The Dissertation Committee for John Benjamin Hedges certifies that this is the approved version of the following dissertation:

Functional characterization of the recycling mechanism for the 60S nuclear export adapter Nmd3p in yeast.

Committee:

Arlen Johnson, Supervisor

Tanya Paull

Makkuni Jayaram

Ellen Gottlieb

David Hoffman

Functional characterization of the recycling mechanism for the 60S nuclear export adapter Nmd3p in yeast.

by

John Benjamin Hedges, BA

Dissertation

Presented to the Faculty of the Graduate School of

The University of Texas at Austin

in Partial Fulfillment

of the Requirements

for the Degree of

Doctor of Philosophy

The University of Texas at Austin

December 2004

Dedication

This dissertation is dedicated to my wife for her love and enduring support throughout my graduate career and to my parents for instilling within me the values upon which I have based my life.

Acknowledgements

I would like to extend my sincere gratitude to Arlen Johnson for allowing me the opportunity to serve in his laboratory and for his patience and guidance throughout my graduate career. I also would like to acknowledge Matt West and George Kallstrom for the establishment of rewarding collaborations, especially Matt for his thorough analysis and helpful discussions. I also would like to thank my former laboratory colleagues, Justin Brown and Jennifer Ho, for providing me with guidance early in my graduate career. My thanks are also extended to Alice Wang and Ivy Hung for their sound advice over the years. I'm also grateful to Anthony Chen for making *sqt1* temperature sensitive and loss of function mutants and *NMD3* suppressor mutants and Grace Chen for making *NMD3* loss of function mutants.

Functional characterization of the recycling mechanism for the 60S nuclear export adapter Nmd3p in yeast.

Publication No._____

John Benjamin Hedges, Ph.D.

The University of Texas at Austin, 2004

Supervisor: Arlen W. Johnson

Ribosomes are essential macromolecular machines that translate, through a messenger RNA intermediate, the information encoded in the DNA sequence of all cells into proteins. Because of their fundamental role in cell survival, an enormous amount of cellular resources must be dedicated to ribosome synthesis. Eukaryotic cells must contend with transport of materials between two compartments, the nucleus and cytoplasm. During ribosome biogenesis, these cells assemble ribosomal subunits at a specific subnuclear structure called the nucleolus and only release them into the nucleoplasm upon completion of initial assembly. The subunits must then traverse the nucleoplasm before reaching the nuclear pore complex (NPC) where they are exported to the cytoplasm to act in translation. Processing of the small (40S) subunit through this pathway occurs relatively quickly. However, processing of the large subunit (60S) involves a greater number of maturation steps. One of the last of these steps being export of the large subunit through the NPC, mediated through the export adapter protein Nmd3.

The large ribosomal subunit protein Rpl10 is required for 60S export and subunit joining in yeast. It is believed that the role of Rpl10p in export is to provide the 60S binding site for Nmd3p in the nucleus. Through examination of *rpl10* mutant effects on the 60S export pathway, I've instead found that the role of Rpl10p is indirect. This work

shows that disruption of either Rpl10p or the Rpl10p 60S loading factor, Sqt1p, leads to a block in export due to entrapment of Nmd3p on 60S subunits in the cytoplasm. For *rpl10* mutants these effects are suppressed by specific alleles of *NMD3* that restore recycling to the nucleus. To gain a better understanding of the export function of Nmd3p, this work also examines the NES and 60S binding domains of Nmd3p and, in light of the Rpl10p results shown here, establishes an assay to identify other 60S components required for this binding. From these findings, I propose the model that Rpl10p is required for the release of Nmd3p from subunits in the cytoplasm to support further rounds of 60S export and to provide a final "quality control" step in 60S maturation prior to 40S joining.

Table of Contents

List of Tables

List of Figures

List of Illustrations

Chapter 1: General Introduction

1.1 OVERVIEW

Ribosome biogenesis is the most energy costly activity a rapidly growing cell undertakes. In eukaryotes, 40S and 60S ribosomal subunits are manufactured in the nucleolus, the sub-nuclear structure(s) where rDNA repeats and biogenesis factors are sequestered. Remarkably, nucleolar processing and assembly is only the beginning of life for subunits in the cell. Once exiting the nucleolus, the 60S subunit is further assembled as it traverses the nucleoplasm, while 40S is immediately exported for final maturation in the cytoplasm. Large and small ribosomal subunits are initially derived from a single 35S rRNA containing precursor particle. From here, each subunit matures down a distinct processing pathway until joining as mature particles in the cytoplasm to form the final 80S translation machine. The complexity of the pre-60S molecule gradually decreases as it moves from the nucleolus to the cytoplasm. However, very little is known about late events during ribosome export and cytoplasmic maturation. Although I began my dissertation work to understand assembly of the 60S export complex, my work has led to a greater understanding of these late maturation events including release of the 60S nuclear export adapter Nmd3p. Furthermore, I have established a link between these final steps and rate of export modulated through Nmd3p release.

1.2 RIBOSOME STRUCTURE AND FUNCTION

The fully matured 80S ribosome of eukaryotes is a large macromolecular machine that functions in translation of proteins in the cytoplasm. It consists of two subunits that, in eukaryotes, can be resolved into 40S and 60S species by velocity sedimentation. 40S

subunits are each composed of a single 18S ribosomal RNA (rRNA) and 33 ribosomal proteins (r-proteins) (Planta and Mager 1998; Sengupta, Nilsson et al. 2004). The small subunit contains the decoding region needed for recognition of cognate tRNAs in the mature ribosome (Carter, Clemons et al. 2000). The 60S subunit is made up of 3 rRNAs consisting of 5S, 5.8S and 25S (28S in higher eukaryotes) as well as 46 different r-proteins (Planta and Mager 1998). Peptidyl-transferase activity is intrinsic to the large subunit as translation of short phenylalanine chains can be carried out in the absence of the small subunit (Maden, Traut et al. 1968).

In bacteria, translation is carried out by the 70S ribosome. This is also composed of two subunits of unequal mass, each of which differ significantly in size but not function from their eukaryotic counterparts. The 30S subunit is composed of a single 16S rRNA and about 21 proteins. The 50S subunit is composed of 23S and 5S rRNAs and just over 30 proteins (Garrett 2000).

The bacterial/archaeal ribosome is approximately 2.5 MDa in size, with about 1.7 MDa contributed from the mass of the large subunit and 800kDa contributed from the small subunit. Most r-proteins are highly basic in nature lending to their ability to interact with RNA. rRNA makes up the core of the ribosome while ribosomal proteins are scattered along the outer boundaries of this core to aid in stability of the RNA tertiary structure (Ban, Nissen et al. 2000; Yusupov, Yusupova et al. 2001). In addition, many ribosomal proteins, especially those involved in active site base arrangement, contain long linear domains that penetrate deep into the rRNA structure (Nakagawa, Nakashima et al. 1999; Ban, Nissen et al. 2000; Yusupov, Yusupova et al. 2001). Amazingly, active bacterial ribosomes have been reconstituted in vitro from purified rRNA and r-protein components (Rohl and Nierhaus 1982; Sanchez, Urena et al. 1990) indicating that bacterial ribosome assembly does not require the participation of trans-acting factors. On

the other hand, eukaryotic ribosomes have only been reconstituted in vitro from *D. discoideum*, where accessory factors from nuclear extracts are still needed for formation of a functional product (Mangiarotti and Chiaberge 1997). This clearly indicates that the assembly of eukaryotic ribosomes is more complex and requires the presence of trans-acting factors.

In recent years, the structure of the ribosome has been resolved in extraordinary detail. Early work in this field consisted of immuno-electron microscopy using antibodies against specific ribosomal proteins for orientation purposes (Lake 1976; Lake 1982). By using antibodies against r-proteins encompassing all parts of the ribosome periphery, preliminary depictions of the ribosomes 3-D structure were created. Most recently, the 50S ribosome structure of the Achaeon *Haloarcula marismortui* has been resolved at 2.4 angstroms by x-ray crystallography (Ban, Nissen et al. 2000), while the yeast 60S ribosome has been resolved at 15 angstroms by cryo-EM (Spahn, 2000). The high conservation of ribosome structure between bacteria and eukaryotes has also allowed threading of the yeast RNA and protein sequence onto the archeal structure to give an approximate atomic resolution model for the yeast ribosome (Spahn, Beckmann et al. 2001). Interestingly, even with such high structural conservation, the yeast ribosome is still approximately 30% larger in size than that of bacteria.

Based on biochemical (Noller, Hoffarth et al. 1992) and structural (Ban, Nissen et al. 2000; Nissen, Hansen et al. 2000) studies it is now known that the ribosome is a ribozyme that facilitates RNA-catalyzed peptide bond formation during protein synthesis. Great strides have been made in defining active residues in the catalytic core of the 50S subunit through modern crystallography techniques. This includes crystallization of ribosomes bound to specific antibiotic conjugants such as the Yarus inhibitor that act as transition-state analogs within the peptidyl transferase site (Nissen, Hansen et al. 2000).

The Yarus inhibitor consists of the antibiotic puromycin, which acts an aminoacylated tRNA analog, fused to the nucleotide sequence CCdA via a phosporamide group (Welch, M and Yarus, 1995). CCA is found at the 3'-end of all tRNAs and positions the tRNA with respect to the large subunit through direct binding (Moazed and Noller 1991). This places the puromycin moiety in the A-site and positions the phosphoramide group in such a way to that it mimics the tetrahedral carbon intermediate that forms in the P-site at the onset of the peptidyl-transferase reaction. X-ray crystals made from the 50S ribosomal subunit of *Haloarcula marismortui* saturated with the Yarus inhibitor as well as other active site inhibitors were then imaged (Nissen, Hansen et al. 2000). This analysis established that the peptidyl-transferase site is r-protein deficient and identified A2451 within 23S rRNA as the nucleotide responsible for initiating the peptidyl-transferase reaction.

Although identification of the active site nucleotide was a major breakthrough in ribosome structural analysis, more recent kinetic studies have found that the ribosome's puromycin-bound behavior is only representative of half of the petidyl-transferase function. This was established by kinetic assays of peptide-bond formation in ribosomes mutated at specific active-site residues (Youngman, Brunelle et al. 2004). This work instead showed that two layers of active nucleotides form the catalytic center of the ribosome. The "inner shell", first established by studies with puromycin and its conjugants, is required for peptide release, while the "outer shell" is responsible for promoting peptide bond formation. These findings indicate that although x-ray crystallography of macromolecules as large as the ribosome can be extraordinarily useful, it has its limitations with respect to fully understanding function at the molecular level.

In addition to the high resolution of the peptidyl-transferase site, the structures of the three distinct tRNA interaction sites that are at the core of the ribosome's function

have been determined from the 70S crystal structure of *Thermus thermophilus* (Yusupov, Yusupova et al. 2001). This was accomplished using ribosomes containing bound mRNA and tRNAs in each of the tRNA binding sites; the A (aminoacyl) site, which accepts the incoming aminoacyl tRNA; P (peptidyl) site, which holds the peptidyl-tRNA with the nascent peptide; and the E (exit) site, which holds the uncharged tRNA prior to release.

According to the hybrid states model of translocation during elongation in bacteria, multiple hybrid states exist between tRNA, the 30S subunit and the 50S subunits of the 70S ribosome (Moazed and Noller 1989). A brief description of this model, which is conserved between archaeabacteria, eubacteria and eukaryotes, follows as reviewed in (Ramakrishnan 2002; Kapp and Lorsch 2004). First, an EF-Tu-GTP-aminoacyl-tRNA ternary complex binds to the 70S ribosome to place a charged tRNA into the recently vacated A-site. The small subunit, containing the "decoding" site, aligns the mRNA codon with the cognate aminoacyl-tRNA anti-codon to appropriately select the next amino acid to be covalently joined to the growing peptide chain. The large subunit, containing the peptidyl-transferase center, utilizes the energy from GTP hydrolysis by EF-Tu to insert the aminoacylated acceptor arm of the cognate aa-tRNA (containing the universal CCA recognition sequence) into its A-site. At this point EF-Tu-GDP is released and the aminoacylated end of the A-site aa-tRNA is positioned into the peptidyl-transferase center. This leads to peptide bond formation with the peptidyl-tRNA located in the P-site. Concomitantly, the deacylated acceptor arm of the newly uncharged P-site tRNA is moved into the E-site. After peptidyl transferase activity, movement of the anticodon ends of the new peptidyl-tRNA into the P-site and the uncharged tRNA into the E-site is driven by the GTPase activity of EF-G. Coincident with this is the movement of the mRNA by one codon in a type of consolidated "ratcheting" motion

between the 30S and 50S subunits. This “resets” the ribosome in anticipation of binding the next cognate tRNA at the A-site.

Although the fundamental aim of forming a translation initiation complex is the same in all organisms, the steps and machinery to accomplish this goal are much more complex in eukaryotes than bacteria (reviewed in (Pestova, Kolupaeva et al. 2001; Ramakrishnan 2002; Sonenberg and Dever 2003; Kapp and Lorsch 2004)). This includes the involvement of 12 different initiation factors in eukaryotes versus only 3 in bacteria. In simplified terms, a round of eukaryotic translation initiation consists of the following: (1) formation of a ternary complex that contains eIF2 bound to GTP and methionyl initiator tRNA (2) binding of the ternary complex, along with other initiation factors, to the 40S ribosomal subunit to form 43S (3) association of the 43S complex to the ^{7}mG cap of mRNA mediated through the eIF4E subunit of eIF4F (4) movement of the mRNA-bound ribosomal complex 5’to 3’ in search of an AUG start codon (5) formation of a 48S initiation complex in which the initiator codon (AUG) is bound by the anticodon of initiator tRNA and finally (6) displacement of factors from the 48S complex to promote joining of the 60S subunit to form an 80S ribosome with Met-tRNAi in the P site.

Although not classified as a step in translation initiation, the loading of the ribosomal protein Rpl10 on the 60S subunit is also a prerequisite for joining to 40S (Dick, Eisinger et al. 1997; Eisinger, Dick et al. 1997). Based on cryo-EM reconstructions, Rpl10p is located just above the A-site and near the GTPase stalk on the joining face of the large subunit (Spahn, Beckmann et al. 2001). This becomes important in the following chapters when testing the possible role of Rpl10p in mediating Nmd3p binding to the 60S subunit and for interpreting the effects of trapping other factors within this region when late 60S maturation is disrupted.

1.3 RIBOSOME BIOGENESIS

The best-characterized rRNA processing pathway to date is that of the yeast *Saccharomyces cerevisiae* (reviewed in (Kressler, Linder et al. 1999) and (Venema and Tollervey 1999)). The 35S and 5S rRNA precursors are transcribed from 100-200 rDNA cassettes located on the long arm of chromosome XII. These cassettes and the trans-acting factors that aid in the formation of the nascent ribosomes, during and after rRNA transcription, form the basis for the nucleolar structure(s) located in the nucleus of eukaryotic cells. The large 35S rRNA precursor, from which 25S (28S in higher eukaryotes), 5.8S and 18S rRNAs are processed, is transcribed by RNA Polymerase I. In contrast, RNA Polymerase III transcribes the 5S rRNA component of the 60S ribosomal subunit.

Both pre-subunit complexes arise from a single 90S ribonucleoprotein (RNP) precursor (Udem and Warner 1972; Trapman, Retel et al. 1975). This 90S particle is then cleaved to form the 43S (pre-40S) and 66S (pre-60S) species ((Trapman, Retel et al. 1975) and Illustration 1.1). This processing, in conjunction with the formation of the final 40S and 60S particles in the cytoplasm, requires over 170 accessory proteins, most of which reside in the nucleolus (reviewed in (Kressler, Linder et al. 1999; Venema and Tollervey 1999; Fromont-Racine, Senger et al. 2003)). Additionally, over 100 small nucleolar RNAs (snoRNAs) that form snoRNP complexes are involved in ribosomal RNA (rRNA) modification for proper active site formation and structural stability that is further enhanced by ribosomal protein binding (Lowe and Eddy 1999). These snoRNP complexes are grouped into two major classes, H/ACA-box and C/D-box, and are mostly involved in pseudouridilation and methylation in addition to less well-characterized cleavage and helicase activities (reviewed in (Kressler, Linder et al. 1999; Venema and Tollervey 1999)).

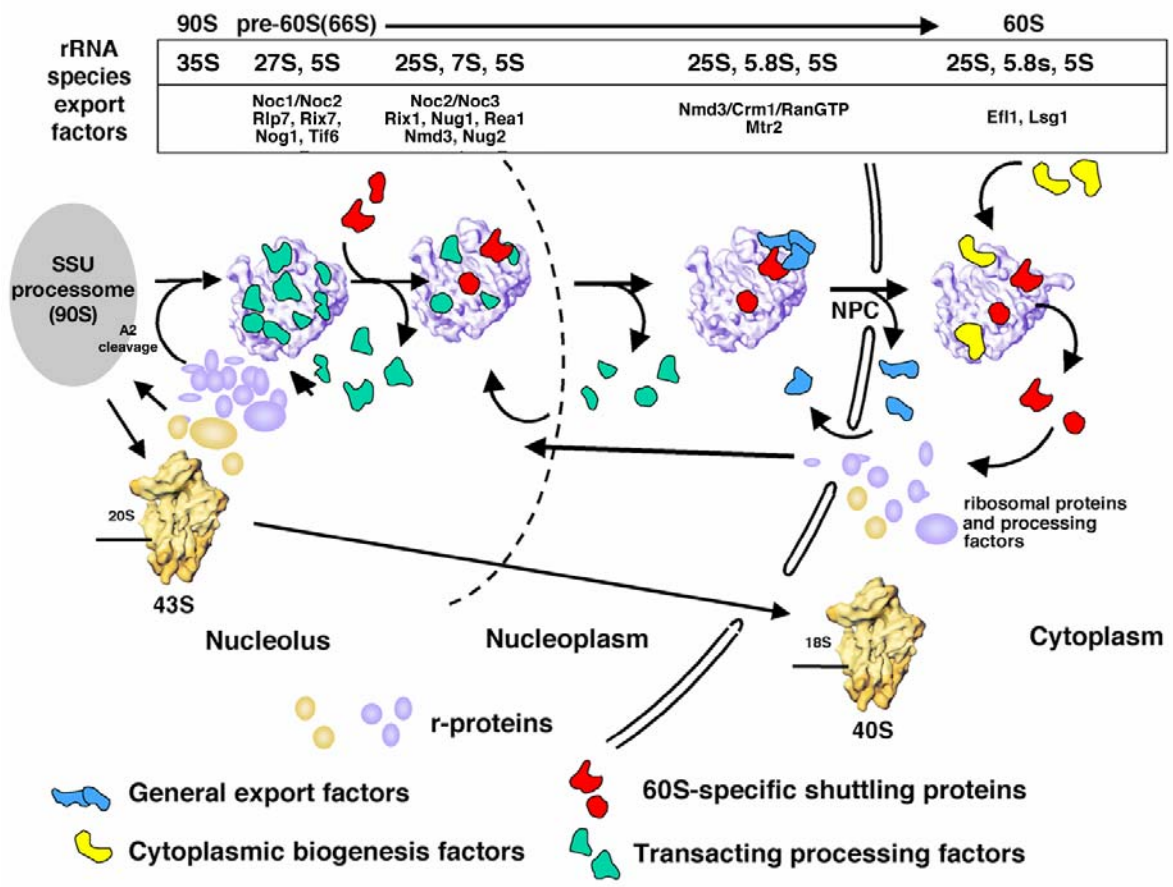

Illustration 1.1 Maturation of ribosomal subunits.

Around 170 trans-acting factors and 100 snoRNAs are required for ribosomal subunit biogenesis. This illustration focuses on the trans-acting factors that are believed to facilitate nucleolar to cytoplamic movement of pre-60S particles. Major rRNAs represented in each of these particles are also given. Adapted from (Johnson 2004).

Although the factors involved in early processing of rRNAs are well characterized, there are divergent thoughts as to what constitutes the 90S precursor particle prior to cleavage at the major A_2 endonucleolytic site to separate the 66S and 43S particles (Reviewed in (Kressler, Linder et al. 1999; Venema and Tollervey 1999; Fromont-Racine, Senger et al. 2003)). The A_2 site is one of many endonucleolytic sites that exist in precursor rRNA that direct enzymatic cleavages during 40S and 60S rRNA processing. Initially, it was believed that the earliest ribonucleoprotein particle consisted of all factors involved in formation of the 40S and 60S subunits including several representative r-proteins from each subunit. This has become known as the "processosome" model. More recently however, the work from the Baserga group has suggested that the precursor particle of the 40S subunit is processed and released by cleavage at A_2 prior to formation of pre-60S as described below in more detail (Dragon, Gallagher et al. 2002). The existence of this processing intermediate is supported by the finding that a recently isolated 90S particle contains many of the same factors found in the Baserga work (Grandi, Rybin et al. 2002).

Although formation of the 40S particle is relatively less complex than for 60S, recent findings have discovered that the 40S ribosomal subunit pathway also requires multiple accessory factors that have only recently been uncovered through discovery of the small subunit (SSU) processome (Dragon, Gallagher et al. 2002). These events occur at a stage in biogenesis prior to pre-60S formation. This is supported by proteomic analysis and electron microscopy of 35S "terminal knobs" at active transcription sites on rDNA chromatin spreads showing that the 35S pre-rRNA is co-transcriptionally associated with small subunit proteins, trans-acting factors and the U3 snoRNP to form the SSU complex. The pre-40S particle is presumably cleaved from this complex at the A_2 site, through guidance by the U3 snoRNP, while 35S transcription is still occurring

(Illustration 1.1). It is not until after this cleavage that large subunit proteins and trans-acting factors associate with the remaining 27S rRNA to form the pre-60S particle. Due to a lack of further nucleoplasmic processing events, the 40S particle is immediately exported to the cytoplasm upon A_2 cleavage (Trapman and Planta 1976; Udem and Warner 1973) where it is processed to maturation by dimethylation and cleavage at site D (Lafontaine, Vandenhaute et al. 1995).

In yeast, mature cytoplasmic 40S immediately binds to transcripts to form the 48S initiation complex, while there is a lag in the incorporatioin of nascent 60S (Warner 1971; Trapman and Planta 1976). Along similar lines, the ribosome biogenesis pathway in HeLa cells also displays a slow cytoplasmic step (Warner 1966). This has been suggested to indicate that further cytoplasmic maturation events occur for 60S prior to subunit joining. The nature and purpose of this late maturation event remains to be determined, however this may suggest that a control point for 60S formation exists in the cytoplasm.

Much work has been done in elucidating the composition of various intermediate forms of the pre-60S particle as it progresses along the road to becoming a mature, "translation competent" subunit ((Fatica and Tollervey 2002; Fromont-Racine, Senger et al. 2003; Tschochner and Hurt 2003) and references therein). Most of the assembly factors are removed from the complex before it leaves the nucleolus, and the complement of trans-acting factors is further reduced in the nucleoplasm prior to export ((Bassler, Grandi et al. 2001; Nissan, Bassler et al. 2002) and diagram 1.1).

Although large-scale proteomic analyses suggest that stable complexes form during various phases of 60S subunit maturation, these are only "snapshots" of ribosome composition. In reality, most of these complexes are enormously dynamic in nature and contain only a minimal core of stably associated trans-acting factors. These large-scale

assays, in conjunction with cell biology and genetic studies, have identified numerous factors involved in transition of specific nascent particles from the nucleolus into and through the nucleoplasm. Around 50 non-ribosomal proteins are associated with the earliest nucleolar pre-60S species while only 5 non-ribosomal proteins are stably associated with the cytoplasmic pre-60S complex (Reviewed in (Tschochner and Hurt 2003)). Associated with these particles are proteins that may control progression through the biogenesis pathway. An example of such factors can be found in what is known as the Noc complex (Milkereit, Gadal et al. 2001). The Noc1/Noc2 protein complex, associated with 90S and 66S pre-ribosomes, is believed to facilitate release of the 66S particle from the nucleolus. Once at the perimeter of the nucleolus, Noc1 is exchanged with Noc3 to form a complex that chaperones the nascent subunit through the nucleoplasm where Noc2 and Noc3 are released prior to export (Illustration 1.1).

Because of the complexity of ribosome biogenesis, the events of pre-rRNA processing and r-subunit assembly are intimately coordinated and linked to ensure proper subunit formation (Venema and Tollervey 1999). Early biogenesis factor mutants accumulate specific rRNA precursors that correspond with defects at specific temporal positions in the processing pathway. Due to the nature of the feedback mechanisms built into this highly regulated process, early biogenesis mutants often accumulate specific pre-rRNAs but not to appreciable levels. Surprisingly, mutants that lead to a blockage in 60S export, including Nug1p, Nog2p and Nmd3p are only slightly defective in pre-rRNA processing ((Ho and Johnson 1999; Bassler, Grandi et al. 2001; Saveanu, Bienvenu et al. 2001), respectively). Nonetheless, mature rRNAs assayed from these mutants are unstable. This suggests that in the event that export is blocked, rRNA processing continues but late nucleoplasmic precursor particles are not able to mature to the point of "export competence". Thus, their lives are short-lived due to nuclear degradation. This

suggests that an active degradation pathway exists to prevent accumulation of defective subunits.

As in other dynamic processes of the cell, GTPases and ATPases also modulate temporal and spatial progression of the 60S ribosome synthesis pathway as determined by large-scale proteomic analysis (reviewed in (Fromont-Racine, Senger et al. 2003)). Although the exact function of these proteins is not well characterized, their interactions with the nascent subunit are likely needed to modulate structural rearrangements to accommodate or release other factors and/or r-proteins.

Recently, it has been found by another lab that the sequential loading of the Nog1p GTPase occurs in conjunction with binding of the ribosomal-like protein Rlp24 (Saveanu, Namane et al. 2003). In this work it is suggested that Rlp24p binds to an early pre-60S particle to provide a binding site for Nog1p. Subsequently, Nog1p association with pre-60S is required for binding of the later pre-60S binding factor Nog2p. Interestingly, depletion of Nog1p leads to the formation of a stable pre-60S intermediate that remains deficient of factors that normally load after Nog1p. This supports the idea that 60S biogenesis, although dynamic, occurs with the formation of various stable intermediates that await binding of factors to allow transition to the next processing step. Thus, the formation of relatively stable intermediates may be required for subsequent association of r-proteins and trans-acting factors in the assembly pathway (Illustration 1.1). Export of the pre-60S subunit from the nucleus requires the assembly of an export complex containing Crm1p and Nmd3p (see section 1.4). Thus, recruitment of Nmd3p may depend on the structural integrity of the pre-60S particle and act as the final step in evaluating “export competence” of the particle.

One of the better characterized G-proteins involved in 60S maturation is Efl1p which affects dissociation of the trans-acting factor Tif6p in the cytoplasm. eIF6, the

mammalian ortholog of yeast Tif6p, was first identified on 60S subunits as a 60S to 40S anti-association factor isolated from rabbit reticulocyte lysates (Raychaudhuri, Stringer et al. 1984). More recently, Tif6p was found to play a similar role in preventing premature subunit joining in yeast as well as acting as an essential factor early in the 60S biogenesis pathway (Basu, Si et al. 2001). Around the same time, others also characterized Tif6 as an essential factor involved in an early 60S biogenesis event (Becam, Nasr et al. 2001; Senger, Lafontaine et al. 2001). From these analyses, it has been proposed that Tif6p associates with pre-60S subunits in the nucleolus to facilitate movement through the nucleoplasm and export into the cytoplasm. In the cytoplasm the G-protein Efl1p is proposed to modulate release of Tif6p to allow recycling to the nucleolus prior to 60S incorporation into the translation apparatus (Senger, Lafontaine et al. 2001). This is based upon the observation that mutants of *EFL1* lead to redistribution of Tif6p from a predominantly nucleolar location to an enhanced presence in the cytoplasm. In turn, *TIF6* dominant mutants may suppress this aberrant relocalization phenotype through weakened interaction with the subunit. This would allow Tif6p to dissociate from subunits in the absence of functional Efl1p. Because of its function as a 60S anti-association factor, Tif6p may play a role in translation control by preventing 60S association with the 48S initiation complex until after Tif6p release.

Previous work in our lab has also characterized the roles of Nog1p and a late trans-acting factor, Lsg1p, in the biogenesis pathway (Kallstrom, Hedges et al. 2003). Both are putative GTPases that are believed to modulate structural rearrangements in the 60S subunit to facilitate binding or release of other biogenesis/export factors. Nog1 was shown to be necessary for early events in 60S biogenesis as disruption of its function leads to early rRNA processing defects and accumulation of the Rpl25-eGFP reporter in the nucleolus. Nucle(ol)ar accumulation of Rpl25-eGFP being indicative of a 60S export

defect because of the role of Rpl25 as a core ribosomal protein (Hurt, Hannus et al. 1999). Conversely, Lsg1p was shown to be a non-shuttling, cytoplasmic protein. Interestingly, disruption of its function leads to a more generalized defect in rRNA processing, as observed for other late-maturation factors including Nmd3p, Nug1 and Nug2 ((Ho and Johnson 1999; Bassler, Grandi et al. 2001; Saveanu, Bienvenu et al. 2001), respectively). In addition, mutations in all of these factors lead to nucleolar accumulation of Rpl25-eGFP.

The above results beg the question of why a 60S trans-acting factor residing in the cytoplasm, such as Lsg1p, would lead to a biogenesis/export defect. The answer to this likely parallels that for the Tif6p/Efl1p interaction in which Efl1p is required for Tif6 recycling to the nucle(ol)us. In the same way, Lsg1p may play a role in recycling a factor involved in large subunit export, such as Nmd3p. In this way, release of Nmd3p, modulated through Lsg1p activity, could present a last opportunity for a 60S "quality control" check prior to 48S initiation complex binding. In turn this would also provide a cytoplasmic control point for the export pathway by sequestering Nmd3p in the cytoplasm in the event that there is a failure in final subunit maturation.

1.4 NUCLEAR EXPORT OF RIBOSOMAL SUBUNITS

In log phase yeast cells, over 2000 ribosomes are produced per minute (Warner 2001). With approximately 150 nuclear pores per nucleus (Winey, Yarar et al. 1997), this means that each pore must accommodate around 25 ribosomal subunits every minute. Even more impressive is the fact that over 160,000 r-proteins, not including trans-acting factors, must be imported every minute to support this rate of biogenesis and export. This corresponds to an enormous volume of traffic that traverses the NPC at any given moment just from the ribosome biogenesis pathway alone.

The transport of materials through the NPC requires facilitated diffusion modulated by soluble transport receptors referred to as “importins” or “exportins” depending on function (reviewed in (Mattaj and Englmeier 1998; Gorlich and Kutay 1999; Fried and Kutay 2003)). These karyopherins, most of which are from the importin-β family, interact with phenylalanine-glycine (FG) repeat sequences in the nucleoporin proteins lining the inner channel of the NPC (Ribbeck and Gorlich 2002). Directionality of movement across the nuclear membrane is controlled by the small GTPase Ran (Gsp1p in yeast). In the nucleus, Ran is loaded with GTP by interaction with the GTP exchange factor (GEF) RCC1 (Prp20p in yeast). In the cytoplasm interaction of Ran with its GTPase activating protein (RanGAP), and accessory proteins such as RanBP1 or RanBP2 in humans, leads to hydrolysis of GTP to GDP.

The constant hydrolysis of RanGTP to RanGDP in the cytoplasm and exchange of GDP for GTP in the nucleus leads to the formation of a RanGTP gradient between the nucleus and cytoplasm. It is this gradient that leads to a constant flux of GTP bound Ran protein complexes out of the nucleus. At the same time, RanGTP is required for export receptors to bind to export cargo. Together, these three components form an export complex. Once in the cytoplasm, GTP hydrolysis leads to disassembly of the export complex to release the export cargo into the cytoplasm (i.e. 60S). Released receptor molecules and RanGDP then recycle back to the nucleus to facilitate further rounds of export.

Multiple nuclear import/export receptor proteins have been identified, and are conserved, in yeast and humans (Fried and Kutay 2003). This is not a surprise when considering the large array of different RNA and protein substrates that traverse the NPC. For cellular mRNA the route of nuclear exit is through interaction with the human TAP (yeast Mex67p) export receptor (Katahira, Strasser et al. 1999). To aid in this TAP

mediated export process is human p15 (yeast Mtr2p), an mRNA export cofactor that must bind to TAP-bound mRNA to help facilitate direct interaction with nucleoporins within the NPC ((Santos-Rosa, Moreno et al. 1998; Suyama, Doerks et al. 2000)). Once this export complex is established, the TAP/p15 complex mediates passage of mRNA through the NPC by facilitated diffusion. Surprisingly, this process is also RanGTP-dependent (Schlenstedt, Wong et al. 1995). This is likely based upon a requirement for maintenance of the RanGTP gradient to recycle non-importin β-like receptors such as TAP back to the nucleus.

Proteins, on the other hand, are preferentially handled by interaction with the export receptor CRM1 (XpoIp or Crm1p in yeast) that binds to leucine-rich nuclear export signals (NESs) of certain cargo adapter proteins (Fornerod, Ohno et al. 1997; Stade, Ford et al. 1997). However, in some cases, viral RNAs also make use of the CRM1 pathway to bypass the prerequisite for splicing that accompanies export through the TAP/p15 pathway ((Popa, Harris et al. 2002) and references therein). By far the best-characterized of the viral particles utilizing CRM1-dependent export is HIV-I. The HIV-1 virus adapter protein Rev contains a leucine-rich NES domain that directly interacts with the CRM1 receptor to modulate unspliced viral RNA export (Fischer, Huber et al. 1995).

Nuclear export of the ribosomal subunits also requires the Crm1p export receptor and maintenance of the RanGTP gradient. The adapter protein Nmd3p provides the leucine-rich NES to mediate 60S subunit interaction with Crm1p ((Ho, Kallstrom et al. 2000; Gadal, Strauss et al. 2001) and illustration 1.2). Although, the export of pre-40S also requires Crm1p, the component that provides the leucine-rich NES, whether a trans-acting adapter or a constituent of the ribosome, has not been identified (Moy and Silver 1999; Moy and Silver 2002). The Nmd3p-mediated export of 60S is conserved from

yeast to humans (Johnson, Lund et al. 2002; Thomas and Kutay 2003; Trotta, Lund et al. 2003). In both yeast and humans it appears that Nmd3p binds to subunits in the nucleolus and may be required for their release into the nucleoplasm. In vitro work with human NMD3 has produced direct evidence for the formation of a complex with RanGTP and CRM1 (Thomas and Kutay 2003). Additionally, removal of the last 27 amino acids of the hNMD3 sequence, containing the primary NES, results in loss of complex formation. Weak formation of this complex has also been shown for yeast Nmd3p (Kallstrom and Johnson, unpublished). However, in vitro reconstitution of export complex binding to 60S has not been established in either system.

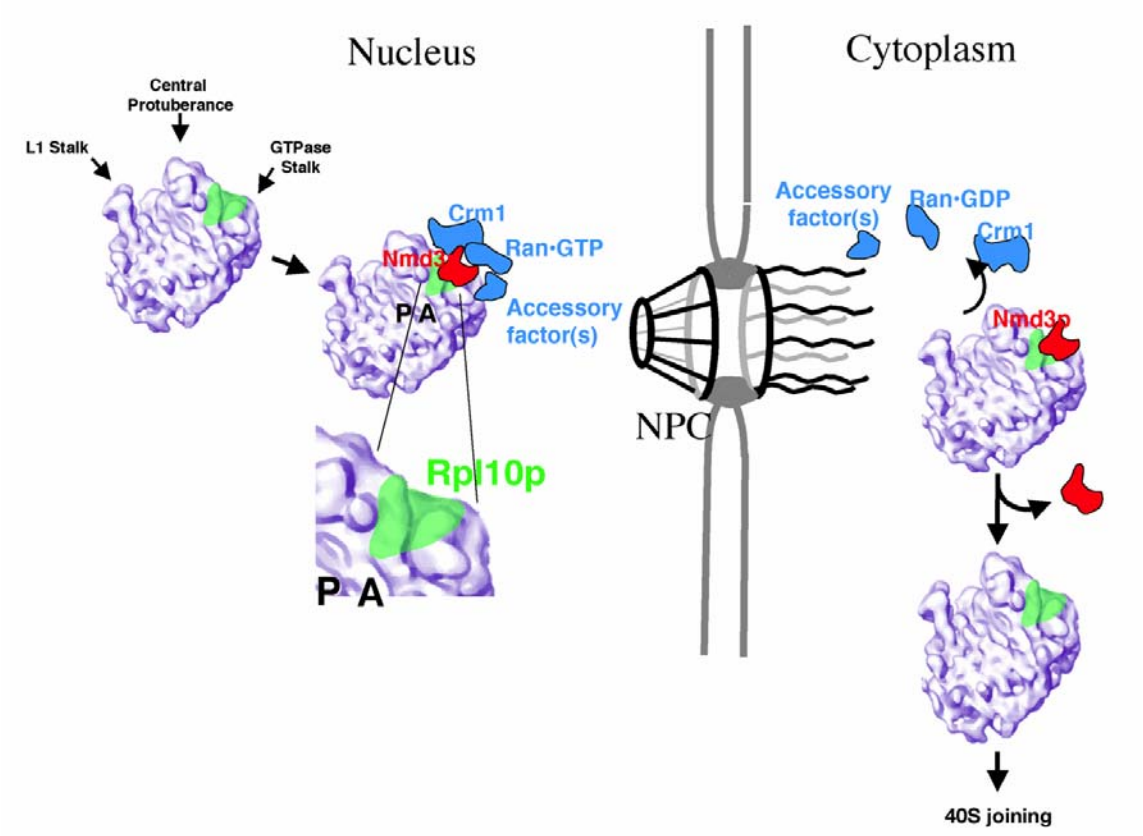

Illustration 1.2 Rpl10p provides the putative 60S binding site for Nmd3p to facilitate interaction with the Crm1p/RanGTP export complex.

Current models for 60S subunit export suggest that Rpl10p is the binding site for Nmd3p. Accessory factors such as Mtr2 may also play a part in 60S export. Once in the cytoplasm, hydrolysis of RanGTP to RanGDP leads to dissociation of the export complex but Nmd3p is retained on 60S. At a later point, prior to 60S joining to 40S, Nmd3p is also released. Rpl10p remains bound to 60S and is required for joining to 40S to form the final, translationally competent, 80S ribosome. Adapted from (Johnson 2004).

Although Nmd3p appears to be the primary factor responsible for pre-60S export, other "accessory factors" have also been implicated in this process. Proteomic analysis of trans-acting factors on a late pre-60S nuclear species identified Mtr2p in conjunction with Nmd3p (Nissan, Bassler et al. 2002). This was unexpected since Mtr2p is also a cofactor in Mex67p modulated mRNA export. Along similar lines, a particularly unusual *mtr2* allele, *mtr2-33*, was shown to impair 60S nuclear export rather than mRNA export (Bassler, Grandi et al. 2001). Interestingly, *mtr2* and *mex67* are also synthetic lethal with *nmd3* mutants ((Ho, Kallstrom et al. 2000; Bassler, Grandi et al. 2001), respectively). These data imply that Mtr2p provides a link between mRNA and ribosome export, possibly through its role as an accessory protein involved in both pathways.

The temporal and spatial points in the 60S biogenesis pathway at which the Nmd3p export adapter binds and releases remain elusive. Previous work suggests that Rpl10p forms at least part of this binding site for Nmd3p on 60S ((Gadal, Strauss et al. 2001) and diagram 1.2). On the other hand, kinetic mapping of r-protein loading suggests that Rpl10p associates with 60S relatively late in the biogenesis pathway, possibly in the cytoplasm (Kruiswijk, Planta et al. 1978). In addition, human Rpl10p (QM) is found exclusively in the cytoplasm of human cells (Nguyen, Mills et al. 1998). This is in contrast to the nuclear and cytoplasmic localization observed for a core ribosomal component, the ribosomal large P antigen that was assayed in the same study. Together these data indicate that a clear picture of when Rpl10p is loaded onto the subunit has not emerged.

1.5 DISSERTATION OBJECTIVES

When I began my dissertation work, my objective was to understand the nature of Nmd3p binding and recruitment to the 60S subunit in the nucleus. This was premised largely on the published work from another laboratory suggesting that Rpl10p provides

the binding site for Nmd3p in the nucleus (Gadal, Strauss et al. 2001). However, my results do not support a role for Rpl10p in recruiting Nmd3p. Furthermore, I have provided evidence that Rpl10p binds after Nmd3p. On the other hand, my work supports a model in which release of Nmd3p requires Rpl10p. This led me to the hypothesis that is supported by the first two results chapters of this dissertation. This focuses on the events that occur late in the large ribosomal subunit biogenesis pathway, including the binding and release of the nuclear export adapter Nmd3p. The last chapter culminates my early work to further characterize Nmd3p spurred through the initial findings of two former students in our lab, Jennifer Ho and George Kallstrom. This includes results and discussion of early attempts to test the binding site for Nmd3p on 60S.

In recent years, numerous studies have tabulated the trans-acting factors that interact with various 60S particles from their origins in the nucleolus to their maturation in the cytoplasm. Although an enormous volume of information was gathered in all of these studies, the interactions between these trans-acting factors have not been extensively studied. This dissertation provides a glimpse into the complex interactions that modulate late events required for sustained export of the 60S subunit.

Five chapters are contained within this body of work. Already, Chapter 1 has provided a general introduction into the extensive research done on the structure and composition of ribosomes with emphasis on factors that modulate late maturation of the large subunit. Chapter 2 will describe the methods and materials utilized to perform the research described herein. The 3rd chapter will characterize the interaction between two proteins, Rpl10 and Sqt1, in maintaining 60S export. Based on work from Chapter 3, Chapter 4 will provide a molecular link between the interactions of Sqt1p and Rpl10p and release of the Nmd3p nuclear export adapter from cytoplasmic 60S subunits. Lastly, Chapter 5 will provide preliminary characterization of the domains of Nmd3p required

for 60S binding and export. This chapter will also present initial attempts at identifying components of the 60S subunit that are necessary for Nmd3p binding. In all, this work significantly expands current knowledge of late events in 60S ribosome maturation. In addition, it shows that 60S biogenesis is coupled to activation of the subunit for translation.

Chapter 2: Experimental Materials and Methods

The experimental materials and methods used in this thesis are described in this chapter. Each section corresponds to a results chapter (3-5) and includes strains, plasmids and methods used in each of these chapters. The first time that a particular method is used it is described in full. Subsequent uses of the same method refer to the first description but with minor modifications.

2.1 MATERIALS AND METHODS FOR CHAPTER 3

2.1.1 Strains, plasmids and media

Strains used in Chapter 3 are listed in Table 2.1. Unless otherwise noted, standard yeast genetics methods and media are used as described in (Kaiser, Michaelis et al. 1994). All strains were grown at 30°C unless otherwise indicated in rich medium (yeast extract-peptone) or dropout medium (synthetic complete) containing either 2% glucose, 1% galactose or 1% raffinose as the carbon source as described previously (Kaiser, Michaelis et al. 1994). The following strains were made for use in this section. A *sqt1::KanMX4* heterozygous diploid (Research Genetics) was transformed with pAJ336 (*GAL10::SQT1*), sporulated and dissected to obtain strain AJY1433 (*MATα sqt1::KanMX4 met15Δ10 leu2Δ0 ura3Δ0 his3Δ1* (pAJ336)). AJY1605 and AJY1640 were made by transforming AJY1433 with pAJ1062 (*SQT1-myc*) and pAJ1065 (*GAL10::SQT1*), respectively, to replace pAJ336. AJY1539, a haploid strain containing a point mutation in genomic *CRM1* that renders it sensitive to the drug LeptomycinB (LMB), was produced as follows. A *crm1::KanMX/CRM1* heterozygous diploid (Research Genetics) was transformed with a derivative of pDC-CRM1(T539C) (Neville and Rosbash 1999) in which *LEU2* was replaced with *URA3*. Cells were sporulated, and

a *crm1::KanMX* containing spore clone was transformed with the *Bgl*II-*Sca*I *CRM1[T539C]*-containing fragment from pDC-CRM1(T539C). Transformants were incubated on YPD plates overnight and then replicated twice to 5FOA-containing plates. 5FOA-resistant clones were scored for G418 sensitivity and integration was confirmed by PCR analysis utilizing the HA-tag within *CRM[T539C]*. AJY1961 (*RPL10-3xHA)* was made as follows. A PCR product made using 5' oligo AJO718 (GAAAACAACATCAGAGAATTCCCAGAATACTTTGCTGCTCAAGCTCGGAT CCCCGGGTTAATTAA), 3' oligo AJO719 (TAATAAACTAGAATTTAAATCAAAAAAATTTCTCTTTTAAGTTAGGAATT CGAGCTCGTTTAAAC) and pFA6a-3HA-KanMX6 as template was transformed into wild-type strain W303. Cells were incubated in 2ml of YPD for 2 hours and plated onto YPD-G418 medium. $G418^R$ colonies were selected and restreaked onto the same medium to verify resistance. Correct isolates were confirmed by PCR.

TABLE 2.1 Strains used in Chapter 3.

Strain	Genotype	Source or Reference
W303 (wt)	*MATa leu2-3,112 his3-11 ura3-1 trp1-1 ade2-1 can1-100 SSD1-d*	J. Warner
CH1305	*MATa ade2 ade3 leu2 lys2-801 ura3-52*	(Kranz and Holm 1990)
DEH221+	*MATα qsr1Δ1::HIS3 ade2-1 trp1-1 leu2-3,112 ura3-1 can1-100* (pDEGQ2)	(Eisinger, Dick et al. 1997)
AJY1433	*MATα sqt1::KanMX4 met15Δ10 leu2Δ0 ura3Δ0 his3Δ1* (pAJ336)	this section
AJY1539	*MATa leu2 ura3 his3 met15 crm1[T539C]*	this section
AJY1605	*MATα sqt1::KanMX4 met15Δ10 leu2Δ0 ura3Δ0 his3Δ1* (pAJ1062)	this section
AJY1640	*MATα sqt1::KanMX4 met15Δ10 leu2Δ0 ura3Δ0 his3Δ1* (pAJ1065)	this section
AJY1961	*MATa leu2-3,112 his3-11 ura3-1 trp1-1 ade2-1 can1-100 SSD1-d RPL10-3xHA::KanMX6*	this section

Plasmids used in Chapter 3 are listed in Table 2.2. Unless otherwise noted, myc denotes 13 tandem copies of the c-myc epitope. pAJ582 (*NMD3-GFP*) was made by amplifying *GFP* with 5' oligo AJO230 (AGAAGATGGAGTCGAGAACACACCCGTTGAATCTCAGCAGCGGATCCC GGGTTAATTAA) and 3' oligo AJO307 (GCGAAGCTTGGCCTCGAAACGTGAGTC) using pFA6a-GFP(S65T)-KanMX6 (Longtine, McKenzie et al. 1998) as template, digesting with PacI and HindIII and ligating it into the same sites of pAJ538. pAJ907 was made by insertion of the *RPL25-eGFP* ORF from pASZ11-RPL25-eGFP into pRS415. The 5' oligonucleotide (oligo) AJO491 (GTGCCATGGCTAGAAGACCAGCT) and the 3' oligos AJO493 (GGTTTAATTAAAGCTTGAGCAGCAAAGTA), AJO494 (GGTTTAATTAAAGCTTCTCTCTTCTTCAA) or AJO513 (GGTTTAATTAAAGCTTCAGAAGACAATTG) were used in PCR with CH1305 genomic DNA as template to amplify full-length *RPL10*, *RPL10N187* or *RPL10N64*, respectively. The products were digested with NcoI and PacI and ligated into the same sites of pAJ544 (*GAL10::NMD3-myc*) to make pAJ792 (*GAL10::RPL10-myc*), pAJ793 (*GAL10::RPL10N187-myc*) and pAJ795 (*GAL10::RPL10N64-myc*), respectively. pAJ1056 (*GAL10::RPL10[26-187]-myc*) was made essentially the same as pAJ793 except the 5' oligo used was AJO556 (GTGCCATGGTTCCAGACTCCAAGATC). pAJ794 (*GAL10::RPL10C43-myc*) was made the same way as pAJ792 except the 5' oligo used was AJO492 (GTGCCATGGGTCCAGAATACTTGAAGAAG). pAJ796 (*GAL10::RPL10-GFP*), pAJ797 (*GAL10::RPL10N187-GFP*), pAJ798 (*GAL10::RPL10C43-GFP*) and pAJ799 (*GAL10::RPL10N64-GFP*) were all made by replacing the PacI-Bsm1 fragments of pAJ792, pAJ793, pAJ794 and pAJ795, respectively, with the PacI-BsmI GFP-containing fragment from pAJ582. pAJ1100

(*GAL10::RPL10N187-GFP*) was made by ligating a BamHI-PstI fragment from pAJ797 into the same sites of YEp352. Single myc-tagged *SQT1* was cut from pSQTMYC1 with BamHI and ligated into the same site of pRS416 to make pAJ1062 (*SQT1-myc*). *GAL::SQT1*, as a BamHI fragment from pAJ336 (*GAL10::SQT1*), was ligated into BamHI-digested pRS416 to make pAJ1065 (*GAL10::SQT1*). *SQT1* was amplified by PCR amplified with 5' oligo AJO521 (CGCGGATCCGAAATTCCCACTCGCCGC) and 3' oligo AJO522 (GAGAAGGATCCCCAAAGAAC), digested with Kpn1, treated with T4 polymerase and then digested with BamHI for ligation into BamHI and SmaI digested pAJ368 (*GAL10::NMD3Δ100*) (Ho, Kallstrom et al. 2000) to make pAJ1063 (*SQT1-myc*).

TABLE 2.2 Plasmids used in Chapter 3.

Plasmid	Relevant markers	Source or Reference
pDC-CRM1(T539C)	LEU2-CEN (*CRM1(T539C)-HA*)	(Neville and Rosbash 1999)
pASZ11-Rpl25eGFP	ADE2-CEN (*RPL25-eGFP*)	(Gadal, Strauss et al. 2001)
pDEGQ2	URA3-CEN (*GAL1-10$_{UAS}$-QSR1*)	(Eisinger, Dick et al. 1997)
pDEGQ64	URA3-CEN (*GAL1-10$_{UAS}$-qsr1-64Δ*)	(Eisinger, Dick et al. 1997)
pDEGQ187	URA3-CEN (*GAL1-10$_{UAS}$-qsr1-187Δ*)	(Eisinger, Dick et al. 1997)
pSQTMYC1	LEU2-CEN (*SQT1-myc*)	(Eisinger, Dick et al. 1997)
pAJ123	LEU2-2μ (*NMD3)*	(Ho and Johnson 1999)
pAJ336	LEU2-2μ(*GAL10::SQT1*)	this section
pAJ368	(*GAL10::NMD3Δ100*)	(Ho, Kallstrom et al. 2000)
pAJ538	LEU2-CEN (*NMD3-myc*)	(Ho, Kallstrom et al. 2000)
pAJ369	URA3-CEN (*GAL10-RPL25-GFP*)	(Ho, Kallstrom et al. 2000)
pAJ582	LEU2-CEN (*NMD3-GFP*)	this section
pAJ792	LEU2-CEN (*GAL10::RPL10-myc*)	this section
pAJ793	LEU2-CEN (*GAL10::RPL10N187-myc*)	this section
pAJ794	LEU2-CEN (*GAL10::RPL10C43-myc*)	this section
pAJ795	LEU2-CEN (*GAL10::RPL10N64-myc*)	this section
pAJ796	LEU2-CEN (*GAL10::RPL10-GFP*)	this section
pAJ797	LEU2-CEN (*GAL10::*RPL10N187-*GFP*)	this section
pAJ798	LEU2-CEN (*GAL10::RPL10C43-GFP*)	this section
pAJ799	LEU2-CEN (*GAL10::RPL10N64-GFP*)	this section
pAJ907	LEU2-CEN (*RPL25-eGFP*)	this section
pAJ1056	LEU2-CEN (*GAL10::RPL10[26-187]-myc*)	this section
pAJ1062	LEU2-CEN (*GAL10::SQT1-myc*)	this section
pAJ1063	LEU2-CEN (*SQT1-myc*)	this section
pAJ1065	URA3-CEN (*GAL10::SQT1*)	this section
pAJ1100	URA2-CEN (*GAL10::RPL10N187-GFP*)	this section
pAJ1252	LEU2-CEN (*sqt1[Q193S/L194V]-myc* ts)	this section
pAJ1264	LEU2-CEN (*sqt1[T356A]-myc* LOF)	this section
pAJ1265	LEU2-CEN (*sqt1[E40G/I370T-myc* LOF)	this section
pAJ1266	LEU2-CEN (*sqt1[N56I]-myc* LOF)	this section

2.1.2 Isolation of *sqt1* temperature sensitive and loss of function mutants

Randomly mutagenized loss of function and temperature sensitive mutants of *SQT1* were made by pooling 40 separate 20 cycle PCR reactions using Taq polymerase (GeneChoice) with 5' oligo AJO620 (ATGGAACCTCAAGAAGAG), 3'oligo AJO621 (CCTCGAACACCAGAGATA) and CH1305 genomic DNA as template. These products were cotransformed into AJY1605 along with MscI-gapped pAJ1063 for *in vivo* homologous recombination. Co-transformants were selected on SC-leu glucose plates and replica plated to 5FOA plates to identify temperature sensitive (37°C) or constitutive slow growth mutants. Plasmids were recovered from selected mutants and transformed into *Escherichia coli* DH5α to obtain pAJ1264 (*sqt1[T356A]-myc* LOF], pAJ1265 (*sqt1[E40G/I370T]-myc* LOF), pAJ1266 (*sqt1[N56I]-myc* LOF) and pAJ1252 (*sqt1[Q193S/L194V]-myc* ts). Out of about 10,000 colonies screened, 15 loss of function and 40 temperature sensitive mutants retained their respective phenotypes throughout the screening process. A list of these and other mutants that were isolated and sequenced from this screen are listed in Appendix A. All sequencing of wild-type and mutant *SQT1* alleles revealed sequence differences (nucleotides C791 and C928) compared to published sequence (A791 and T928, respectively). These represent polymorphisms in strain CH1305 genomic sequence.

2.1.3 Immunoprecipitions

For immunoprecipitations of myc-tagged Rpl10p fragments in figure 3.1, 100ml cultures, diluted to OD_{600}~0.05 from overnight cultures, werre grown to an OD_{600} of ~0.3 in raffinose-containing medium and induced for 3 hours by the addition of galactose. Cultures were pelleted and frozen at -80°C until use. All subsequent steps were carried out on ice or at 4°C. Cells were thawed and washed in lysis buffer (10mM Tris pH 7.6,

40mM NaCl, 10% glycerol, 0.1% NP40, 1mM PMSF and 1μg/ml each of leupeptins and pepstatin A) and repelleted. The cells were resuspended in one volume of lysis buffer, and extracts were made by glass bead lysis (5x50 seconds with 1 minute intervals on ice). Insoluble material was pelleted at 15000xg for 10 minutes at 4°C. 1.5 μl of α-c-myc (9E10 monoclonal, Covance) antibody was added to equal OD_{260} units of sample supernatants and rocked for 1 hour at 4°C. 30μl of BSA-blocked protein A agarose beads (Invitrogen) were then added, and rocking was continued for an additional 1hr. Beads were washed 3x with lysis buffer and eluted in 50μl of 1x Laemmli sample buffer without β-mercaptoethanol. Proteins were run on a 12% SDS-PAGE gel and transferred to nitrocellulose for western blotting as described in section 2.1.9 using α-c-myc, α-Sqt1p (B. Trumpower) or α-Rpl12p (J. Ballesta).

For immunoprecipitations from W303 coexpressing GFP-tagged Rpl10N187p with Sqt1p wild-type or various Sqt1p loss of function alleles in figure 3.4, cultures were grown overnight in appropriate raffinose-containing medium. They were diluted to OD_{600} ~0.15, incubated 4 hours and induced with galactose for 3 hours. Cells were collected, extracts made and immunoprecipitation steps carried out as above except 5μl of α-GFP antibody (Santa Cruz Biotech) were used in place of α-c-myc. Samples were run on an 8% gel and western blotting carried out as for figure 3.1 above using α-c-myc or α-GFP.

For immunoprecipitations from the *RPL10::3xHA* strain co-expressing full-length Rpl10p or Rpl10N64p each with myc-tagged Nmd3p in figure 3.8, cultures were grown overnight and diluted to OD_{600}~0.15 in raffinose containing medium. A control culture with empty vectors was treated the same. After incubation for 3 hours, galactose was added to induce *RPL10* expression for 6 hours. Cultures were treated with 150μg/ml cycloheximide and immediately poured into centrifuge tubes containing ice. Cells were

pelleted and frozen at -80°C. All immunoprecipitation steps were carried out as for figure 3.1, however the lysis buffer also contained 50mM NaCl and 1mM $MgCl_2$. Primary antibodies used in western blotting were α-c-myc, α-Rpl12p or α-HA (16B12 monoclonal, Covance).

2.1.4 Indirect immunofluorescence

Indirect immunofluorescence was performed as described previously (Ho and Johnson, 1999). Cell culture conditions are described in figure legends. Cultures were fixed in the presence of 3.7% formaldehyde for 30 minutes. The cells were washed twice in KSorb buffer (1.2M sorbitol, 0.1M KPO_4 pH6.6). Yeast lytic enzyme (Zymolyase T100) was added to cultures at 0.1mg/ml followed by 10mM final concentration DTT and cells were incubated at 30°C for 20 minutes to spheroplast cells. Following digestion, cells were washed twice with KSorb plus 1mM PMSF and resuspended in 30μl of the same buffer. 15μl of cell suspension was aliquoted onto a poly-lysine coated multi-well slide. Excess liquid was aspirated after 2 minutes. Cells were permeabilized in cold methanol for six minutes followed by treatment with cold acetone for 30 seconds. The slide was allowed to air-dry completely. Cells were blocked in PBS plus 1% BSA for 30 minutes. Primary antibody (α-c-myc, 9E10 from Covance) was added to cells at a 1:1000 dilution in PBS plus 1% BSA and incubated four hours in a damp chamber. Cells were washed three times in PBS plus 1% BSA followed by incubation with Cy2-conjugated goat anti-mouse antibody (Jackson IRL) at a 1:500 dilution in PBS plus 0.1% BSA for one hour in a damp chamber. Cells were again washed three times in PBS plus 0.1% BSA. DNA was stained by adding 1μg/ml of DAPI in PBS plus 0.1% BSA to cells for 1 minute and washing three times with the same buffer without DAPI. Cells were mounted by adding 2.5 μl of AquaPolymount (Poly Biosciences) to each well and attaching a coverslip. Fluorescence was visualized on a Zeiss Axiophot microscope fitted

with a X100 objective lens and a Princeton Electronics Micro-MAX charge-coupled device camera controlled with the IPLab Spectrum P software package from Signal Analytics Corp or on a Nikon E800 microscope fitted with a X100 objective and a Diagnostic Instruments SPOT II camera controlled with SPOT software. Images were prepared using Adobe Photoshop 5.0.

2.1.5 In vivo microscopy

GFP visualization was adapted from a method described previously (Stage-Zimmermann, Schmidt et al. 2000). Culture conditions are given in corresponding figure legends. Cultured cells were fixed with 1:9 volume of 37% formaldehyde for 40 minutes. The cells were washed two times with 0.1M potassium phosphate pH 6.6 and resuspended in Ksorb buffer (0.1M potassium phosphate pH6.6, 1.2M sorbitol). 0.05% Triton X-100 was added to permeabilize cells for 4 minutes and 1μg/ml DAPI was added to stain nuclei. After 2 minutes, cells were washed twice with PBS and visualized as described for indirect immunofluorescence.

2.1.6 LMB treatment

For LMB treatment in figure 3.5, overnight cultures were diluted to an OD_{600} of ~0.1 and incubated for 6 hours at 30°C. They were then concentrated 10-fold in fresh medium. LeptomycinB (LMB) (M. Yoshida) was added at a final concentration of 0.1μg/ml and cultures were incubated an additional 20 minutes before fixation, antibody staining and visualization as described for indirect immunofluorscence.

2.1.7 Growth assays

For growth comparisons, saturated cultures were either plated from ten-fold serial dilutions or streaked onto appropriate medium as indicated in corresponding figures. Conditions for growth are also given in respective figures.

2.1.8 Polysome analysis

For sucrose density gradients in figure 3.7, cultures of either wild-type *SQT1* or *sqt1* ts mutant strains were grown two overnights in raffinose. Cultures were diluted to OD_{600} ~0.1 into 100ml of fresh raffinose-containing medium and incubated at 25°C. At OD_{600} ~0.25, cultures were shifted to 37°C for 1hr. *RPL25-GFP* expression was induced by the addition of galactose and incubation at 37°C was continued for 2 hours more. Cycloheximide (150μg/ml final concentration) was then added to each culture followed by a 20-minute incubation on ice. Cells were pelleted and frozen at –80°C until use. All of the following steps were carried out on ice or at 4°C. Culture pellets were washed with two ml of polysome lysis buffer (10mM Tris-HCl pH 7.6, 100mM KCl, 10mM $MgCl_2$, 6mM BME, 150μg/ml cycloheximide, 1mM PMSF and 1μg/ml each of leupeptins and pepstatin A). Cells were pelleted, resuspended in one volume of the same buffer and broken open by glass bead lysis (4x30 second cycles each separated by 1 minute intervals on ice). Insoluble material was pelleted by centrifugation at 15000xg for 10min. 9 OD_{260} units of supernatant were loaded onto linear 7-47% sucrose gradients in polysome lysis buffer without protease inhibitors. After a 2.5 hour spin at 40,000 rpm in a Beckman SW40 rotor, gradient fractions were collected on an ISCO density gradient fractionator continuously measuring A_{254}. Fractions were precipitated by the addition of 10% trichloroacetic acid, a 30-minute incubation on ice and centrifugation at 15,000 rpm for 10 minutes. After resuspension in 50μl of 1x Laemmli buffer, fractions were run on 12% SDS-PAGE gels and western blotting performed as described in section 2.1.9 using either α-GFP or α-Rpl12p antibodies.

2.1.9 Western blotting

After separating proteins on SDS-PAGE gels, they were electrophoretically transferred to nitrocellulose membranes. After blocking in TBS (10mM Tris-HCl pH 8.0,

150mM NaCl) plus 3% powdered milk for 30 minutes, the membranes were incubated four hours with primary antibody and 30 minutes with secondary antibody each in TBST (TBS + 0.1 Tween 20). Primary antibodies used are given in respective figure legends and/or methods section. Blots were developed for visualization using standard colorimetric (alkaline phosphatase-conjugated secondary) or chemiluminescent (horseradish peroxidase-conjugated secondary) methods.

2.2 MATERIALS AND METHODS FOR CHAPTER 4

2.2.1 Strains, plasmids and media

The strains used in Chapter 4 are listed in Table 2.3. The *NMD3-GFP* genomic fusion was made by homologous recombination as described (Longtine, McKenzie et al. 1998). The oligonucleotide primers 5'-AGAAGATGGAGTCGAGAACACACCCGTTGAATCTCAGCAGCGGATCCCCG GGTTAATTAA and 3'-ACTGAAATGCTAGTGTTTGTTAAGAGTATATACTACTCTCGAATTCGAGC TCGTTTAAAC were used in PCR to amplify plasmid pFA6a-KanMX6-GFP(S65T). The PCR product was transformed into the wild-type haploid CH1305. Geneticin-resistant transformants were selected, and integration was confirmed by PCR and fluorescence microscopy to yield the strain AJY1708. AJY1548, a haploid strain containing a point mutation in genomic *CRM1* that renders it sensitive to the drug LeptomycinB (LMB), was produced from the same integration and cross used to isolate AJY1539 in Section 2.1.1. AJY1708 was then crossed with AJY1548, and the resulting heterozygous diploid was sporulated to give the spore clone AJY1705 (*NMD3-GFP crm1[T539C]-HA*). An *rpl10::KanMX4* haploid (Research Genetics) containing pDEGQ2 (*GAL1-10::RPL10*) was mated with AJY1705 to make AJY1836 (*NMD3-*

GFP::KanMX6 crm1[T539C] rpl10::KanMX4 (pDEGQ2)). The following scheme was used to make AJY1657 (*rpl10[G161D]*). *Rpl10[G161D]* in the integrating vector pRS406 was made by three-part ligation. The 5'-portion of *RPL10* was amplified by PCR using AJO264, 5'-CGCGGATCCGAAACTAGTTAGCAC, and the mutagenic primer 5'-GCCTGATCAGGGAACTTGTATCTGG. The 3'-portion of *RPL10* was amplified using the mutagenic primer 5'-CTGCCTGATCAACAAAAGATTATTTTGTC and AJO268, 5'-CGCGGATCCTACCCAACATGCTGAAC. The mutagenic primers introduced the G161D mutation as well as a silent BclI site. The PCR products were digested with SpeI and BclI (5'-product) and BclI and HindIII (3'-product) and ligated into pAJ735 digested with SpeI and HindIII to give pAJ736. pAJ735 was made by amplifying *RPL10* from CH1305 genomic wild-type DNA using AJO264 and AJO268, digesting with BamHI, filling in the ends and ligating into PvuII-cut pRS406. *RPL10* alleles were confirmed by sequencing. pAJ736 was digested with BsaB1 and transformed into wild-type CH1305. Ura^+ transformants were screened by PCR and BclI-digestion for integration of *rpl10[G161D]*. Correct integrants were mated to the wild-type strain AJY1168 (Research Genetics). Pop-outs were selected on 5FOA-containing media and screened for retention of the *rpl10[G161D]* allele by PCR and BclI digestion. Heterozygous diploids were then sporulated and tetrads dissected to give AJY1657. AJY1440 (*rpl10[F85S]*) was made as follows. *rpl10* was amplified from AJY1320 (*grc5ts942*) using 5' oligo AJO264 and 3' oligo AJO265 (CGCCCATGGCTACCCAACATGCTGAAC). This PCR product was transformed into AJY1435 (*rpl10::KanMX4*/pDEGQ2) and cells were plated onto YPD. At the same time, the PCR product was sequenced and found to contain the single F85S point mutation. After two days of growth on YPD at 25°C, colonies were replica plated to 5FOA to select for loss of the *URA3* plasmid. Out of those colonies that grew on 5FOA, eight were

streaked onto YPD-G418 to select for loss of resistance due to replacement of *rpl10::Kan* with *rpl10[F85S]*. Out of these, the clone providing the tightest temperature sensitive phenotype was determined to be *rpl10[F85S]* by sequencing

TABLE 2.3 Strains used in Chapter 4.

Strain	Genotype	Source or Reference
W303 (wt)	*MATa leu2-3,112 his3-11 ura3-1 trp1-1 ade2-1 can1-100 SSD1-d*	J. Warner
DEH221+	*MATα qsr1Δ1::HIS3 ade2-1 trp1-1 leu2-3,112 ura3-1 can1-100* (pDEGQ2)	(Eisinger, Dick et al. 1997)
CH1305	*MATa ade2 ade3 leu2 lys2-801 ura3-52*	(Kranz and Holm 1990)
AJY1320	*MATa ade2-101 his3-200 tyr1 ura3-52 grc5ts942*	(Zuk, Belk et al. 1999)
AJY1134	*MATα pep4-3 prb1-1122 ura3-52 leu2-3,112 reg1-501 gal1*	(Hovland, Flick et al. 1989)
AJY1435	*MATa lys2Δ0 met15Δ0 his3Δ1 leu2Δ0 ura3Δ0 rpl10::KanMX4* (pDEGQ2)	this section
AJY1440	*MATa lys2Δ0 met15Δ0 his3Δ1 leu2Δ0 ura3Δ0 rpl10[F85S]*	this section
AJY1548	*MATα leu2 ura3 his3 met15 crm1[T539C]*	this section
AJY1640	*MATα sqt1::KanMX4 met15Δ10 leu2Δ0 ura3Δ0 his3Δ1* (pAJ1065)	section 2.1.1
AJY1657	*MATa ura3 leu2 rpl10[G161D]*	this section
AJY1705	*MATa leu2 ura3 NMD3-GFP::KanMX6 crm1[T539C]*	this section
AJY1708	*MATa ade2 ade3 leu2 lys2-801 ura3-52 NMD3:GFP::KanMX6*	this section
AJY1836	*MATa NMD3-GFP::KanMX6 crm1[T539C] rpl10::KanMX4 ura3 leu2* (pDEGQ2)	this section

The plasmids used in Chapter 4 are listed in Table 2.4. Unless otherwise noted, myc denotes 13 tandem copies of the c-myc epitope. The myc-tagged *NMD3* loss of function mutants V340D (pAJ1299), H108P (pAJ1295), L82P (pAJ1296) and H108R (pAJ1297) were isolated from a PCR mutagenized library by screening for 5FOA-sensitive clones in an *nmd3::HIS3* strain. pAJ410 (*NMD3*) was made by moving the SmaI-HindIII fragment from pAJ123 and ligated into pRS425. pAJ1002 (*NMD3-myc*) was made by moving a BglII-HindIII fragment from pAJ538 and placing it into the same sites of pAJ412 (*NMD3-myc*). To make pAJ415 (*NMD3[L291F]*) and pAJ1070 (*NMD3[L291F]-myc*), inverse PCR was carried out with the 5' oligo AJO303 (GCGGATCTGTCACCATCT) and the mutagenic 3' oligo AJO304 (GGTTTGGAAAGTAGTCGGGTCCATAAACTG) to incorporate the mutations underlined into the *NMD3* ORF (the second mutation, which is silent, was used to eliminate an internal BamHI site). The BglII to MscI fragment containing the L291F mutation was then used to replace the corresponding fragment of pAJ123 and pAJ1002 to give pAJ415 and pAJ1070, respectively. pAJ1069 (*NMD3[L291F]AAA-GFP*) was made by three-part ligation of BglII-PacI and PacI-HindIII fragments from pAJ755 (*NMD3-GFP*) and BglII-HindIII cut pAJ415. To make pAJ754 (*NMD3AAA-GFP*), 5' oligo AJO247 (CGGAATTCACTGTCCAGTTTATGGATC) and 3' oligo AJO389 (5'GCAAGCTTAGATTAATGTCATT

TCATCTGCCTCGTCGGCTAATTCATCAGCGTTGATTT) were first used in PCR to amplify nt843-1516 of *NMD3* while introducing missense mutations as underlined. This product was amplified with AJO247 and 5' oligo AJO413 (GGCAAGCTTAGTTAATTAA

CCCGGGGATCCGCTGCTGAGATTCAACGGGTGTGTTCTCGACTCCATC

TTCTAATGTCATTTCAT). The product was cut with BglII-PacI and ligated into BglII-

PacI cut pAJ535 to make pAJ752. GFP, amplified from pFA6a-GFP(S65T)-KanMX using 5'-oligo AJO230 (AGAAGATGGAGTCGAGAACACACCCGTTGAATCTCAGCAGCGGATCCCCG GGTTAATTAA) and AJO307 (GCGAAGCTTGGCCTCGAAACGTGAGTC) was cut with PacI-HindIII and ligated into the same sites of pAJ752 to give pAJ754. pAJ690 was made by inserting *NMD3* on a XhoI(filled in)-HindIII fragment from pAJ118 into the SmaI-HindIII sites of pEG(KT) (Mitchell, Marshall et al. 1993). pAJ698 was derived from pAJ690 and contains an *nmd3* allele deleted of 194 C-terminal amino acids. PAJ1291, pAJ1292 and pAJ1293 were made by subcloning fragments from pAJ1070, pAJ1315 and pAJ1299, respectively, into pAJ698. pAJ1287 (*NMD3[I112T,I362T]-GFP*) was constructed by ligating the BglII/PacI and PacI/HindIII fragments from pAJ582 into the BglII and HindIII sites of pAJ1315. pAJ1109 (*GAL10::myc-LSG1[K349T]*) and pAJ1131 (*GAL10::myc-LSG1[N173Y,L176S]*), each with *LSG1* N-terminal single myc-tags, were isolated from an *LSG1* dominant negative screen using randomly mutatgenized PCR products of the *LSG1* ORF (West and Johnson, unpublished). pAJ1108 (*GAL10::LSG1[K349T]-myc]*) was made by moving the BsaBI-SalI fragment from pAJ903 (*LSG1-myc*) and ligating it into pAJ1109. pAJ1105 (*GAL10::LSG1[N173Y,L176S]-myc*) was made by moving the NcoI-BsaBI fragment from pAJ1131 and ligating it into the same sites of pAJ1108. pAJ1107 (*GAL10::LSG1-myc*) was made by cutting a NcoI-BsaBI fragment from pAJ879 (*myc-LSG1*) and ligating it into pAJ1108 cut with the same enzymes. pAJ879 was made by moving the NcoI-NheI fragment from pAJ289 (*myc-LSG1*) and ligating it into NcoI-NheI digested pAJ368 (*GAL10::NMD3Δ100*).

TABLE 2.4 Plasmids used in Chapter 4.

Plasmid	Relevant markers	Source or Reference
pASZ11-Rpl25eGFP	ADE2-CEN (*RPL25-eGFP*)	(Gadal, Strauss et al. 2001)
pSQTMYC1	LEU2-2μ (*SQT1-myc*)	(Eisinger, Dick et al. 1997)
pDEGQ2	URA3-CEN (*GAL1-10$_{UAS}$-QSR1*)	(Eisinger, Dick et al. 1997)
pDEGQ187	URA3-CEN (*GAL1-10$_{UAS}$-qsr1-187Δ*)	(Eisinger, Dick et al. 1997)
pAJ123	LEU2-CEN (*NMD3)*	(Ho and Johnson 1999)
pAJ289	LEU2-CEN (*myc-LSG1*)	(Kallstrom, Hedges et al. 2003)
pAJ410	LEU2-2μ (*NMD3*)	this section
pAJ415	LEU2-CEN (*NMD3[L291F]*)	this section
pAJ538	LEU2-CEN (*NMD3-myc*)	(Ho, Kallstrom et al. 2000)
pAJ582	LEU2-CEN (*NMD3-GFP*)	section 2.1.1
pAJ689	URA3-2μ (*GAL10::GST*)	this section
pAJ690	URA3-2μ (*GAL10::GST-NMD3*)	this section
pAJ752	LEU2-CEN (*NMD3AAA-myc*)	this section
pAJ754	LEU2-CEN (*NMD3AAA-GFP*)	this section
pAJ755	URA3-CEN (*NMD3-GFP*)	this section
pAJ879	URA3-CEN (*GAL10::myc-LSG1*)	this section
pAJ1002	URA3-CEN (*NMD3-myc*)	this section
pAJ1069	LEU2-CEN (*NMD3[L291F]AAA-GFP*)	this section
pAJ1070	LEU2-CEN (*NMD3[L291F]-myc*)	this section
pAJ1100	URA3-2μ (*GAL10::RPL10-GFP*)	section 2.1.1
pAJ1105	LEU2-CEN (*GAL10::LSG1[N173Y,L176S]-myc*)	this section
pAJ1107	LEU2-CEN (*GAL10::LSG1-myc*)	this section
pAJ1108	LEU2-CEN (*GAL10::LSG1[K349T]-myc*)	this section
pAJ1287	LEU2-CEN (*NMD3[I112T,I362T]-GFP*)	this section
pAJ1291	URA3-2μ (*GAL10::GST-NMD3[L291F]*)	this section
pAJ1292	URA3-2μ (*GAL10::GST-NMD3[I112T,I362T]*)	this section
pAJ1293	URA3-2μ (*GAL10::GST-NMD3[V340D]*)	this section
pAJ1295	LEU2-CEN (*NMD3[H108P]-myc*)	this section
pAJ1296	LEU2-CEN (*NMD3[L82P]-myc*)	this section
pAJ1297	LEU2-CEN (*NMD3[H108R]-myc*)	this section
pAJ1299	LEU2-CEN (*NMD3[V340D]-myc*)	this section
pAJ1315	LEU2-CEN (*NMD3[I112T,I362T]-myc*)	this section
pAJ1316	LEU2-CEN (*NMD3[R113G]-myc*)	this section
pAJ1402	URA3-2μ (*GAL10::RPL10N64-GFP*)	this section

2.2.2 Isolation of *NMD3* suppressor alleles of *rpl10* mutants

Randomly mutagenized *NMD3* suppressor mutants of *rpl10(G161D)* and *rpl10(F85S)* were made by pooling 20 separate 20 cycle PCR reactions using Taq polymerase (GeneChoice) with 5' oligo AJO106 (GCCGCTCGAGACACCATGGAATTCACACCTATAG), 3'oligo AJO305 (TCCCCCGGGCTGCTGAGATTCAACGGG) and CH1305 genomic DNA as template. The product was co-transformed into AJY1657 (*rpl10[G161D]*) or AJY1440 (*rpl10[F85S]*) along with Bsg1-gapped pAJ538 for *in vivo* homologous recombination. Plasmid-borne suppressors were identified as fast-growing colonies at 35°C. Positive clones were isolated from yeast and transformed into *E. coli* to obtain pAJ1315 (*NMD3[112T,I362T]-myc*) and pAJ1316 (*NMD3[R113G]-myc*). Several other suppressor alleles were isolated and sequenced as well and are listed in Appendix B.

2.2.3 In vivo microscopy

Preparation and visualization of cells containing GFP fusion proteins was carried out as described in section 2.1.5. Cells were cultured as described in respective figure legends.

2.2.4 LMB treatment

For LMB treatment in figure 4.2, overnight cultures in galactose were diluted to an OD_{600} of ~0.1 and incubated for 4 hours. Cultures were divided in half and 2% glucose was added to one half while the other was left in galactose. Cultures were incubated 4 hours more before being concentrated 10-fold in fresh medium. LeptomycinB (LMB) (M. Yoshida) was added at a final concentration of 0.1μg/ml and cultures were incubated an additional 20 minutes before fixation and visualization as described for in vivo microscopy.

2.2.5 Polysome analysis

For sucrose density gradients in figure 4.3, cultures containing galactose inducible alleles of either *RPL10* or *SQT1* as the sole source of Rpl10p or Sqt1p proteins, respectively, were grown and collected as described in the figure legend. Cells were pelleted and frozen at –80°C until use. All other steps, including gradient fractionation and SDS-PAGE analysis, were carried out as described in section 2.1.8. Western blotting was carried out as described in section 2.2.11 using α-Nmd3p or α-Rpl12p.

For gradients in figure 4.7, cultures of AJY1657 (*rpl10[G161D]*) containing empty vector or various *NMD3* alleles were grown two overnights at 25°C and diluted to OD_{600}~0.15 in 150ml of fresh medium. After incubating at 25°C until cell density reached OD_{600}~0.3, cultures were shifted to 37°C and incubated an additional 3 hours. Cells were treated with cycloheximide, pelleted and frozen until use as described above, except gradient fractions were not collected.

2.2.6 Growth assays

Growth assays were carried out as in section 2.1.7 at the temperatures and conditions given in respective figure legends.

2.2.7 Purification of GST-Nmd3 proteins

GST-fusion proteins were expressed from pAJ690 (*NMD3*), pAJ1291 (*NMD3[L291F]*), pAJ1292 (*NMD3[I112T,I362T]*) or pAJ1293 (*NMD3[V340D]*) in strain AJY1134 (*reg1-501*) and purified from yeast as described previously (Ho, Kallstrom et al. 2000). Overnight cultures were diluted into 500ml of glucose-containing medium to give OD_{600}~0.10. Cultures were incubated for 4 hours before galactose was added to induce GST-Nmd3p expression for 6 hours. Cells were collected by centrifugation and frozen at -80°C until use. Pellets were thawed on ice and washed in

two volumes of lysis buffer (20mM Tris pH 7.6, 500mM LiCl, 1mM EDTA, 10% glycerol, 1mM DTT and protease inhibitors). After washing, cells were resuspended in 1 volume of ice-cold lysis buffer and 3/4 volume of glass beads was added. Cells were broken open by vortexing at highest setting for 5 cycles of 1 minute each with at least 1 minute intervals on ice between cycles. Extracts were transferred to eppendorf tubes on ice and supplemented with 1mM more PMSF (protease inhibitor). 1% triton was then added and extracts were rocked at 4°C for 1 hour to aid in solublization of proteins. After rocking, extracts were clarified by two centrifugation cycles of 10 minutes each at 15,000 rpm and 4°C. For binding free GST-Nmd3p, 1/10 bed volume of Glutathione Sepharose 4B (Amersham) was added to clarified extracts and rocked for two hours at 4°C. After rocking, these mixtures were placed over a BioRad micro-spin chromatography column and extract was eluted. The resin was washed three times with ten volumes of ice-cold high-salt wash buffer (20mM Tris-HCl pH 7.6, 500mM LiCl, 1mM EDTA and protease inhibitors). The column was then washed two times with ten volumes of low-salt wash buffer (20mM Tris-HCl pH 7.6, 100mM NaCl, 1mM EDTA and protease inhibitors). After the wash buffers had fully eluted, the column was capped and one bed volume of glutathione elution buffer (50mM Glutathione and 50mM Tris-HCl pH 8.0) was added. The column was then allowed to equilibrate at room-temperature for 20 minutes prior to GST-Nmd3p elution. The column was uncapped and the eluate was collected as fraction 1. Immediately, another bed volume of elution buffer was added and eluted as fraction 2. This continued until five total fractions of one bed volume each were collected. Fractions containing GST-Nmd3p were determined through SDS-PAGE analysis. Once identified, these fractions were pooled and dialyzed against 100 volumes of storage buffer (10mM Tris-HCl pH 7.6, 50mM KCl and 6mM BME) with two subsequent buffer exchanges overnight at 4°C. Final protein concentrations

were measured using the Bradford assay as well as by comparison on SDS-PAGE gels with proteins of known concentrations.

2.2.8 Purification of free 60S subunits

Purified ribosomal subunits were isolated in a method similar to that described in (Ho, Kallstrom et al. 2000). Several liters of W303 (wild-type) were grown to mid-log phase in YPD and collected by centrifugation in the absence of the translation inhibitor cycloheximide. Pellets were frozen at -80°C prior to subunit isolation. Pellets were thawed on ice and washed in two volumes of lysis buffer (20mM Tris-HCl pH 7.6, 500mM KCl, 10mM $MgCl_2$, 6mM β-mercaptoethanol (BME) and protease inhibitors). Pellets were resuspended in one volume of ice-cold lysis buffer. Cells were broken open by glass-bead lysis by vortexing for 5 cycles of one minute each with one-minute intervals on ice between cycles. Extracts were clarified twice by centrifugation at 15,000 rpm at 4°C. Clarified extracts were placed at 4°C for 2 hours in order to allow dissociation of 80S ribosome couples and polysomes into free 40S and 60S subunits. Up to 350 OD_{260} units of extract were then layered onto linear 10-40% sucrose gradients (SW28) made up in lysis buffer (without protease inhibitors). Gradients were centrifuged at 20,000 rpm in a SW-28 rotor in a Beckman ultracentrifuge for 17 hours at 4°C. After centrifugation, gradients were fractionated using an ISCO gradient fractionator with continuous measuring of A_{280} signal to isolate 40S and 60S containing peak fractions. Multiple fractions from several centrifuge tubes were pooled and dialyzed overnight at 4°C against 100 volumes of storage buffer (10mM Tris-HCl pH 7.6, 10mM $MgCl_2$, 50mM KCl and 6mM BME). The storage buffer was exchanged twice during the course of dialysis.

2.2.9 Composite gel assays of in vitro binding

Composite gels were made essentially as described previously (Dahlberg and Grabowski 1990). A buffer containing 25mM Tris-OAc pH 7.6, 60mM KOAc, 1mM $MgOAc_2$, 0.4% Dimethylpropionitrile and 2.5% (29:1) bis-acrylamide (final concentrations) was made up with continual mixing. Separately, 0.5% (final concentration) agarose was melted in 23.5 ml of ddH_2O. Once the agarose was cooled to about 60°C, it was added to the acrylamide mixture with stirring to give a final volume of 30ml. 80ul of 10% APS was then added to the mixture with brief stirring, followed by syringe injection into Hoefer 8x10x0.0015cm gel forms containing 10-well combs.

For *in vitro* reconstitutions, increasing amounts of each GST-Nmd3 protein (see figure 4.9, 1X~30ng) were mixed with 2µl (0.018 OD_{260} U) of purified free 60S subunits (prepared in section 2.2.8) in 10 ul of low Mg^{2+} TKM buffer (25mM Tris-OAc pH 7.6, 60mM KOAc and 1mM $MgOAc_2$) plus protease inhibitors on ice. After 30min of incubation at room temperature samples were placed back onto ice and 5X sucrose loading dye (TKM + 5% sucrose + bromophenol blue) was added to each reaction. During sample prep, gels were pre-run at 60V for 1hr in low Mg^{2+} TKM buffer with continual cooling at 4°C. After a fresh buffer change, samples were loaded and run with cooling for 4 hours at 60V with a second fresh buffer change after 2 hours. The gels were transferred to nitrocellulose and western blotting performed using α-GST (Sigma) as described in section 2.2.11. The post-transfer gels were stained with ethidium bromide to visualize 60S subunit position.

2.2.10 Immunoprecipitations

Co-immunoprecipitations and subsequent sample analyses of Nmd3-myc proteins in figure 4.10 were carried out as described for myc-tagged Rpl10p fragments in section 2.1.3. Cultures of wild-type strain W303 containing various myc-tagged *NMD3*

constructs or an empty vector control were collected in mid-log phase and frozen at -80°C until use. The lysis buffer used at all steps consisted of the following: 20mM Tris-HCl pH7.5, 150mM NaCl, 10% glycerol, 0.1% NP40, 1mM $MgCl_2$ and protease inhibitors. Western blotting was carried out using α-c-myc or α-Rpl8p primary antibodies as described in section 2.2.11.

For co-immunoprecipitations in figure 4.11, overnight cultures of wild-type strain CH1305 containing various combinations of galactose inducible *LSG1* and *RPL10* dominant negative alleles or empty vector controls were diluted to OD_{600}~0.15 in raffinose-containing medium. Cultures were incubated for 5 hours prior to the addition of galactose to induce protein expression. After 3 hours, cultures were pelleted and frozen at –80°C until use. All immunoprecipitation and sample analysis steps were carried out as above, however the lysis buffer contained 50mM rather than 150mM NaCl.

2.2.11 Western blotting

After running SDS-PAGE gels, proteins were transferred to nitrocellulose and western blotting performed as described in section 2.1.9 using antibodies indicated in respective figure legends and/or methods sections.

For composite gels, proteins were electrophoretically transferred to nitrocellulose in 25mM Tris-OAc pH 7.6 buffer after pre-soaking gels and membranes in the same buffer containing 0.1% SDS for 10 minutes. After transfer, western blotting was performed on the membrane as described above for SDS-PAGE analysis.

2.3 MATERIALS AND METHODS FOR CHAPTER 5

2.3.1 Strains, plasmids and media

The strains used in Chapter 5 are listed in Table 2.5. AJY1849 (*MATa his3 leu2 ura3 Nic96-mRFP::KanMX6 crm1[T539C]*) was made by crossing AJY1539 (*MATα*

leu2 ura3 his3 met15 crm1[T539C]) from section 2.1.1 with AJY1848 (*MATa Nic96-mRFP::KanMX6*), selecting HIS^+ $G418^R$ diploids and isolating haploids that were $G418^R$. These haploids were then tested for the presence of the *crm1[T539C]* allele by PCR.

TABLE 2.5 Strains used in Chapter 5.

Strain	Genotype	Source or Reference
W303 (wt)	*MATa leu2-3,112 his3-11 ura3-1 trp1-1 ade2-1 can1-100 SSD1-d*	J. Warner
CH1305	*MATa ade2 ade3 leu2 lys2-801 ura3-52*	(Kranz and Holm 1990)
AJY529	*MATα his3 leu2 ura3 nmd3::TRP1* (pAJ112)	(Ho and Johnson 1999)
AJY1848	*MATa Nic96-mRFP::KanMX6*	(Huh, Falvo et al. 2003)
AJY1849	*MATa his3 leu2 ura3 Nic96-mRFP::KanMX6 crm1[T539C]*	this section

The plasmids used in Chapter 5 are listed in Table 2.6. Unless otherwise noted, myc denotes 13 tandem copies of the c-myc epitope. Also, XNG represents an Xrn1-NLS(SV40)-GFP fusion. pAJ670 (*XNG*) was made by moving the NheI-HindIII fragment from pAJ667 (*XNG*) and placing it into NheI-HindIII digested pAJ237 (*XNG*) to provide a compatible site 3' of GFP to introduce Nmd3p NES fragments. pAJ665 (*XNG-NES(489-501)*) was made by kinasing oligos AJO364 (GATCCCCACAAATCAACATTGATGAATTATTGGACGAGTTAGATTA) and AJO365 (AGCTTAATCTAACTCGTCCAATAATTCATCAATGTTGATTTGTGGG) and dropping them into BamHI-HindIII cut pAJ667. An NheI to HindIII fragment was cut from pAJ665 and ligated into pAJ237 cut with the same enzymes to make pAJ671. The PCR product from a reaction using 5' oligo AJO384 (CGCGGATCCGATGAAGACGCTCCACAA), 3' oligo AJO329 (CTGCATCCAGTATACACACCCA) and pAJ123 as template was digested with BamHI-HindIII and ligated into BamHI-HindIII cut pAJ675 (*XNG*) to make pAJ673 (*XNG-NES(485-519)*). pAJ676 (*XNG-NES(485-505)*) was made by placing the PCR product from 5' oligo 3160 and 3' oligo AJO382 (CTAAGCTTAGATTAATGTCATTTCATCTAA) using pAJ673 as template as a NheI-HindIII cut fragment into pAJ675 cut with the same enzymes. pAJ677 (*XNG-NES(AA)*) and pAJ678 (*XNG-NES(AAA)*) were made similarly to pAJ676, but using 3' oligos AJO388 (GCAAGCTTAGATTAATGTCATTTCATCTAACTCGTCGGCTGCTTCATCAATG) or AJO389 (GCAAGCTTAGATTAATGTCATT TCATCTGCCTCGTCGGCTAATTCATCAGCGTTGATTT), respectively, with each oligo incorporating the missense mutations underlined. Both pAJ583 (*NMD3CΔ50-GFP*) and pAJ584 (*NMD3CΔ100-GFP*) were made the same as pAJ582 in section 2.1.1,

however GFP was cloned into pAJ534 or pAJ535, respectively. pAJ751 (*NMD3AA-myc*) was made by using two sequential PCR steps prior to cloning. First, 5' oligo AJO247 (CGGAATTCACTGTCCAGTTTATGGATC) and 3' oligo AJO388 were used to PCR amplify nt843-1516 of NMD3 using pAJ123 as template. This product was then amplified with AJO247 and 3' oligo AJO413 (GGCAAGCTTAGTTAATTAA CCCGGGGATCCGCTGCTGAGATTCAACGGGTGTGTTCTCGACTCCATC TTCTAATGTCATTTCAT) to add the complete 3' NMD3 ORF. Finally, this product was cut with BglII-PacI and ligated into BglII-PacI cut pAJ535 (*NMD3CΔ100-myc*). pAJ753 (*NMD3AA-GFP*) was made by cutting GFP from pAJ582 with PacI-HindIII and ligated it into PacI-HindIII cut pAJ751. pAJ752 (*NMD3AAA-myc*) was made the same as pAJ751 except the 3' oligo used in the first PCR reaction was AJO389. All other steps were the same. GFP was cut from pAJ582 with PacI-HindIII and ligated into PacI-HindIII cut pAJ752 to make pAJ754 (*NMD3AAA-GFP*). pAJ377 (*NMD3CΔ33-myc*) was made by digesting a PCR product made using 5' oligo AJO245 (CGGAATTCGCTAAGGACGGGTTGGAT), 3' oligo AJO348 (GCACTTAATTAACCCGGGCTGCAGCTCGTCTTCATCCATTTC) and pAJ538 as template with BglII-PacI and ligating into BglII-PacI cut pAJ538. pAJ378 (*NMD3ΔCC[418-468]-myc*) was made by digesting a PCR product made using 5' oligo AJO349 (CTGCCCGGGAACCGCGAAGCAAATGTA), 3' oligo AJO329 and pAJ538 as template with SmaI and ligating into SmaI cut pAJ535. pAJ414 was made by removing *NMD3-myc* from pAJ408 (*NMD3-myc*) using EheI-HindIII and ligating it into SmaI-HindIII cut pRS416. A BglII-BglII fragment, containing *myc*, was cut from pAJ401(*myc-NMD3*) and ligated into pAJ521 (*nmd3NΔ123*) cut at the same sites to make pAJ515 (*nmd3NΔ123-myc*). pAJ516 (*nmd3NΔ167-myc*) was made the same as pAJ515, but *myc* was ligated into pAJ522 (*nmd3NΔ167*).

TABLE 2.6 Plasmids used in Chapter 5.

Plasmid	Relevant markers	Source or Reference
pAJ112	URA3-2μ (*His_6-NMD3*)	(Ho and Johnson 1999)
pAJ377	LEU2-CEN (*NMD3CΔ33-myc*)	this section
pAJ378	LEU2-CEN (*NMD3ΔCC[418-468]-myc*)	this section
pAJ414	URA3-2μ (*NMD3-myc*)	this section
pAJ515	URA3-2μ (*nmd3NΔ123-myc*)	this section
pAJ516	URA3-2μ (*nmd3NΔ167-myc*)	this section
pAJ534	LEU2-CEN (*NMD3CΔ50-myc*)	(Ho, Kallstrom et al. 2000)
pAJ535	LEU2-CEN (*NMD3CΔ100-myc*)	(Ho, Kallstrom et al. 2000)
pAJ536	LEU2-CEN (*nmd3CΔ120-myc*)	(Ho, Kallstrom et al. 2000)
pAJ537	LEU2-CEN (*nmd3CΔ194-myc*)	this section
pAJ538	LEU2-CEN (*NMD3-myc*)	(Ho, Kallstrom et al. 2000)
pAJ582	LEU2-CEN (*NMD3-GFP*)	section 2.1.1
pAJ583	LEU2-CEN (*NMD3CΔ50-GFP*)	this section
pAJ584	LEU2-CEN (*NMD3CΔ100-GFP*)	this section
pAJ670	URA3-2μ (*XRN1-NLS(SV40)-GFP*)	this section
pAJ671	URA3-2μ (*XNG-NES[489-501]*)	this section
pAJ673	URA3-2μ (*XNG-NES[485-519]*)	this section
pAJ676	URA3-2μ (*XNG-NES[485-505]*)	this section
pAJ677	URA3-2μ (*XNG-NES[AA]*)	this section
pAJ678	URA3-2μ (*XNG-NES[AAA]*)	this section
pAJ690	URA3-2μ (*GAL10::GST-NMD3*)	this section
pAJ751	LEU2-CEN (*NMD3AA-myc*)	this section
pAJ752	LEU2-CEN (*NMD3AAA-myc*)	section 2.2.1
pAJ753	LEU2-CEN (*NMD3AA-GFP*)	this section
pAJ754	LEU2-CEN (*NMD3AAA-GFP*)	section 2.2.1

2.3.2 Composite gel assays of extracts

Composite gels were made as described in section 2.2.9, however they contained 16mM instead of 1mM $MgOAc_2$ as well as 10% glycerol and 150μg/ml cycloheximide. Overnight cultures of wild-type CH1305 without a vector or containing pAJ414 (*NMD3-myc*), pAJ515 (*NMD3NΔ123-myc*) or pAJ516 (*NMD3NΔ167-myc*) were diluted into 10ml of fresh YPD or SC-leu glucose medium, respectively, to give an OD_{600}~0.1. Cultures were incubated for 6 hours prior to treatment with 150 μg/ml of cycloheximide for 20 minutes on ice to arrest translation. Cells were pelleted and frozen at -80°C until use. The following steps were carried out on ice. Pellets were thawed and washed with two volumes of composite buffer (25mM Tris-OAc pH 7.6, 60mM KOAc, 16mM $MgOAc_2$, 150μg/ml cycloheximide and protease inhibitors). After resuspension in one volume of the same buffer, cells were broken open by the addition of 3/4 volume glass beads and vortexing at high speed for 5 x 1 minute cycles each separated by 1 minute intervals one ice. Extacts were clarified by centrifugation at 15,000 rpm at 4°C for 10 minutes. The A_{260} of each clarified extract was taken in order to standardize the concentration of each sample with additional composite buffer. A composite gel was prerun at 50V in TKM running buffer (25mM Tris-OAc pH 7.6, 60mM KOAc, 10mM $MgOAc_2$) for one hour with ice water cooling. Buffer was removed and wells were cleaned of all debris. 5μl of each standardized sample was mixed with 25μl of pre-warmed agarose loading buffer (composite buffer containing 0.5% agarose and bromophenol blue) and immediately loaded into each well. After solidification, pre-chilled TKM buffer was re-added to the gel-running apparatus. The gel was run for 5 hours at 50V with continual ice water cooling. Buffer was exchanged every 1.5 hours during the run. Proteins were transferred to nitrocellulose and western blotting

performed using α-c-myc as described in secion 2.3.9. The post-transfer gel was stained with Coomasie Blue to visualize ribosome positions.

2.3.3 In vivo microscopy

Cultures were grown as indicated in respective figure legends. Cells were fixed and prepared for visualization as described in section 2.1.5.

2.3.4 Purification of GST-Nmd3p

Wild-type GST-Nmd3p protein was purified as described in section 2.2.7.

2.3.5 Purification of free 60S subunits

Purification of free 60S subunits was carried out as in section 2.2.8.

2.3.6 Purification of free 60S subunits in the absence of magnesium

Free 60S subunits were isolated by sucrose density sedimentation in buffer absence of magnesium essentially as decribed in (Dick, Karamanou et al. 1997). A one liter culture of wild-type strain W303 was grown to mid-log phase in YPD and collected by centrifugation in the absence of cycloheximide. Cells were frozen at –80°C until use. Cell lysis was carried out as in section 2.2.8 but in dissociation buffer (10mM Tris-HCl pH 7.6, 500mM KCl, 1mM DTT, 0.2mg/ml heparin and protease inhibitors). Up to 35 A_{260} units of extract were immediately loaded onto linear 10-40% sucrose gradients (SW40) made up in dissociation buffer (without protease inhibitors). Samples were spun at 35,000 rpm for 4 hours at 4°C in a Beckman ultracentrifuge. After centrifugation, gradients were fractionated using an ISCO gradient fractionator with continuous measuring of A_{254} signal to isolate 40S and 60S containing peak fractions. Immediately following collection, fractions were supplemented with 10mM $MgCl_2$ to stabilize subunits. 1/10 of each fraction was TCA-precipitated and samples were run on a 12% SDS-PAGE gel. This was followed by protein transfer to nitrocellulose and western

blotting with α-Rpl5p (D. Brow), α-Rpl10p (B. Trumpower), or α-Rpl12p (J. Ballesta) antibodies as described in section 2.3.9. Multiple free 60S fractions from several centrifuge tubes were pooled and dialyzed overnight at 4°C against 100 volumes of storage buffer (10mM Tris-HCl pH 7.6, 10mM $MgCl_2$, 50mM KCl and 6mM BME). The storage buffer was exchanged twice during the course of dialysis.

2.3.7 Size exclusion chromatography of "stripped" free 60S subunits

The following steps were carried out at 4°C or on ice. Free 60S subunits purified under normal magnesium concentrations (10mM) as described in section 2.2.8 were dialyzed into low magnesium storage buffer (10mM Tris-HC1 pH 7.6, 50mM KCl, 1mM $MgCl_2$ and 6mM BME). At the same time P300 polyacrylamide size exclusion resin (300kDa MWCO, BioRad) was equilibrated with four different "stripping" buffers at 0.1, 0.2, 0.3 or 0.4mM magnesium concentrations. The equilibrated resins were carefully poured into 30ml BioRad columns, one for each magnesium concentration, to a final bed volume of 15ml. Buffer was allowed to flow through the column until the meniscus was at the top of the resin bed. Each column was subsequently washed with 5ml of each respective buffer. Once the last of the 5ml flow-through had just entered the columns, 1.5ml of appropriately pre-treated 60S subunits were added to each resin bed. This pre-treatment of subunits consisted of adding appropriate concentrations of EDTA to bring the free magnesium concentrations in each sample down from 1mM to 0.1, 0.2, 0.3 or 0.4mM, respectively. Immediately after samples were added to columns, the first elution fractions (1.5ml) were immediately collected. Once the sample had fully entered the column, 1ml of "stripping" buffer, at appropriate magnesium concentration, was added and eluted as the second fraction (1ml) from each column. Thereafter, 5ml of the same respective buffer was loaded onto each column and six consecutive 500µl fractions were collected for a total of 8 fractions. Each fraction was immediately supplemented with up

to 10mM magnesium to stabilize subunits. This was followed by running fractions on 12% SDS-PAGE gels, western blotting with α-Rpl5p or α-Rpl10p as described in section 2.3.9 and Coomasie Blue staining of post-transfer gels. Once identified, 60S fractions were combined and exchanged with storage buffer (10mM Tris-HCl pH7.6, 50mM KCl, 10mM $MgCl_2$ and 6mM BME) using Centrex UF-2 (10k MWCO) centrifugal filter units.

2.3.8 Composite gel assays of in vitro binding reactions

The 2.5% polyacrylamide/0.5% agarose composite gel used in figure 5.7 was made as described in section 2.2.9, except the final magnesium concentration was 10mM rather than 1mM. About 150ng of purifed GST-Nmd3p was mixed with about $3X10^{-3}$ A_{260} units of 60S subunits isolated under various conditions, including 10mM magnesium (section 2.3.5), no magnesium (section 2.3.6), or 0.1, 0.2, 0.3, or 0.4mM magnesium (section 2.3.7), on ice. These binding reactions were supplemented with ice-cold TKM buffer (25mM Tris-OAc pH 7.6, 60mM KOAc and 10mM $MgOAc_2$) containing protease inhibitors to bring the total volume of each reaction to 20µl. Reactions were incubated at 25°C for 30 minutes prior to being placed on ice for 15 minutes before the addition of 5X sucrose loading buffer (TKM + 5% sucrose + bromophenol blue). After pre-running the gel in TKM buffer at 60V for 1hr, buffer was exchanged and samples were loaded. Samples were run at 60V for 3.5 hours with buffer exchanges every 1.5 hours. Transfer of proteins to nitrocellulose and western blotting was performed as described is section 2.3.9 using α-GST or α-Rpl1ap.

2.3.9 Western blotting

Composite gels were transferred to nitrocellulose and western blotting performed as described in section 2.2.11. For the membrane in figure 5.7, probing with two different antibodies was carried out as follows. After blocking in 3% milk, the blot was

probed with α-Rpl1ap primary antibody for 4 hours then with horseradish peroxidase-conjugated α-rabbit secondary antibody for 30 minutes. The blot was developed and exposed to x-ray film to capture signal. The membrane was then stripped by incubating at 50°C for 45 minutes in stripping buffer (100mM BME, 2% SDS, 63mM Tris pH6.8). The membrane was reblocked with 3% milk and probed using α-GST primary antibody and horseradish peroxidase-conjugated α-rabbit secondary antibody. GST-Nmd3p signal was visualized as described for Rpl1ap.

2.3.10 Northern blotting

A composite gel was made and samples were run as in section 2.3.9. After electrophoresis, the composite gel and a nylon membrane (Zeta-probe GT, BioRad) were each soaked separately in 0.3X TBE buffer (90mM Tris-borate pH7.6 and 2mM EDTA) for 15 minutes. The addition of 0.1% SDS was made to the gel buffer during this pre-incubation to aid in dissociation of proteins. rRNA was then electrophoretically transferred to the membrane using a BioRad semidry transfer apparatus at 5V for 2 hours. The nylon membrane was briefly washed in 0.3X TBE and UV-crosslinked. The membrane was then incubated in pre-hybridization solution (1mM EDTA, 0.5M Na_2HPO_4 pH7.2, 7% SDS) for 5 minutes at 50°C. The pre-hybridization solution was then changed and denatured [^{32}P] end-labeled oligonucleotide probe specific for 25S rRNA (AJO192 – CCCGCCGTTTACCCGCGCTTGG) was added. The membrane was incubated with probe overnight at 50°C. It was then washed twice with wash buffer #1 (1mM EDTA, 40mM Na_2HPO_4 pH7.2, 5% SDS) and twice with wash buffer #2 (1mM EDTA, 40mM Na_2HPO_4 pH7.2, 1% SDS). Finally, the plastic wrap covered membrane was subjected to autoradiography in order to visualize hybridized radiolabeled probes. To probe for 5S rRNA, the same membrane was stripped by washing twice for 20 minutes each in stripping buffer (0.1X SSC, 0.5% SDS) at 95°C. The membrane was

checked for removal of hot probe and reprobed with a 5S specific oligo (AJO249 – TCTGGTAGATATGGCCGCAACC) as is described for 25S above.

Chapter 3: Molecular characterization of the interaction between Sqt1p and Rpl10p

3.1 INTRODUCTION

The work in this chapter was begun with the intention of testing the model that Rpl10p recruits Nmd3p to the 60S ribosomal subunit in the nucleus. It was suggested that truncated Rpl10 proteins prevent efficient incorporation of full-length Rpl10p into nuclear subunits that, in turn, prevents subsequent Nmd3p binding (Gadal, Strauss et al. 2001). The work presented in this chapter begins with the demonstration that these fragments do not stably associate with subunits but rather sequester Sqt1p, an essential WD-repeat protein that acts as a chaperone for Rpl10p. I then present the biochemical and genetic characterization of the interaction between Rpl10p dominant fragments and Sqt1p. Furthermore, the cellular localization of these proteins was assayed using fluorescent microscopy, and the effects of these proteins on 60S ribosomal subunit export are determined. The chapter concludes with a discussion on the significance of these results in the context of current literature and on what work remains for future investigations.

3.2 BACKGROUND

Rpl10p interacts with the essential WD-repeat protein Sqt1p, identified as a high-copy suppressor of dominant-negative, truncated *RPL10* mutants (Eisinger, Dick et al. 1997). Additionally, Rpl10p shows strong 2-hybrid interaction with Sqt1p and depletion of Sqt1p from cells leads to free 60S subunits deficient for Rpl10p (Eisinger, Dick et al. 1997). From these previous results, it has been suggested that Sqt1p is required for Rpl10p loading onto subunits. Although Sqt1p shows only transient interaction with 60S through sucrose gradient sedimentation, no direct evidence for a role in loading has been

provided. Interestingly, multiple WD-repeat proteins have been found associated with pre-60S particles (Grandi, Rybin et al. 2002). It has been suggested that WD-repeat proteins act as molecular scaffolds to allow binding of other trans-acting factors that may have a more direct role in 60S formation. Thus, it is likely that Sqt1p is needed to stabilize free Rpl10p prior to subunit loading. This function would parallel that observed for the WD-repeat protein Rrb1p that is proposed to be a chaperone for free Rpl3p prior to or during its loading onto pre-60S subunits in the nucleolus (Iouk, Aitchison et al. 2001).

3.3 RESULTS

3.3.1 Rpl10p dominant negative fragments are not stably incorporated into 60S subunits

C-terminal truncations of Rpl10p are dominant lethal when overexpressed (Eisinger, Dick et al. 1997). Previous work alluded to the idea that Rpl10p dominant negative fragments are incorporated into nascent 60S subunits in the nucleus, thus blocking full-length Rpl10p interaction and, subsequently, recruitment of Nmd3p for 60S nuclear export (Gadal, Strauss et al. 2001). In order to test whether these fragments were indeed incorporated into subunits, immunoprecipitations with myc-tagged fragments were performed. Full-length and truncated Rpl10p fragments were expressed from a galactose inducible (*GAL10*) promoter in vivo as fusions to an oligomeric myc epitope and could be immunoprecipitated from extracts (Figure 3.1A). 60S subunits, monitored by western blotting for the ribosomal protein Rpl12p, were efficiently co-immunoprecipitated with full-length Rpl10-myc, but not with Rpl10N187-myc (containing amino acids 1-187), Rpl10N64-myc (containing amino acids 1-64) or with the C-terminal 43 amino acid fragment Rpl10C43-myc (Figure 3.1A). These results indicate that only the full-length protein was stably incorporated into subunits. Thus, the

dominant negative effect of overexpressing these truncated proteins does not appear to arise from their incorporation into subunits, thereby blocking subsequent assembly events.

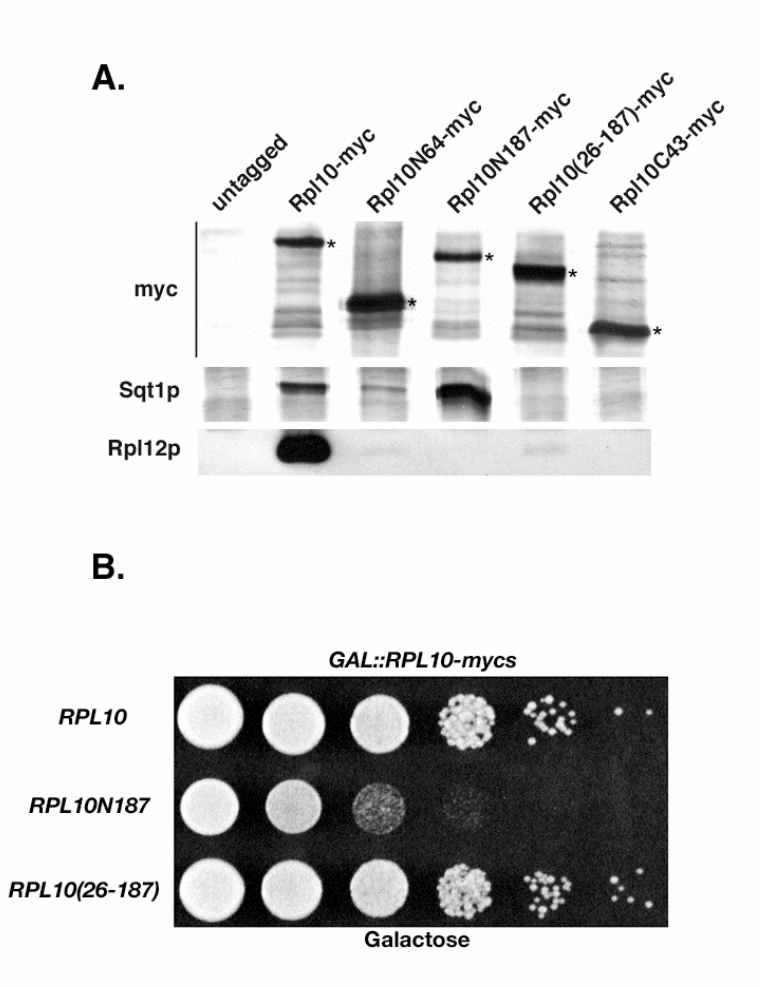

Figure 3.1 Co-immunoprecipitation of proteins associated with Rp10p dominant negative fragments and relief of the dominant negative growth phenotype by deletion mapping.

(A) Extracts were prepared from strain W303 (wt) transformed with pAJ792 (*GAL10::RPL10-myc*), pAJ793 (*GAL10::RPL10N187-myc*), pAJ794 (*GAL10::RPL10C43-myc*), pAJ795 (*GAL10::RPL10N64-myc*), pAJ1056 (*GAL10::RPL10[25-187]-myc*) or pAJ24 (empty vector) and immunoprecipitations performed as described in Chapter 2. The proteins associated with the affinity-purified complexes were separated on a 12% SDS-PAGE gel and transferred to nitrocellulose for western blotting of myc-tagged Rpl10p fragments, Sqt1p or Rpl12p, as a ribosomal marker. Asterisks indicate positions of various myc-tagged Rpl10p alleles. (B) 10X serial dilutions of W303 containing pAJ792, pAJ793 or pAJ1056 were spotted onto a SC-leu galactose plate and incubated 3 days at 30°C.

3.3.2 Localization of Rpl10p C-terminal truncations

If Rpl10p fragments blocked recruitment of Nmd3p to subunits in the nucleus, these fragments would be expected to be nuclear. To see if myc-tagged Rpl10p fragments accumulated in the nucleus, the localization of full-length and truncated forms of Rpl10p was observed by indirect immunofluorescence (IF). The first 64 N-terminal amino acids of Rpl10p are highly basic and have been shown to localize GFP to the nucleus, suggesting the presence of an NLS (Gadal, Strauss et al. 2001). Because the amino terminus of Rpl10p is predicted to be buried in the interface of Rpl10p and the 60S subunit (Ban, Nissen et al. 2000), the NLS would be masked in the assembled subunit. Surprisingly, none of the myc-tagged proteins, including Rpl10N64p, accumulated in the nucleus after three hours of expression (Figure 3.2A).

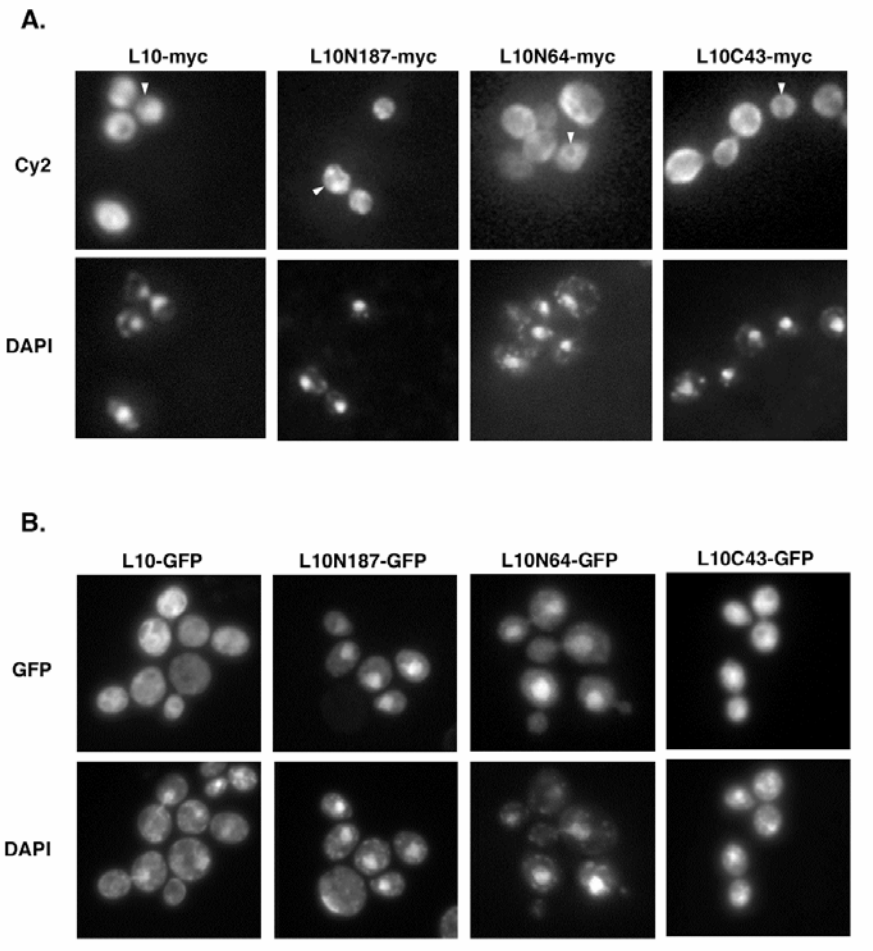

Figure 3.2 Localization of Rpl10p fragments.

Cultures of strain W303 (wt) transformed with either (A) pAJ792 (*GAL10::RPL10-myc*), pAJ793(*GAL10::RPL10N187-myc*), pAJ794 (*GAL10::RPL10C43-myc*) or pAJ795 (*GAL10::RPL10N64-myc*) or (B) pAJ796 (*GAL10::RPL10-GFP*), pAJ797 (*GAL10::RPL10N187-GFP*), pAJ798 (*GAL10::RPL10C43-GFP*) or pAJ799 (*GAL10::RPL10N64-GFP*) were grown overnight in SC-leu raffinose medium and diluted to OD_{600} ~0.3 in fresh medium. After 4 hours, galactose was added and the cultures were grown an additional 3 hours. Cells were fixed and treated for microscopy as described in Chapter 2. Arrowheads point to nuclei in A.

To confirm the results reported with GFP-tagged Rpl10N64 (Gadal, Strauss et al. 2001), the localization of GFP-tagged proteins was also examined. As previously reported, GFP-tagged Rpl10N64 was predominantly nuclear (Figure 3.2B). However, both GFP-tagged Rpl10N187 and Rpl10C43 also showed significant nuclear accumulation while full-length Rpl10p was cytoplasmic. The nuclear accumulation of Rpl10C43 is particularly surprising given that a putative NLS is suggested to exist only in the N-terminus of the full-length protein (Gadal, Strauss et al. 2001). After closer evaluation, however, the relative amount of C43 in the cytoplasm is more substantial than the amounts of N64 or N187 suggesting that GFP rather than the C43 fragment could be providing an additional nuclear import signal. Nonetheless, overexpression of the myc-tagged, as well as the GFP-tagged, N-terminally truncated fusion proteins impaired cell growth to a degree similar to that observed with untagged proteins (Figure 3.3 and (Eisinger, Dick et al. 1997)).

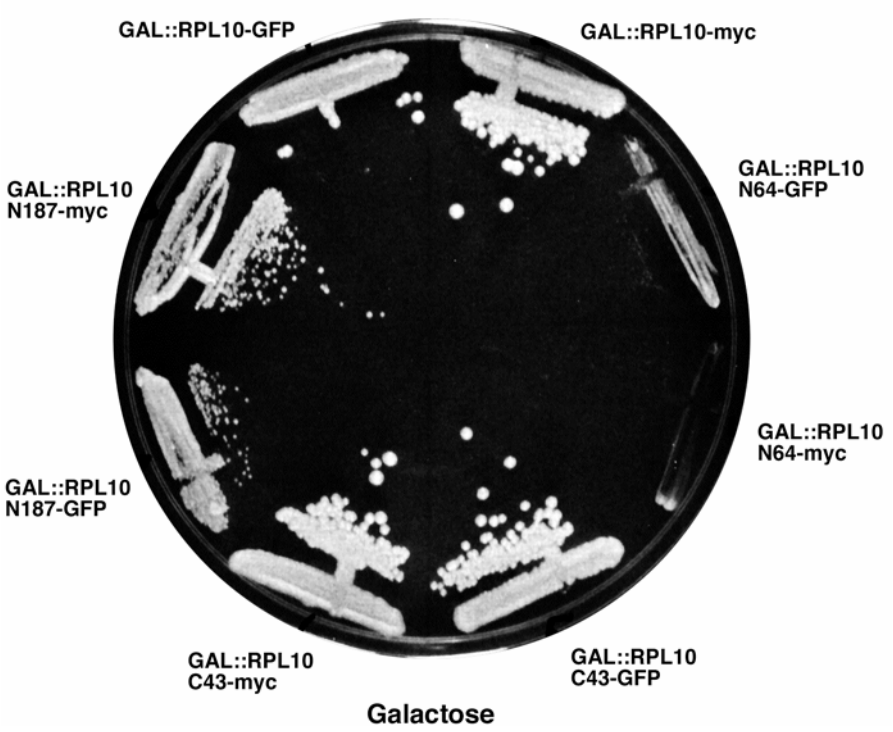

Figure 3.3 Rpl10p dominant negative fragments inhibit growth regardless of differences in C-terminal epitope tags.

Wild-type strain W303 containing the various galactose inducible Rpl10p fragments from figure 3.2 were streaked onto galactose-containing medium. Plates were incubated at 30°C for 3 days. Note: although Rpl10-GFP is less densely streaked than Rpl10-myc, colony size indicates a similar rate of growth which was validated through restreaks.

The disparity between localization of GFP and myc-tagged proteins led to the examination of the effects of GFP and myc fusions on the localization of another protein. The localization of GFP-tagged Nmd3p in live and fixed cells was compared with the localization of myc-tagged and native versions of Nmd3p by indirect immunofluorescence using anti-myc and anti-Nmd3 antibodies, respectively. Here again, the GFP-tagged protein in live and fixed cells showed greater nuclear accumulation than both the myc-tagged and untagged proteins (data not shown). A similar nuclear bias has been observed for signal recognition particle proteins in yeast when tagged with small epitopes versus GFP ((Ciufo and Brown 2000; Grosshans, Deinert et al. 2001), respectively). This difference in localization is probably not due to inhibition of import by the myc epitope because myc-tagged mutant Nmd3 proteins readily accumulate in the nucleus (Ho, Kallstrom et al. 2000). Free GFP has also been observed in the nucleus of LeptomycinB (LMB)-sensitive yeast when treated with LMB (Kallstrom and Johnson, unpublished). Because LMB disrupts the interaction between Crm1p and its cargo molecules, this suggests that GFP may contain a weak nuclear localization signal. Thus GFP may contribute to the nuclear accumulation of some fusion proteins, especially those that may already have a higher steady state level at the nuclear membrane. Regardless of the effect of GFP, the data presented here suggests that the dominant negative fragments of Rpl10p do not need to enter the nucleus to inhibit growth. Thus, these results do not concur with the idea that Rpl10p dominant negative fragments block full-length Rpl10p loading in the nucleus.

3.3.3 Rpl10p dominant negative fragments sequester Sqt1p

Previous work has shown that Rpl10p loads onto the nascent 60S subunit late in the biogenesis pathway (Kruiswijk, Planta et al. 1978) and is one of several exchangeable proteins (Zinker and Warner 1976). Although Rpl10p makes extensive contacts with 25S

rRNA and 5S rRNA in the cleft between the central protuberance and the GTPase stalk ((Ban, Nissen et al. 2000; Spahn, Beckmann et al. 2001) and diagram 1.2), Rpl10p is released from the subunit under high salt and low magnesium conditions in vitro (Dick, Karamanou et al. 1997) consistent with the suggestion that Rpl10p exchanges on the subunit in vivo (Dick, Eisinger et al. 1997).

In attempting to co-immunoprecipitate 60S subunits with truncated Rpl10 proteins, a protein of approximately 47 kDa was co-purified with full-length Rpl10p, Rpl10N64p and Rpl10N187p that was not apparent in the immunoprecipitate obtained with the C-terminal fragment Rpl10C43p. Based on its apparent size and the reported interaction of Sqt1p with Rpl10p (Eisinger, Dick et al. 1997), the immunoprecipitates were tested by western blotting for the presence of Sqt1p. Indeed, the 47-kDa protein strongly cross-reacted with Sqt1p antisera (Figure 3.1A). This result raised the possibility that the dominant negative effects of the C-terminally truncated Rpl10p proteins are caused by sequestering Sqt1p. This would be consistent with the observation that overexpression of Sqt1p suppresses the dominant negative phenotype of Rpl10p C-terminal truncations (Eisinger, Dick et al. 1997).

In order to test if the dominant negative phenotype of Rpl10p fragments was due to sequestering Sqt1p, the loss of the dominant negative phenotype of the Rpl10N187p mutant by disruption of its interaction with Sqt1p was examined. It is reasonable to assume that the interaction between these two proteins is mediated in part by electrostatic interactions between the acidic N-terminus of Sqt1p and the basic N-terminus of Rpl10p (See figure 3.4B and C). Thus, N-terminal truncations of myc-tagged Rpl10N187p were made in order to try to disrupt its interaction with Sqt1p. Removal of the first 25 amino acids of Rpl10N187-myc eliminated binding to Sqt1p (Figure 3.1A) and relieved the dominant negative growth phenotype (Figure 3.1B). Since this double truncation mutant

was expressed at levels similar to or even higher than the single C-terminal deletion (Rpl10N187-myc) in extracts (data not shown), these results support the idea that the Rpl10N187p dominant negative phenotype is due to sequestering Sqt1p thereby effectively preventing its association with endogenous Rpl10p. In turn, this would indirectly decrease the efficiency of Rpl10p loading onto 60S subunits.

3.3.4 Sqt1p binding to free Rpl10p is important for its function

SQT1 was randomly mutagenized by PCR as described in Chapter 2 and temperature-sensitive (ts) and loss of function (LOF) mutants were identified to correlate a function with biochemical activity. A list of sequenced mutants from this collection can be found in Appendix A. Interestingly, *sqt1* LOF mutants were found to have a reduced affinity for Rpl10N187-GFP (Figure 3.4A). Sqt1 is a WD-repeat protein with 5 well-predicted blades that is predicted to fold into a typical disc with an acidic amino terminal extension as determined by BMERC-PSA (bmerc-www.bu.edu/psa)(Stultz, Nambudripad et al. 1997) and 3D-PSSM (www.sbg.bio.ic.ac.uk/~3dpssm) (Kelley, MacCallum et al. 2000) server protein sequence threading analysis (Figure 3.4B). The predicted PSSM structure was modeled from the C-terminal domain of the Tup1p transcription repressor from *S. cerevisiae*. Because Tup1p contains 7 WD-repeat domains, two additional WD domains were predicted in the PSSM model for Sqt1p as compared to the PSA results (Figures 3.4B, dashed boxes). Regardless, in such a structure the two termini are expected to be close together and on the same surface of the protein. Sequence analysis revealed that the *sqt1* LOF mutants contained point mutations throughout the protein sequence. However, point mutations within the WD repeats and/or C-terminal portion of the protein (T356A, T165P/R346G, C115R, W92R/L134P/K357R) did not completely block binding to Rpl10N187-GFP, whereas a single mutation in the N-terminus alone or double mutations with one in each terminus

(N56I, E40G/I370T) led to a more significant loss of binding (Figure 3.4A and data not shown). To rule out the possibility that these mutant proteins were unstable, the cellular levels of these mutants in extract were compared to that of myc-tagged wild-type Sqt1p by western blotting. The mutant proteins were expressed at levels similar to wild-type protein indicating that protein stability was not significantly affected (data not shown). These results are consistent with the idea that the amino terminal extension of Sqt1p is important for its interaction with Rpl10p through electrostatic interactions.

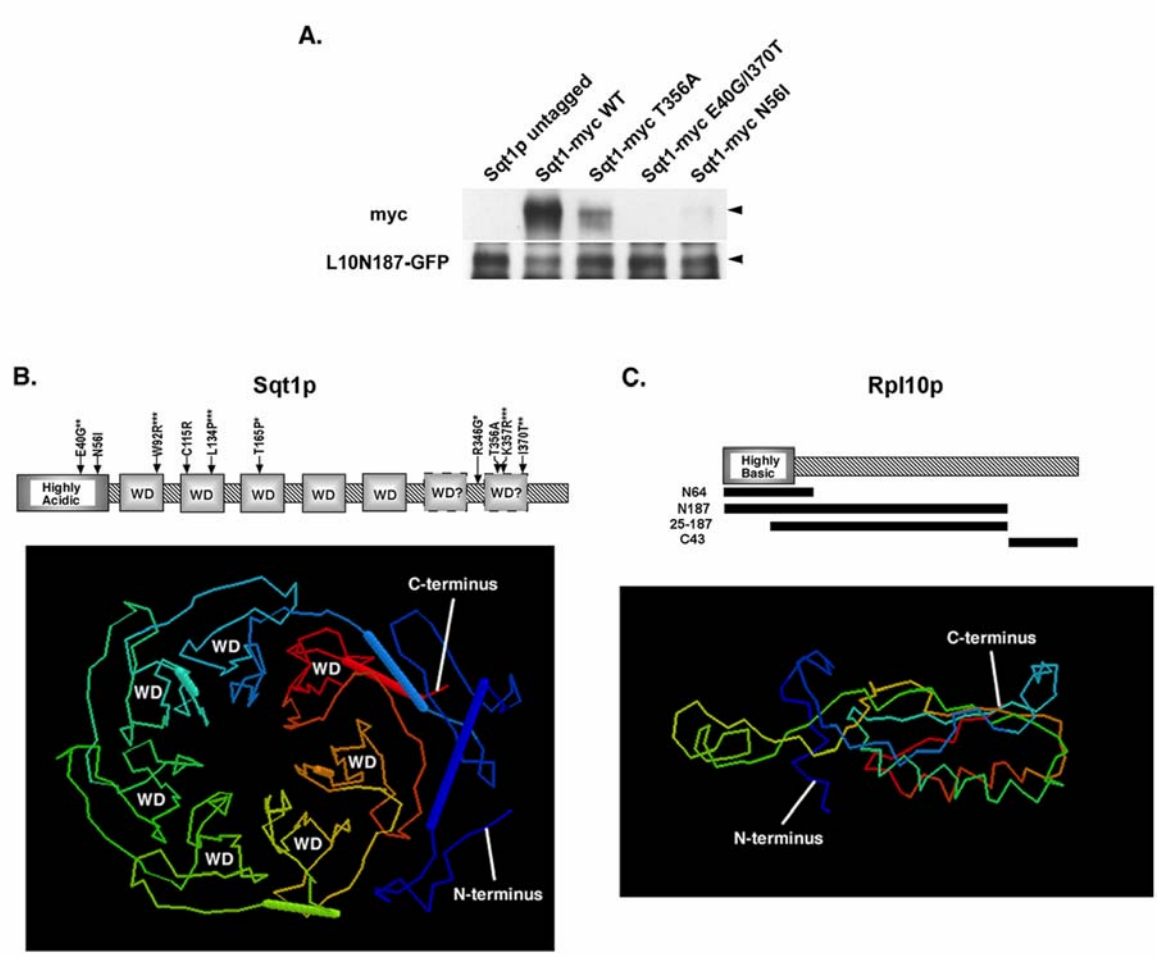

Figure 3.4 Mutations in Sqt1p lead to loss of interaction with an Rpl10p dominant negative fragment.

(A) Extracts were made from strain W303 containing pAJ1100 (*GAL10::L10N187-GFP*) with either pAJ1063 (WT *Sqt1-myc*), pAJ1264 (*sqt1[T356A]-myc* LOF), pAJ1265 (*sqt1[E40G/I370T]-myc* LOF) or pAJ1266 (*sqt1[N56I]-myc* LOF) and immunoprecipitations performed with α-GFP as described in Chapter 2. (B) Schematic diagram and predicted structure of Sqt1p. The two C-terminal WD-repeats of Sqt1p are predicted by PSSM threading but not by PSA domain assessment. The first 60 amino acids of Sqt1p are highly acidic. Arrows indicate mutations in the *SQT1* sequence that lead to a decrease in Rpl10p binding. Asterisks indicate multiple mutations that occur in the same allele. (C) Schematic diagram and predicted structure of Rpl10p. Bars indicate Rpl10p truncation mutants used in this work. The first 40 amino acids of Rpl10p are highly basic.

These results tie in well with the predicted structures of Rpl10p and Sqt1p (Figure 5.4B and C). As mentioned above, the N- and C-terminal ends of Sqt1p are predicted to be in close proximity with one another. In addition, the N-terminus of the protein contains a cluster of acidic residues that could provide an excellent binding surface for the highly basic N-terminus of Rpl10p. On the other hand, the predicted structure of Rpl10p shows the basic N-terminal extension loosely wraps around the protein, suggesting that it may be in a relatively dynamic conformation. Insertion of Rpl10p into the ribosome could necessitate displacement of Sqt1p from the N-terminus of Rpl10p. Without subunit insertion of Rpl10p, Sqt1p displacement would not occur. This would lead to a continual cycle of nonproductive binding to and subsequent release from the subunit.

3.3.5 Cellular localization of Sqt1p

If Rpl10p loads onto nascent 60S subunits in the nucleus and requires Sqt1p for binding, Sqt1p would be expected to shuttle. Sqt1p fractionates as a cytoplasmic protein (Eisinger, Dick et al. 1997), and an HA-tagged version has been localized to the cytoplasm by indirect immunofluorescence (Triples immunofluorescent database, http://ygac.med.yale.edu/triples). Interestingly, when fused with GFP at its C-terminus, Sqt1p localizes to the nucleus ((Huh, Falvo et al. 2003) and data not shown). Recent proteomic data also suggests that Sqt1p may shuttle since it can be co-purified with nuclear pre-60S subunits (Nissan, Bassler et al. 2002). However, Sqt1p containing a C-terminal oligomeric c-myc epitope was dispersed throughout the cytoplasm and mostly excluded from cell nuclei (Figure 3.5A).

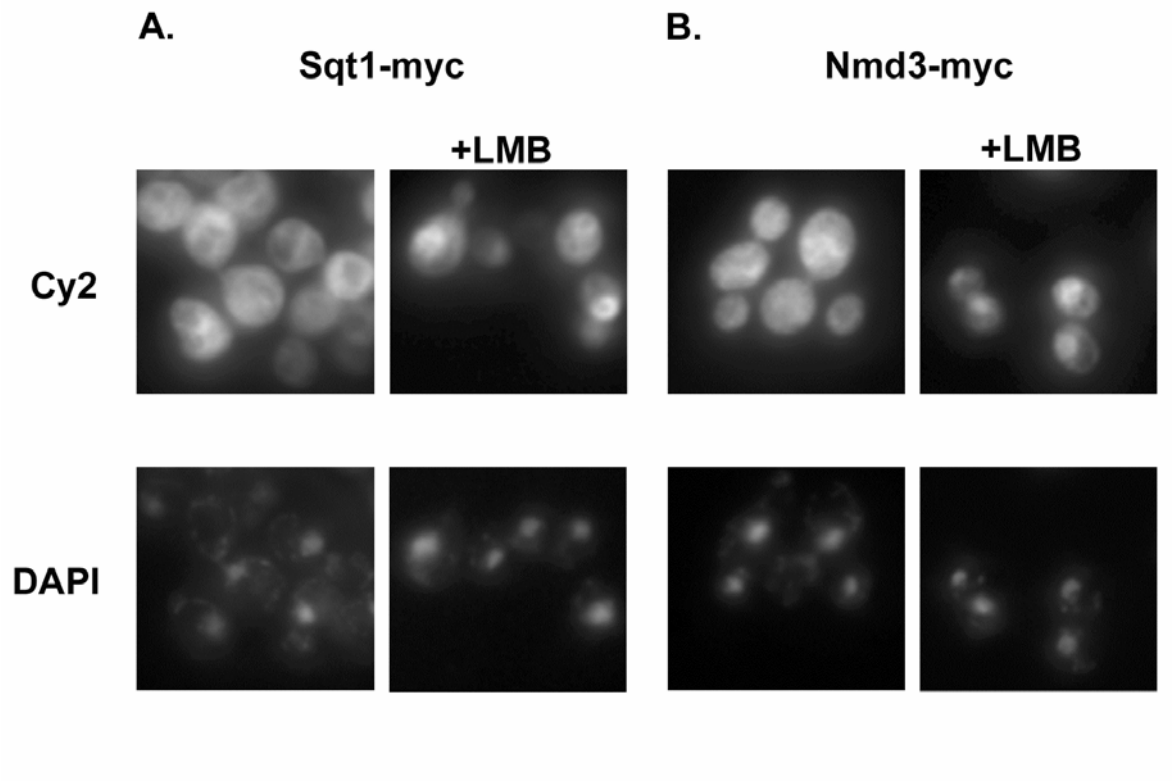

Figure 3.5 Sqt1p localizes to a perinuclear position in the absence of 60S export.

(A) AJY1539 (*crm1[T539C]*) containing pAJ1063 (*SQT1-myc*) was grown to mid-log phase and either treated with LMB as described Chapter 2 or left untreated. Cells were fixed, stained and visualized by indirect immunofluorescence as also described in Chapter 2. (B) AJY1539 containing pAJ538 (*NMD3-myc*) was treated as in A.

To examine the possibility of Sqt1p shuttling in vivo, Sqt1-myc was visualized by indirect immunofluorescence under conditions in which Crm1p meditated export was inhibited. It is known that Crm1p-mediated export of the 60S subunit via interaction with the Nmd3p adapter is disrupted by leptomycin B (LMB) treatment in LMB sensitive yeast (Ho, Kallstrom et al. 2000; Gadal, Strauss et al. 2001). LMB inhibits binding between Crm1p and the leucine-rich NESs of its adapter substrates. Thus, any factors that are associated with the 60S subunit during export should be retained within the nucleus under this condition. Sqt1-myc was expressed in LMB sensitive yeast and observed for nuclear mislocalization upon addition of LMB. Sqt1-myc appeared to be enriched at the nuclear envelope of these LMB treated cells (Figure 3.5A). Interestingly, a similar localization phenotype was observed for Rp10N64-myc, but in the absence of LMB as observed by indirect immunofluorescence in figure 3.3A.

As a control, Nmd3-myc was also observed and, as previously published, was predominantly nuclear upon LMB treatment (Figure 3.5B). At closer observation there are areas of clearing within the nuclei of some cells, however these areas are not as pronounced as in the case of Sqt1p. Although not previously documented, this may indicate that Nmd3p is being trapped at the inside of the nuclear envelope or is sequestered to particular areas of the nucleus upon LMB treatment. This issue remains to be resolved by confocal or electron microscopy. Nonetheless, from these preliminary results, it does not appear that Sqt1p shuttles between the nucleus and cytoplasm.

3.3.6 Defects in Rpl10p or Sqt1p function disrupt ribosome export

RPL10 was identified in a screen for conditional mutants that blocked nuclear export of 60S subunits (Gadal, Strauss et al. 2001). This screen employed an Rpl25-eGFP fusion as a fluorescent reporter that is incorporated into 60S subunits and is functional (Hurt, Hannus et al. 1999). Mutants in the 60S export pathway accumulate

this reporter in the nucleus and/or nucleolus. Considering the intimate link between Rpl10p and Sqt1p, the effects of overexpression of *RPL10N187* or repression of *SQT1* on ribosome export were determined by monitoring the localization of Rpl25-eGFP. The effects of these conditions on Nmd3-GFP were also examined. When *SQT1* was repressed or *RPL10N187* was expressed, Rpl25-eGFP but not Nmd3-GFP accumulated in the nucleus (Figures 3.6A & 3.6B, respectively). Similar results were observed in cells repressed for *RPL10* expression (see following chapter) and in temperature sensitive *sqt1* and *rpl10* mutants (data not shown and (Gadal, Strauss et al. 2001)). The common effects observed upon reducing cellular levels of *RPL10* or *SQT1* are consistent with the idea that Sqt1p is required for maintaining the stability of free Rpl10p (see discussion).

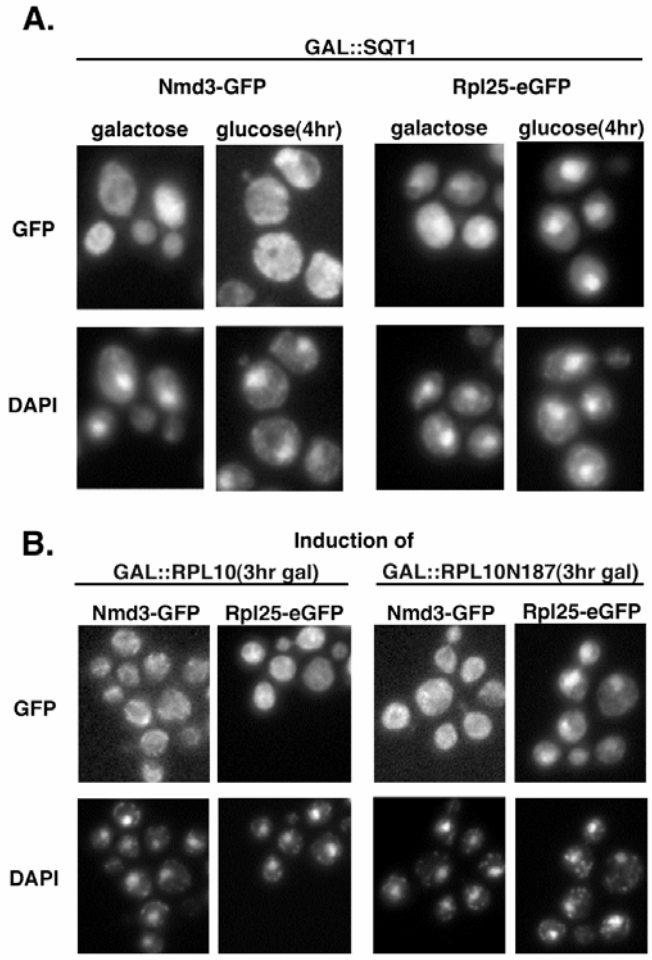

Figure 3.6 Repression of *SQT1* expression and overexpression of *RPL10N187* both lead to inhibition of ribosome export without Nmd3p nuclear entrapment.

(A) AJY1640 (*GAL::SQT1*) containing pAJ582 (*NMD3-GFP*) or pAJ907 (*RPL25-eGFP*) were grown overnight in medium containing galactose. Cultures were diluted to OD_{600} ~0.15 and split into two aliquots. *NMD3-GFP* cultures were incubated 4hr prior to addition of glucose to one set of aliquots while glucose was immediately added to one set of *RPL25-eGFP* aliquots during recovery from lag phase. After 4hr, cells were fixed and DAPI stained according to Chapter 2. (B) W303 containing either pDEGQ2 (*GAL1-10::RPL10*) or pDEGQ187 (*GAL1-10::RPL10N187*) each with either pAJ582 (*NMD3-GFP*) or pAJ907 (*RPL25-eGFP*) were grown overnight in medium containing raffinose. *NMD3-GFP* cultures were diluted to OD_{600} ~0.15 and incubated for 4 hr before the addition of galactose to induce expression of wild-type and truncated *RPL10* for 3hr. *RPL25-eGFP* cultures were also diluted to OD_{600} ~0.15, but galactose was immediately added to induce wild-type and truncated *RPL10* for 3hr during recovery from lag phase. Cells were treated and visualized as in A.

The nuclear accumulation of Rpl25-eGFP under conditions where either *SQT1* or *RPL10* functions are disrupted suggests that nascent subunits are blocked for export. To confirm that Rpl25-eGFP was incorporated into free 60S subunits when Sqt1p function is disrupted, the sedimentation of Rpl25-GFP in a *sqt1* ts mutant was examined. In this experiment, cells were grown at semi-permissive temperature followed by induction of Rpl25-GFP expression. Extracts were prepared and analyzed by sucrose gradient velocity sedimentation in the presence of the translation elongation inhibitor cycloheximide. The various ribosomal subunit and/or mRNA species involved in the translation process can be resolved using this type of analysis. By trapping translating ribosomes (polysomes) on mRNAs using cycloheximide, populations of these different structures, including free 40S, 60S and 80S couples as well as polysomes containing mRNAs bound by one to several elongating 80S ribosomes, can be tracked by tracing of a polysome profile based on constant measurement of A_{254} units coming off linear sucrose gradients. Under these conditions, wild-type cells showed Rpl25-GFP present in 60S, 80S and polysome fractions (Figure 3.7). In contrast, in a *sqt1* ts mutant, Rpl25-GFP was incorporated into free 60S, but its incorporation into polysomes was markedly reduced (Figure 3.7). Furthermore, halfmer shoulders on polysome peaks were obvious in the *sqt1* ts profile. These are indicative of 48S initiation complex entrapment on mRNAs without subsequent binding of a 60S subunit. They arise from a depletion of the free 60S pool or from subunit joining defects. Since 60S levels were not depleted and Rpl25-eGFP was being incorporated into pre-60S subunits, these results indicate that subunits were not efficiently entering the translationally active (polysome) pool in *sqt1* mutant cells.

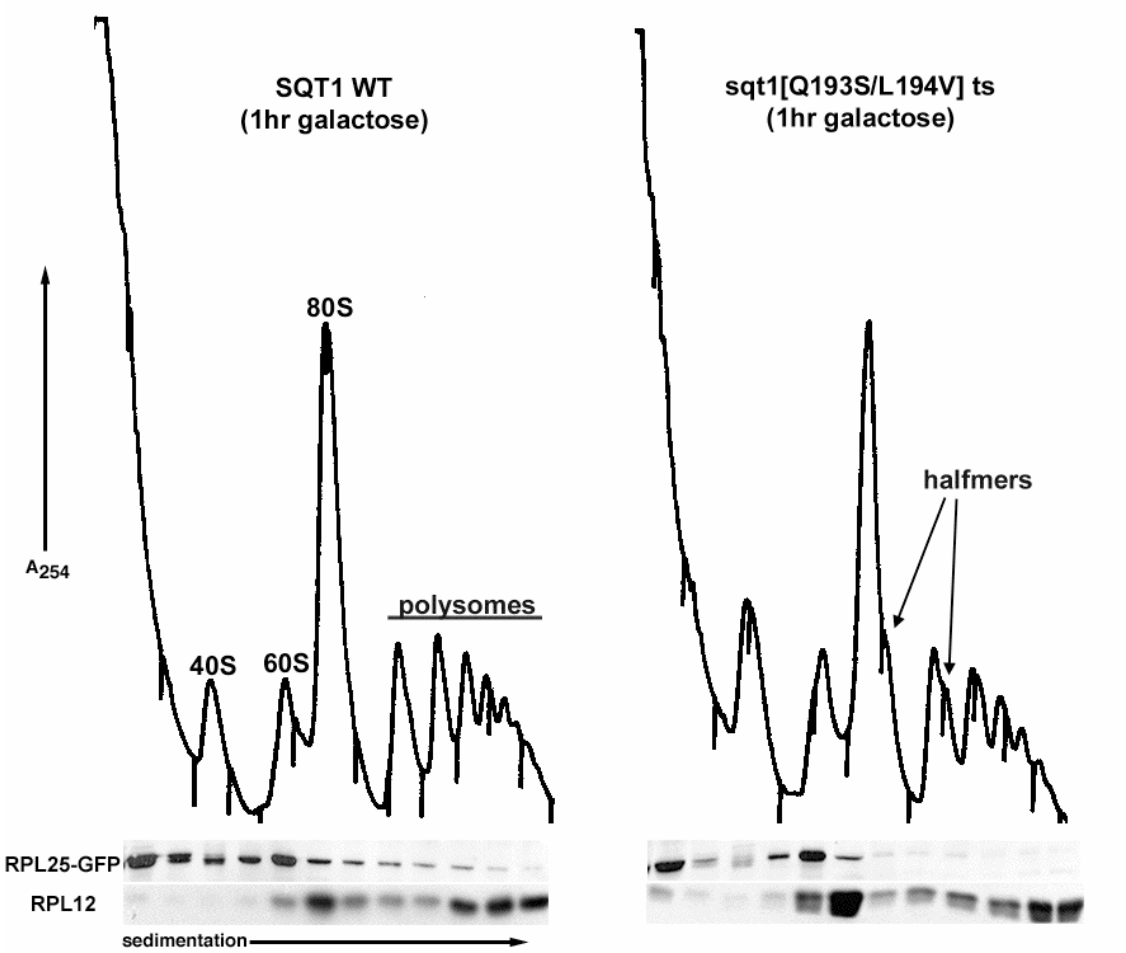

Figure 3.7 Nascent 60S subunits do not progress into the translating pool of subunits in *sqt1* mutants.

AJY1640 (*GAL::SQT1*) with either pAJ1063 (*SQT1-myc*) or pAJ1252 (*sqt1[Q193S/L194V]-myc* ts) replacing pAJ1065 and each with pAJ369 (*GAL10::RPL25-GFP*) were collected and analyzed by sucrose gradient fractionation as described in Chapter 2. Fractions were run on 12% SDS-PAGE gels and transferred to nitrocellulose for western blotting with α-GFP or α-Rpl12p. Halfmer shoulders on polysome peaks are denoted in the *sqt1* ts profile.

3.3.7 Nmd3p binds to 60S subunits lacking Rpl10p

Although it has been reported that Nmd3p and Rpl10p interact directly through an in vitro binding assay (Gadal, Strauss et al. 2001), direct evidence for Rpl10p dependent Nmd3p binding to 60S is lacking. In addition, as will be discussed in Chapter 5, I was unable to demonstrate specific interaction between Nmd3p and Rpl10p in vitro. Additional evidence that contradicts the idea of Rpl10p recruitment of Nmd3p to 60S in the nucleus is the cytoplasmic localization of myc-tagged Rpl10N64, as assayed by indirect immunofluorescence (see figure 3.2A). This fragment showed a peri-nuclear localization in the cytoplasm, while its GFP fused counterpart mislocalized to the nucleus ((Gadal, Strauss et al. 2001) and figure 3.2B). This is likely due to the existence of a weak NLS in GFP that has not been previously reported, as fusion of this tag to other proteins has a similar effect (see section 3.2.2). Thus, by most indications, Sqt1p-dependent Rpl10p loading occurs in the cytoplasm and is not required for loading Nmd3p in the nucleoplasm.

To determine whether sequestering Sqt1p prevents the loading of Rpl10p onto Nmd3p bound subunits, co-immunoprecipitations of myc-tagged Nmd3p in the presence of Rpl10N64p or Rpl10N187p dominant negative fragments were carried out. Expression of *GAL* driven *RPL10* wild type or dominant negative fragments was induced for three hours in a *RPL10-HA* integrant strain harboring a plasmid containing myc-tagged Nmd3p. Cells were treated with cycloheximide to prevent dissociation of polysomes into the free 40S and 60S pools.

Coimmunoprecipitations showed that, in the presence of either full-length Rpl10p or Rpl10N64p overexpression, Nmd3p bound 60S subunits to a similar extent. This was indicated by the ability of Nmd3-myc to co-immunoprecipitate equivalent amounts of the

60S r-protein marker Rpl12p (Figure 3.8). However, endogenous Rpl10-HA protein signal was significantly depleted from Nmd3p immunoprecipitated subunits when co-expressed with Rpl10N64p (Figure 3.8). Similar observations were obtained with Rpl10N187p (data not shown). The variable levels of Rpl10p in subunits affinity-purified with Nmd3p indicate that not all subunits bound by Nmd3p contain Rpl10p. Thus, Rpl10p is not required for Nmd3p binding. Because Sqt1p is cytoplasmic, these results support the notion that Rpl10p is loaded, via Sqt1p, onto 60S subunits in the cytoplasm once Nmd3p-mediated export has occurred. Work in Chapter 4 will show how this depletion of Rpl10p leads to entrapment of Nmd3p on free 60S subunits in the cytoplasm.

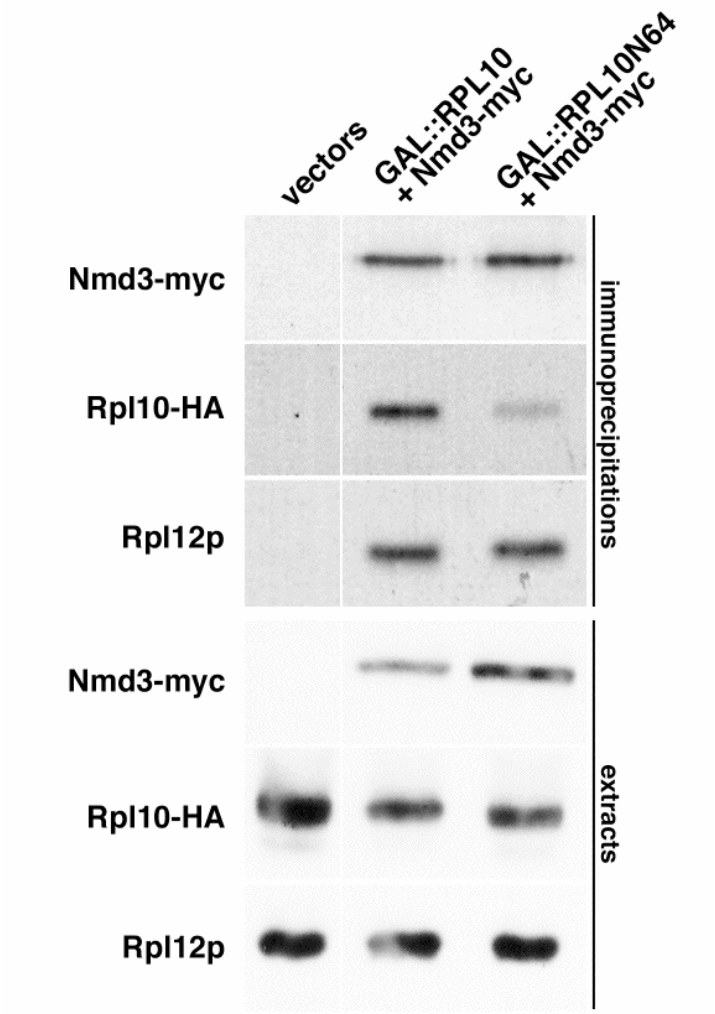

Figure 3.8 Nmd3p binds to 60S subunits deficient for Rpl10p.

Extracts were made from strain AJY1961 (*RPL10::3xHA*) containing pDEGQ2 (*GAL1-10::RPL10*) or pDEGQ64 (*GAL1-10::RPL10N64*) each with pAJ538 (*NMD3-myc*). The same strain containing empty vectors pRS425 and pRS426 was used as a negative control. Immunoprecipitations using α-c-myc, sample analysis on 12% SDS-PAGE gels and western blotting using α-c-myc, α-HA or α-Rpl12p were carried out as described in Chapter 2. Pre-immunoprecipitation extracts are provided as protein expression level controls.

3.4 DISCUSSION

Rpl10p is an integral component of the large ribosomal subunit, positioned between the central protuberance and the GTPase stalk, and makes contacts with 25S and 5S rRNAs (Diagram 1.2 and (Ban, Nissen et al. 2000)). Eukaryotic Rpl10 proteins contain a C-terminal extension of approximately 50 amino acids. Yeast Rpl10p, lacking this C-terminal extension, is comparable in size and predicted structure to its prokaryotic counterparts and can be modeled into the 15 angstrom cryo-EM map of the yeast ribosome (Spahn, Beckmann et al. 2001) using the known crystal structure from *Haloarcula marismortui* (Ban, Nissen et al. 2000) (Diagram 1.2, cryo-EM reconstruction). Consequently, it seemed reasonable that truncated Rpl10p, lacking only the C-terminal 43 amino acids, would be incorporated into subunits. Similarly, a deletion that removes all but the amino-terminal 64 amino acids yields a peptide that could pack into the subunit via interactions with 25S rRNA. These fragments inhibit cell growth when expressed in yeast (Eisinger, Dick et al. 1997), which could be explained if their incorporation into subunits in the nucleus blocked subsequent assembly or export events. It was found here that these Rpl10p fragments do not stably assemble into 60S subunits, indicating that their dominant negative effect comes from interactions separate from the subunit. These fragments were dominant negative regardless of whether they localized to the nucleus or cytoplasm (Figures 3.2 and 3.3), consistent with the idea that they act independently of assembly of subunits in the nucleus.

In addition to its interactions within the 60S subunit, Rpl10p physically interacts with both the WD repeat protein Sqt1 (Eisinger, Dick et al. 1997) and the 60S export adapter Nmd3p (Gadal, Strauss et al. 2001). In attempting to show that Rpl10p fragments were incorporated into 60S subunits, these fragments were found to bind,

perhaps irreversibly, to Sqt1p, a protein previously suggested to act as a chaperone for loading Rpl10p onto subunits (Figure 3.1A and (Eisinger, Dick et al. 1997)). These results suggest that the dominant negative effect of Rpl10p truncations is due to titrating out Sqt1p and not a direct effect on subunit assembly. Rpl10p appears to interact with Sqt1p at least partly through electrostatic interactions. Sqt1p is predicted to form a disc, typical of WD repeat proteins, with a highly negatively charged amino-terminal extension (amino acids 1- 50 have a calculated pI of 3.9). This amino terminus could bind electrostatically to the highly basic amino-terminal 40 amino acids of Rpl10p. Indeed, deletion of 25 amino acids from the N-terminus of Rpl10p prevented its binding to Sqt1p and, at the same time, relieved the dominant negative effect of a C-terminal truncation. Because the Rpl10p C-terminal truncations do not assemble into 60S and remain bound to Sqt1p, the C-terminus must be necessary for its release from Sqt1p as it assembles into the subunit. It may be necessary for Rpl10p to achieve a conformation appropriate for 60S binding. Alternatively, it may initiate the loading onto the subunit by its own binding to the subunit or to other proteins transiently on the subunit. In the cryo-EM map of yeast ribosomes, an unassigned mass was observed near the C-terminus of the conserved core of Rpl10p and adjacent to 5S as well as helix 38 of 25S rRNA (Spahn, Beckmann et al. 2001). This mass may represent the C-terminal extension of Rpl10p.

When *RPL10* expression is induced in a *sqt1* ts mutant under restrictive conditions, newly made Rpl10p is not detected (data not shown), indicating that Sqt1p is necessary for stabilizing Rpl10p. This is consistent with long-term repression of *SQT1* expression leading to depletion of Rpl10p from free 60S subunits (Eisinger, Dick et al. 1997). Additionally, *sqt1* ts mutants show reduced levels of endogenous Rpl10p in extracts (data not shown). *SQT1* was originally identified as a high copy suppressor of dominant negative Rpl10p fragments (Eisinger, Dick et al. 1997). That the *RPL10*

dominant negative mutants can be suppressed by high copy *RPL10* or high copy *SQT1* and that Rpl10p is unstable in *sqt1* mutants is consistent with the original proposal that Sqt1p acts as a chaperone for free Rpl10p, prior to and during its loading into a subunit (Eisinger, Dick et al. 1997). This, combined with its late loading onto the subunit, suggests that the presence of Rpl10p could act as a means of controlling 60S incorporation into the translation apparatus.

Multiple WD-repeat proteins have been identified as trans-acting factors in the 60S biogenesis pathway. Sqt1p loading of Rpl10p closely parallels the role of the WD-repeat protein Rrb1p in Rpl3p assembly into the large subunit (Iouk, Aitchison et al. 2001). In this case, depletion of Rrb1p leads to co-depletion of Rpl3p while overexpression of Rrb1p leads to accumulation of Rpl3p in the nucleus of cells. Additionally, the WD-repeat protein Pwp2 was found to copurify an early 90S pre-ribosomal particle. This was one of the earliest precursor particles examined to date (Grandi, Rybin et al. 2002). Interestingly, a subcomplex containing Pwp2 was removed from this 90S particle upon disruption of U3 snoRNP formation. Through mass spec analysis, the other proteins found in this subcomplex were also WD-repeat proteins. This, combined with the functions of Rrb1 and Sqt1 in loading r-proteins onto 60S, suggests that WD-repeat proteins perform important scaffolding roles at all stages of ribosome biogenesis.

A number of conditional *rpl10* mutants, including *rpl10[G161D*] and *rpl10[F85S]*, have been identified (Eisinger, Dick et al. 1997; Karl, Onder et al. 1999; Zuk, Belk et al. 1999; Gadal, Strauss et al. 2001). Because Rpl10p is an essential component of the ribosome, these mutant proteins must be able to assemble into subunits under permissive conditions. Under restrictive conditions, *rpl10[G161D]* does not lead to rapid loss of 60S subunits, indicating that pre-existing subunits are not severely

destabilized by the mutant Rpl10 protein (Oender, Loeffler et al. 2003). Interestingly, none of the *rpl10* mutants that have been tested are suppressed by high copy Sqt1p ((Eisinger, Dick et al. 1997) and data not shown). Because Sqt1p acts to stabilize Rpl10p prior to incorporation into subunits, the lack of suppression by *SQT1* suggests that the defect in these *rpl10* mutants is downstream of Sqt1p function and possibly downstream of Rpl10p assembly into the ribosome. This is consistent with similar observations made in *sqt1* ts mutants that show loss of free Rpl10p signal.

Repression of *SQT1* or *RPL10* expression as well as induction of dominant negative Rpl10p fragments prevented export of the 60S reporter Rpl25-eGFP, consistent with the defect in 60S export reported for *rpl10* conditional mutants (Gadal, Strauss et al. 2001). The Rpl25-GFP that accumulates in the nucleus in an *sqt1* ts mutant at semi-permissive temperature is incorporated into pre-60S subunits, but these subunits are not efficiently incorporated into the translation apparatus (Figure 3.7). Under the same conditions, Nmd3-GFP remains in the cytoplasm (Figure 3.6), suggesting that either 1.) 60S subunits are not maturing to a point that an Nmd3p binding site is formed or 2.) Nmd3p is not being imported into the nucleus to support export of otherwise "export competent" subunits. In Chapter 4, I will show that Nmd3p is not released from cytoplasmic subunits in the absence of Rpl10p.

The Rix7p AAA ATPase is also involved in the late nucleoplasmic maturation of the pre-60S particle. Rix7p is found in the nucleolus during stationary phase, however it accumulates at the nuclear envelope in early log phase cells (Gadal, Strauss et al. 2001). This is in contrast to its localization during logarithmic growth, at which time it is in the nucleoplasm. Its redistribution to the nuclear envelope from stationary phase to log phase closely matches the localization of myc-tagged Sqt1p in the presence of LMB. This colocalization, in combination with similar effects on 60S export, may indicate that

both factors have roles in restructuring (Rix7p) or in loading factors to restructure (Sqt1p) the 60S subunit before and after transit through the nuclear pore complex, respectively.

In conclusion, results from this chapter support a role for Sqt1p in stabilizing and loading Rpl10p onto subunits immediately following nuclear export of the pre-60S particle. One of the most important observations from this work is that, contrary to current thinking, Rpl10p does not appear to mediate the interaction of Nmd3p with the pre-60S subunit. Instead, Rpl10p seems to load onto pre-60S subunits in the cytoplasm for activation of the subunit prior to incorporation into the translation apparatus. Characterization of the role of Rpl10p in late subunit maturation is the cornerstone of Chapter 4.

Chapter 4: Sqt1p and Rpl10p are required for Nmd3p nuclear recycling

4.1 INTRODUCTION

The preceding chapter focused on the requirement for Sqt1p-mediated stability of Rpl10p prior to Rpl10p incorporation into 60S subunits to maintain subunit nuclear export. In this chapter I further characterize the role of Rpl10p in ribosome export. Contrary to previously published work suggesting that Rpl10p is directly required for 60S export by recruiting the export adapter Nmd3p, I show that Rpl10p plays an indirect role in this process. First, data is presented that shows that Nmd3p recycling to the nucleus depends on fully functional Sqt1p and Rpl10p. I then examine the basis for the genetic interaction between *RPL10* and *NMD3*. I show that *nmd3* mutations that suppress *rpl10* conditional mutants are able to recycle to the nucleus more efficiently. Lastly, I provide evidence that these *NMD3* suppressor mutations reduce the binding of Nmd3p to 60S subunits to facilitate release of the Nmd3 mutant proteins from 60S. Thus Rpl10p and Sqt1p are needed for Nmd3p recycling to the nucleus. A discussion of the impact that characterization of this recycling mechanism has on current thinking in the area of ribosome export and its potential linkage to translation control will also be provided.

4.2 BACKGROUND

As mentioned in Chapter 1, work from the laboratory of Dr. Ed Hurt has suggested that Rpl10p forms at least a part of the binding site for the 60S nuclear export adapter, Nmd3p, on 60S subunits (Gadal, Strauss et al. 2001). However, earlier work on the kinetics of r-protein incorporation during biogenesis showed that Rpl10p loads into subunits relatively late in the pathway, even possibly in the cytoplasm (Kruiswijk, Planta et al. 1978). As further indication that Rpl10p acts late in the biogenesis pathway, human

Rpl10p (QM) is found exclusively in the cytoplasm of human cells by indirect immunofluorescent staining (Nguyen, Mills et al. 1998).

Multiple types of interactions between *RPL10* and *NMD3* have been established. Interaction was first observed in a genetic screen for spontaneous suppressors of an *rpl10* temperature sensitive (ts) mutant (*rpl10[G161D]*) (Karl, Onder et al. 1999). Additionally, high copy *NMD3* was found to suppress an *rpl10* ts mutant (*rpl10[F85S]*) (Zuk, Belk et al. 1999), and Nmd3p and Rpl10p have been reported to interact in an in vitro binding assay as stated previously (Gadal, Strauss et al. 2001). However, these two factors do not interact through two-hybrid analysis (Karl, Onder et al. 1999). The in vitro and genetic interaction data have led to the plausible model that Rpl10p provides the binding site for Nmd3p on the 60S subunit, thereby recruiting the export adapter to the subunit in the nucleus. Once in the cytoplasm, release of Nmd3p from the subunit appears to occur prior to subunit joining during translation initiation, as it is not found on translating polysomes (Ho and Johnson 1999). Conversely, Rpl10p remains associated and is required for subunit joining (Dick, Eisinger et al. 1997; Eisinger, Dick et al. 1997).

4.3 RESULTS

4.3.1 Nmd3p fails to shuttle in the absence of functional Sqt1p or Rpl10p

Disrupting Sqt1p or Rpl10p function leads to an inhibition in ribosome export as indicated by accumulation of an Rpl25-eGFP reporter protein in the nucleus (as shown in Chapter 3). This is consistent with the model that Rpl10p recruits Nmd3p to nuclear subunits. On the other hand Nmd3p remains in the cytoplasm under these conditions. This could be explained if Nmd3p shuttles but does not accumulate in the nucleus because its binding site is not present. On the other hand, Nmd3p import could be blocked or, contrarily, it is possible that Nmd3p is trapped on cytoplasmic 60S subunits.

In order to determine if the cytoplasmic localization of Nmd3-GFP is caused by a failure of Nmd3-GFP to recycle to the nucleus in the absence of functional Sqt1p or Rpl10p, a Nmd3p mutant (*NMD3AAA*) that contains three point mutations within its NES (I493A, L497A, L500A) and shows a predominantly nuclear localization under wild-type conditions was utilized (Figure 4.1, presence of galactose). Nmd3AAA-GFP was redistributed to the cytoplasm when Sqt1p was repressed (Figure 4.1). A similar redistribution was observed with repression of *RPL10* expression and in the *rpl10[G161D]* ts mutant (Figure 4.1). Nmd3AAA-GFP is predominantly nuclear in wild-type cells (See figures 5.3B and 5.4), because nuclear export is rate limiting. Thus, the cytoplasmic accumulation of this protein suggests that import has become the rate-limiting step under these conditions.

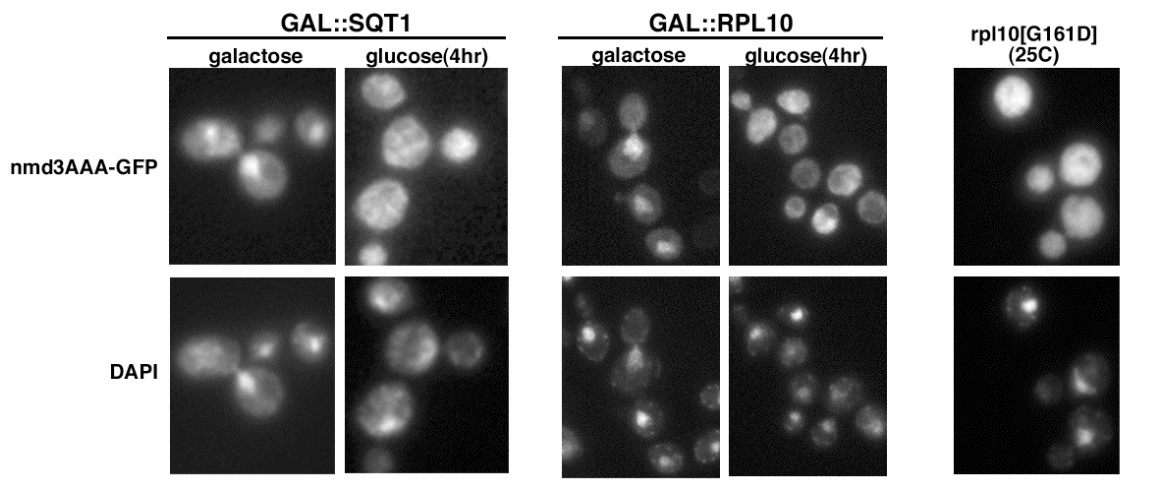

Figure 4.1 Disruption of Rpl10p or Sqt1p function leads to Nmd3p entrapment in the cytoplasm.

Nmd3AAA-GFP (pAJ754) was visualized in strains DEH221+ (*GAL1-10::RPL10*) or AJY1640 (*GAL10::SQT1*) after growth into mid-log phase followed by 4 hours of glucose repression or in the *rpl10[G161D]* mutant AJY1657 constitutively grown into mid-log phase at 25°C.

As a means to support the interpretation of the relocalization of the Nmd3AAA-GFP allele under *RPL10* repressed conditions, genomically expressed Nmd3-GFP in a LeptomycinB (LMB) sensitive strain was observed under these conditions. Actively shuttling Nmd3-GFP can be trapped in the nucleus by the addition of LMB (Ho, Kallstrom et al. 2000). However, when *RPL10* was repressed for 4 hours followed by treatment with LMB for 20 minutes, Nmd3-GFP remained cytoplasmic in the presence of LMB (Figure 4.2). This was consistent with the findings with Nmd3AAA-GFP that Nmd3p shuttling into the nucleus is blocked (Figure 4.1).

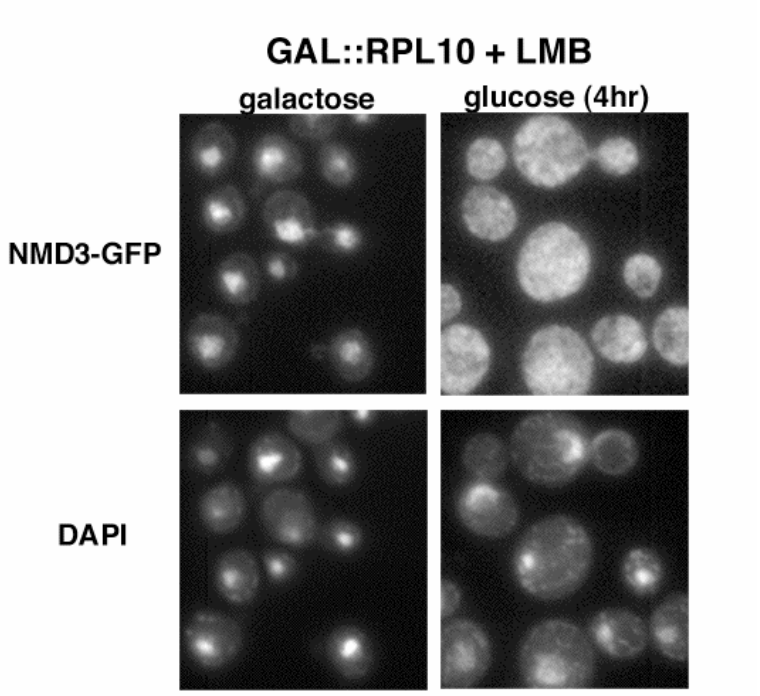

Figure 4.2 Disruption of Rpl10p function leads to entrapment of Nmd3-GFP in the cytoplasm of LMB treated cells.

After growing into mid-log phase in the presence of galactose, *RPL10* expression was maintained in AJY1836 (*GAL1-10::RPL10 NMD3-GFP crm1[T539C]*) by growth in galactose or repressed in glucose before addition of LMB and visualization of Nmd3-GFP as described in Chapter 2.

The Nmd3p that was retained in the cytoplasm could be either free protein that is not imported or associated with 60S subunits. To examine this possibility, the sedimentation of Nmd3p in sucrose density gradients was assayed. Under these conditions, no free Nmd3p accumulated at the top of the gradient, indicating that most Nmd3p was 60S associated (Figure 4.3). These results show that the loss of Rpl10p, by repression of either *RPL10* or *SQT1* expression, leads to cytoplasmic retention of Nmd3p on 60S subunits, suggesting that release of Nmd3p from cytoplasmic subunits depends on the presence of Rpl10p.

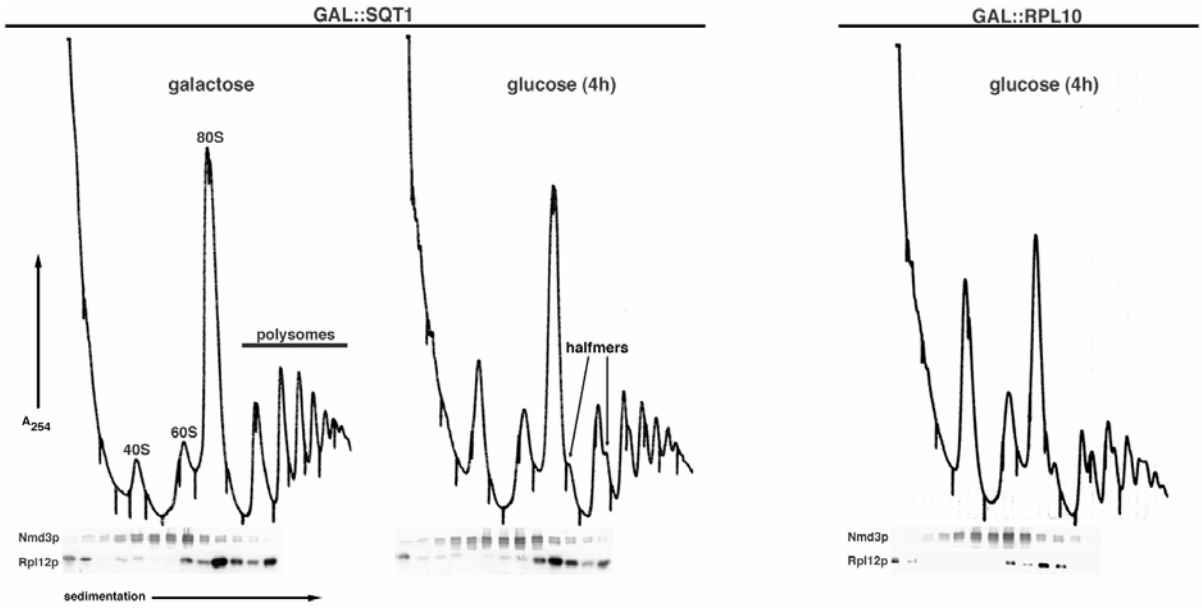

Figure 4.3 Nmd3p is trapped on 60S in the cytoplasm of cells disrupted for Rpl10p or Sqt1p function.

Strains DEH221+ (*GAL1-10::RPL10*) or AJY1640 (*GAL10::SQT1*) were diluted from overnight cultures to OD_{600}~0.05 in fresh galactose-containing medium. Cultures were incubated to OD_{600}~0.20 during which point glucose was added to repress *RPL10* or *SQT1* expression or cells were left untreated for 4 hours. Cultures were treated with 150μg/ml cycloheximide and incubated for 20 minutes on ice prior to collection and analysis as described in Chapter 2 for polysome profile analysis and sucrose gradient fractionation. Western blotting of proteins in each fraction was carried out using α-Nmd3p or α-Rpl1ap (Lacroute) as also described in Chapter 2.

4.3.2 *NMD3* suppressors of *rpl10* contain mutations in specific domains

Three spontaneous *NMD3* mutants were identified previously as suppressors of the temperature sensitive *rpl10[G161D]* (Karl, Onder et al. 1999). These mutations map to I279F, L291F and A336P and alter hydrophobic residues in this region of Nmd3p. To understand the interaction of Nmd3p with Rpl10p more completely, a screen for additional *NMD3* suppressors was carried out. This screen utilized strains containing genomically integrated copies of the *rpl10[G161D]* or *rpl10[F85S]* (Zuk, Belk et al. 1999) mutant alleles. The *NMD3* ORF was randomly mutagenized by PCR and cotransformed into the *rpl10* mutant strains with a vector containing only flanking sequence of the *NMD3* ORF to allow for recombination of the mutant sequences into the vector in vivo. These transformants were plated onto SC-leu plates to select for recombinants. All transformants were pooled to give a mutant library for each respective *rpl10* ts strain. Cells were diluted from these frozen stocks and plated onto SC-leu medium to give about 300 colonies per plate. *NMD3* suppressors were selected for their ability to permit growth of the *rpl10* ts strains at 35°C. Using this strategy, about 20 suppressors were isolated from 3000 colonies replated from the frozen stock for each of the two strains assayed.

Plasmids harboring *NMD3* mutants providing the best suppression were isolated and sequenced. A list of these various *NMD3* alleles can be found in Appendix B. This analysis identified two highly mutated regions in the Nmd3p protein sequence (Diagram 4.4A, orange boxes). One region (aa~100-115) contains several basic residues and may be responsible for RNA binding. The second domain (aa~290-360) is hydrophobic, suggesting that it facilitates protein-protein interaction. Not surprisingly, the C-terminal domain corresponds with a suppressor-rich region originally isolated during the previous

rpl10[G161D] suppressor screen ((Karl, Onder et al. 1999) and diagram 4.4A, C-terminal box). These previous mutants (L291F) along with those more recently isolated (I112T/I362T, R113G, L359P) significantly alter amino acid properties within each suppressor domain.

NMD3 mutants isolated from each *rpl10* mutant screen were transformed into AJY1657 (*rpl10[G161D*) to compare their ability to suppress the same *rpl10* mutation. In general, it was found that the extent of suppression corresponded with the location of mutations in the Nmd3 protein sequence. Mutations in the N-terminal suppressor domain (eg R113G) provided less suppression than mutations in the C-terminal domain (eg L291F) (Figure 4.4A, red lettering and figure 4.4B). However, the strongest suppressor contained mutations in both domains (I112T/I362T) suggesting that both suppressor domains are additive with respect to suppressive effects (Figure 4.4A, red lettering denoted by asterisks and figure 4.4B). Subsequent subcloning of the I112T and I362T mutations indicated that this is indeed the case, since neither mutation on its own suppressed to the same extent as the double mutant allele (West and Johnson, unpublished). In addition, similar to the difference between R113G and L291F, the suppression provided by I362T was more robust than I112T.

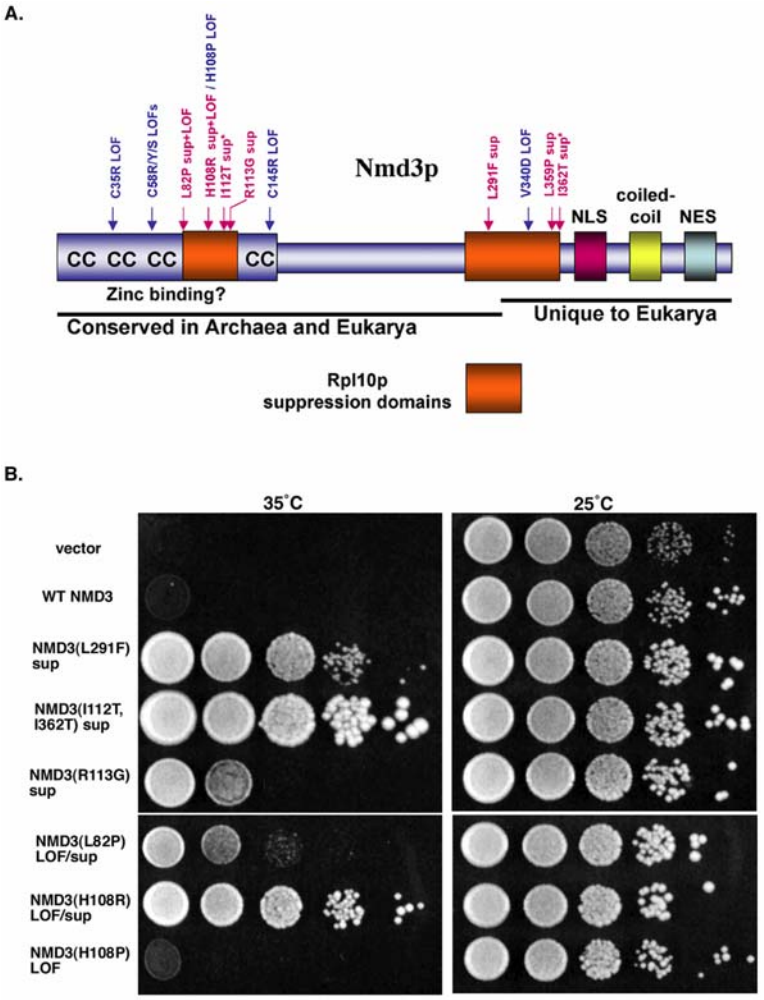

Figure 4.4 Comparison of *NMD3* suppressor and loss of function mutant effects on *rpl10[G161D]* ts mutant growth.

(A) Schematic diagram of Nmd3p. Blue: loss of function mutations. Red: suppressor mutations, some of which were originally found in the loss of function screen. Also shown are the cys-x-x-cys motifs (CC), nuclear localization signal (NLS), coiled-coil and primary NES. Orange boxes indicate domains in which suppressor mutations were most commonly found. The C-terminus of Nmd3p containing the nuclear pore complex transit signals and part of one suppressor domain is specific to eukaryotes. (B) *NMD3* alleles from either suppressor or loss of function screens were transformed into strain AJY1657 (*rpl10[G161D]*), including pAJ1315 (*NMD3[I112T,I362T]* sup), pAJ1316 (*NMD3[R113G]* sup), pAJ1296 (*NMD3[L82P]* LOF), pAJ1297 (*NMD3[H108R]* LOF) or pAJ1295 (*NMD3[H108P]* LOF). pAJ24 (vector alone), pAJ538 (*NMD3*) or pAJ415 (*NMD3[L291F]*) were each transformed as growth controls. Cells were spotted onto plates as described in Chapter 2 and grown for 5 days at either 25°C or 35°C as indicated.

Around the same time that the *NMD3* suppressor screens were carried out, another screen was carried out to identify *nmd3* loss-of-function (LOF) mutants. Of particular interest were mutants that lost 60S binding. The residues most commonly hit during this screen were the multiple cysteines that lie at the N-terminus of the protein, however these caused only moderate loss of 60S binding through immunoprecipitation analysis under low salt (50mM) conditions (Diagram 4.4A, blue lettering and A. Johnson, unpublished). Surprisingly, another LOF mutation, that changed valine 340 to aspartic acid (V340D), occurred within the C-terminal suppressor domain. This mutant also showed moderate loss of 60S binding by immunoprecipitation under low salt conditions (A. Johnson, unpublished). However, unlike its suppressor counterparts, it did not suppress the temperature sensitivity of *rpl10[G161D]* (data not shown).

Several other Nmd3p LOF mutations also overlapped with suppressor domains. Because several of these LOF mutants were viable, albeit they grew slowly, I tested their ability to suppress *rpl10[G161D]*. Interestingly, two different LOF alleles (L82P and H108R) suppressed the *rpl10* ts mutant. In contrast to V340D, these two alleles showed no obvious loss of binding under low salt conditions (A. Johnson, unpublished). *NMD3[L82P]*, showed relatively weak suppression of *rpl10[G161D]* (Figure 4.4A, blue and figure 4.4B) while H108R suppressed the *rpl10* ts mutant significantly (Figure 4.4A, red and figure 4.4B). Surprisingly, mutation of histidine 108 to proline (H108P) led to a loss of function, without the ability to suppress *rpl10[G161D]* (Figure 4.4A, blue and figure 4.4B). The overlap of suppressor and loss of function mutations suggests that suppression is elicited through some partial loss of activity rather then a gain of activity. This, again, is not consistent with Nmd3p recruitment. Instead, it is consistent with the idea that release of Nmd3p is a necessary requirement for suppression. This will be addressed further in following sections.

4.3.3 An Rp10p dominant negative mutant is suppressed by *SQT1* and *NMD3*

Previous work has shown that *SQT1* overexpression rescues the growth inhibition caused by various *RPL10* dominant negative mutants, but not by *rpl10* conditional mutants (Eisinger, Dick et al. 1997). Additionally, certain dominant mutant alleles of *NMD3* have been shown to suppress an *rpl10[G161D]* mutant (above and (Karl, Onder et al. 1999)). In order to determine whether *NMD3* could also suppress *RPL10* dominant negative mutants, an *rpl10[G161D]*ts-suppressing allele of *NMD3* (L291F) was co-expressed in wild-type cells with Rpl10p C-terminal truncation fragments. On galactose-containing medium, *NMD3[L291F]* showed modest suppression of the *RPL10N187* mutant (Figure 4.5A) but not the *RPL10N64* mutant (data not shown). However, the degree of suppression was less than observed with *SQT1* (Figure 4.5A). Because Sqt1p stabilizes Rpl10p, this result suggests that suppression of the Rpl10p dominant negative phenotype by *NMD3* is by a mechanism other than stabilizing wild-type Rpl10p.

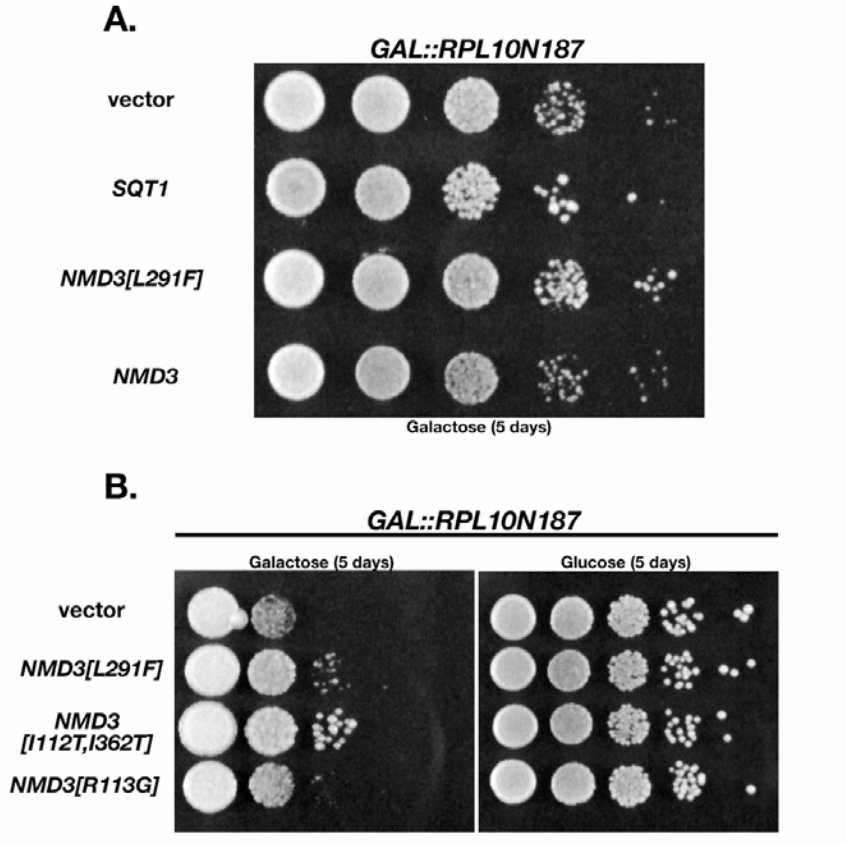

Figure 4.5 *NMD3* suppressors of *rpl10* ts mutants also suppress expression of an Rpl10p dominant negative fragment.

(A) Wild-type strain W303 containing pDEGQ187 (*GAL1-10::RPL10N187*) with either pAJ24 (vector), pSQTMYC1 (*SQT1*), pAJ415 (*NMD3[L291F]*), or pAJ538 (*NMD3*) was serially diluted onto galactose containing plates as described in Chapter 2. (B) Growth of W303 containing pDEGQ187 and either pAJ24, pAJ415, pAJ1315 (*NMD3[I112T,I362T]*) or pAJ1316 (*NMD3[R113G]*) was compared on galactose as in A. As a positive control, cells were also plated onto glucose to show that *NMD3* suppressor mutants do not alter growth under normal conditions.

When suppression by various *NMD3* alleles was compared, the I112T,I362T allele again provided the most dramatic affects with R113G being less effective (Figure 4.5B). This is consistent with the differences observed for suppression of *rpl10[G161D]*. Again, none of the *NMD3* alleles significantly suppressed the growth inhibition caused by Rpl10N64p overexpression (data not shown). These results suggest that Rpl10N187p retains some function necessary to allow suppression by *NMD3* that is not shared with the Rpl10N64 protein or with depletion of wild-type Rpl10p levels through repression.

4.3.4 *NMD3* suppressors of *rpl10* mutants restore Nmd3p shuttling

In order to determine whether *NMD3* suppressor point mutations could also suppress the cytoplasmic redistribution of Nmd3p in *rpl10* mutants, the L291F and I112R,I362T point mutations were introduced into the Nmd3AAA-GFP reporter. These "combination" alleles, Nmd3[L291F]AAA-GFP and Nmd3[I112T,I362T]AAA-GFP, were transformed into the *rpl10[G161D]* mutant, and cells were visualized by fluorescent microscopy. In contrast to Nmd3AAA-GFP, which was cytoplasmic in *rpl10[G161D]* (Figure 4.1), the introduction of the L291F or I112T,I362T mutations allowed the protein to be relocalized to the nucleus (Figure 4.6).

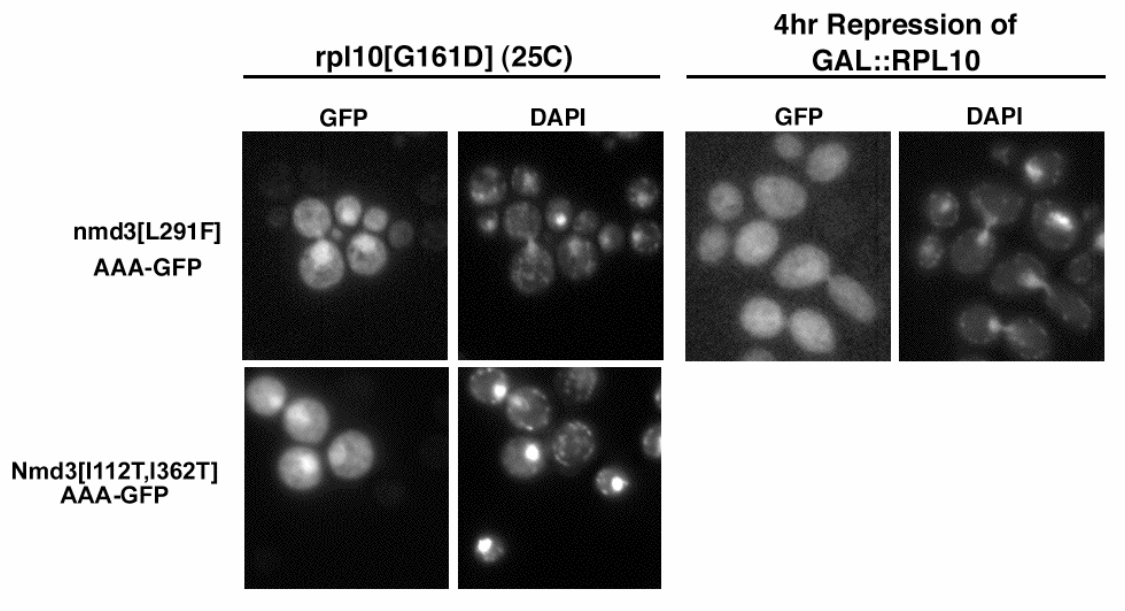

Figure 4.6 Introduction of suppressor mutations allows Nmd3-GFP to recycle in the presence of *rpl10* mutants.

AJY1657 (*rpl10[G161D]*) containing either pAJ1069 (*NMD3[L291F]AAA-GFP*) or pAJ1288 (*NMD3[I112T, I362T]AAA-GFP*) was grown into mid-log phase at 25°C prior to diluting ten-fold into fresh medium and incubating 6 hours more at the same temperature. Cells were then treated with LMB, fixed, DAPI stained and visualized as described for in vivo fluorescence in Chapter 2. For *RPL10* repression, an overnight culture of DEH221+ containing pAJ1069 (*NMD3[L291F]AAA-GFP*) was diluted ten-fold into fresh galactose-containing medium. After incubating for 4 hours, glucose was added to repress *RPL10* expression for 4 hours. Cultures were fixed and prepared for microscopy as described for the *rpl10* ts mutant.

To determine if the same suppressor mutations could bypass a complete loss of Rpl10p function, the localization of Nmd3[L291F]AAA-GFP was also examined in *RPL10* repressed cells. Under these conditions, Nmd3[L291F]AAA-GFP did not efficiently re-enter the nucleus (Figure 4.6), further indicating a requirement for some aspect of Rpl10p function that is retained in the *rpl10[G161D]* mutant. The *NMD3[L291F*] mutant on its own has no obvious detrimental effect when expressed in wild-type cells and does not block nuclear export of 60S subunits (data not shown). Thus, the redistribution of Nmd3[L291F]AAA-GFP to the nucleus in *rpl10[G161D]* mutant cells appears to be due to enhanced release of Nmd3p from cytoplasmic subunits, allowing nuclear re-entry, rather than an increased block in export (see discussion).

4.3.5 *NMD3* suppressors of *rpl10* mutants restore polysome levels

It has previously been shown that disruption of Rpl10p function leads to modest free 60S instability with a dramatic disruption in subunit joining indicated by the formation of halfmers in polysome profiles (Eisinger, Dick et al. 1997; Oender, Loeffler et al. 2003). As explained in Chapter 3, halfmers are indicative of stalled 48S initiation complexes on mRNAs that await binding by a 60S subunit. They can result either from a deficiency in the free 60S population or from disruptions in subunit joining.

The results in section 4.3.1 showed that Nmd3p is trapped on free 60S subunits in *rpl10* mutants. On the other hand, suppressor mutations in Nmd3p restore its ability to shuttle in the same *rpl10* mutant cells. Thus, to see if *NMD3* suppressors also led to recovery from translation defects observed in *rpl10* mutants, polysome profile analysis of an *rpl10* mutant in the presence of an *NMD3* suppressor was carried out. These results clearly show a recovery of polysome levels with a significant reduction in halfmers in the presence of *NMD3[I112T,I362T]* as compared to both vector alone or low-copy overexpression of wild-type Nmd3p (Figure 4.7). Although this result is not surprising

when considering the significant recovery of growth in these cells, it is unusual that this occurs through *NMD3*, which is not known to play a role in translation. These results suggest that there is a two-tiered mode of recovery (1) Nmd3p suppressor alleles, rather than being trapped on cytoplasmic subunits and blocking joining, are released more readily allowing 60S to become "translation competent" (2) in the presence of renewed Nmd3p shuttling, free 60S subunits that were accumulating and being slowly degraded in the nucleus are exported more efficiently. Thus enhanced release of Nmd3 suppressor proteins from cytoplasmic free 60S leads to enhanced polysome levels. This ties in well with the observations that Rpl25-eGFP accumulates in the nucleus when Rpl10p or Sqt1p function is disrupted and that newly made subunits more slowly enter the translational pool in *sqt1* mutants. Together these results show that recovery of export is a direct effect of Nmd3p release from the cytoplasmic pool of free 60S subunits. Additionally, subunits containing mutant Rpl10p, although defective for wild-type Nmd3p release, are still capable of functioning in subunit joining if Nmd3p is released through an alternative mechanism such as partially disrupting the binding interface with suppressor mutations. On the other hand, subunits devoid of Rpl10p are defective for release of Nmd3p as well as for subunit joining.

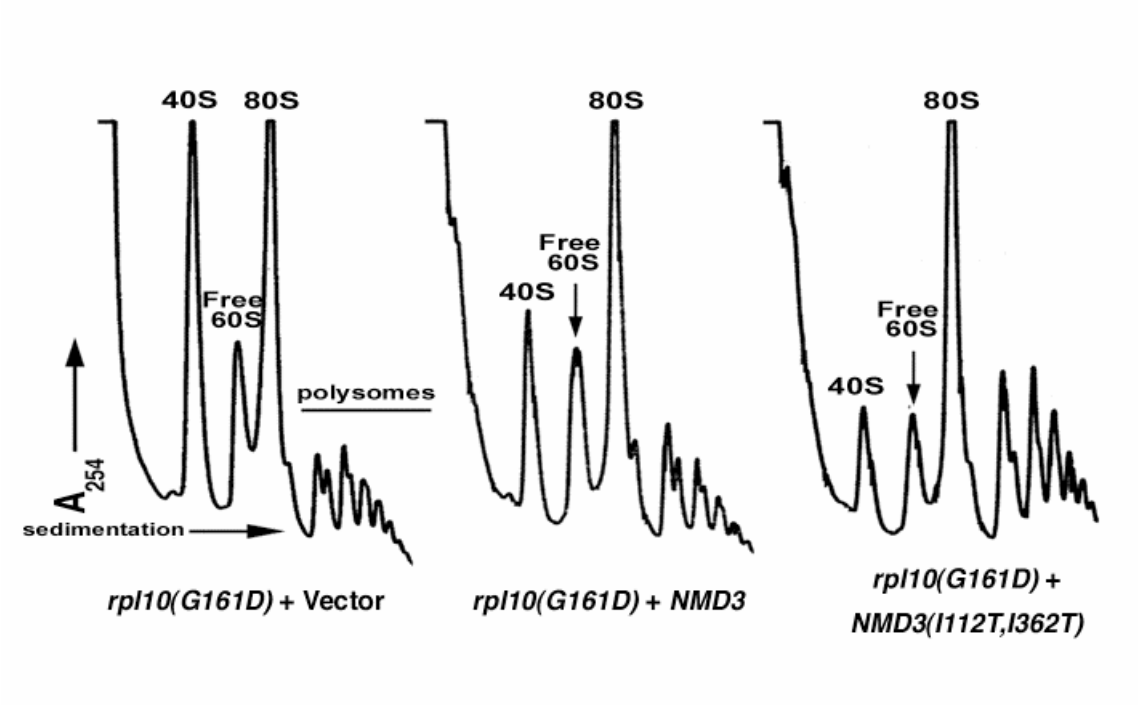

Figure 4.7 *NMD3* suppressors partially restore translation levels in *rpl10* mutant cells.

Cultures of AJY1657 (*rpl10[G161D]*) cells carrying empty vector (pRS425), pAJ538 (*NMD3-myc*) or pAJ1315 (*NMD3[I112T, I362T]-myc*) were harvested after growth at 37°C and sucrose density sedimentation analysis was carried out as described in Chapter 2. Data contributed by Matt West.

4.3.6 Overexpression of *NMD3* supports 60S export in Rpl10p deficient cells

Work presented here and that of others (Eisinger, Dick et al. 1997; Gadal, Strauss et al. 2001) has shown that *RPL10* repression and *rpl10* ts mutants each cause similar defects in ribosome export and subunit joining. However, high-copy *NMD3* and certain *NMD3* point mutants suppress the growth defect of *rpl10* mutants but not the inviability of cells that arises when *RPL10* is repressed ((Karl, Onder et al. 1999; Zuk, Belk et al. 1999) and data not shown). From these results it is obvious that Nmd3p cannot substitute for Rpl10p, an essential ribosomal protein. Nevertheless, it was possible that overexpression of Nmd3p could suppress specific defects, such as the block in nuclear export of 60S subunits, that result from loss of Rpl10p.

To address this, I examined if the overexpression of Nmd3p could alleviate the nuclear export block of 60S subunits in *RPL10* repressed cells. *RPL10* expression was repressed for 4 hours and Rpl25-eGFP localization in the presence or absence of ectopically expressed Nmd3p was monitored. Consistent with observations made in Chapter 3, Rpl25-eGFP accumulated in the nucle(ol)us of these repressed cells in the presence of endogenous levels of Nmd3p (Figure 4.8). Remarkably, expression of Nmd3p from a high-copy (2μ) plasmid led to relocalization of Rpl25-eGFP to the cytoplasm (Figure 4.8), suggesting that Nmd3p can bypass the requirement for Rpl10p in nuclear export of 60S. On the other hand, Nmd3p expressed from a low-copy (centromeric) vector or low-copy *NMD3[L291F]* did not support redistribution of Rpl25-eGFP to the cytoplasm (Figure 4.8). These results show that, in the absence of newly synthesized Rpl10p, the 60S export defect can be alleviated by overexpression of *NMD3*. This suggests that the export defect in these cells is indirect.

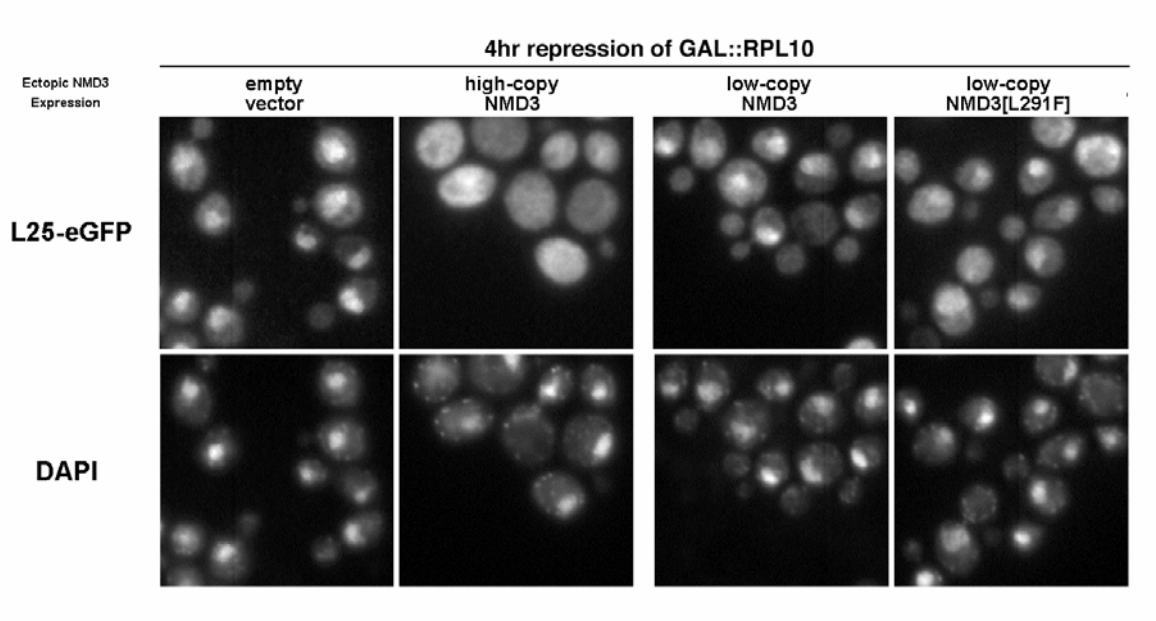

Figure 4.8 Overexpression of Nmd3p bypasses a requirement for Rpl10p in 60S export.

DEH221+ (*GAL1-10::RPL10*) cells containing pASZ11-RPL25-eGFP (*RPL25-eGFP*) with either pRS315 (empty vector), pAJ410 (*NMD3 2μ*), pAJ123 (*NMD3 CEN*) or pAJ415 (*NMD3[L291F] CEN*) were grown overnight in galactose-containing medium and diluted four-fold into glucose-containing medium to repress *RPL10* expression. After 4 hours, cells were prepared for in vivo fluorescence visualization as described in Chapter 2.

Suppression of 60S export in *RPL10* repressed cells by high-copy Nmd3p but not *NMD3[L291F]* suggests that their mechanism of suppression may be different. As observed here, high-copy *NMD3* bypasses the release defect entirely. On the other hand, *NMD3[L291F]* is released more readily but requires at least partially functional Rpl10p to mediate this release. The lack of suppression of the 60S export defect in *RPL10* repressed cells by *NMD3[L291F]* is consistent with the suggestion that *NMD3[L291F]* facilitates release of Nmd3p from Rpl10p associated ribosomes but does not directly enhance 60S subunit export. Additionally, this finding may indicate that subunit joining, occurring only in the presence of Rpl10p, is a prerequisite for Nmd3p release.

4.3.7 Nmd3p suppressors of *rpl10* have a reduced affinity for the 60S subunit

The observation that *NMD3* suppressor alleles are capable of accumulating in the nucleus in *rpl10* mutants suggested that the mechanism of suppression was through facilitating release of Nmd3p from cytoplasmic 60S subunits. Such enhanced release could be due to bypass of the dependence of Nmd3p release on a particular Rpl10p function, possibly by lowering the affinity of mutant Nmd3p for the 60S subunit. To test this idea, a native gel assay (Dahlberg and Grabowski 1990) was adapted to qualitatively measure the affinity of Nmd3p for 60S subunits in vitro. Wild-type and mutant Nmd3 proteins were purified as GST fusions from yeast and wild-type 60S subunits were prepared by dissociating 80S ribosomes as described in Chapter 2. 60S subunits were then incubated with purified Nmd3p under conditions to promote binding, and complexes were electrophoresed on native 0.5% agarose/2.5% polyacrylamide gels as also described in Chapter 2. The migration of 60S subunits was determined by ethidium bromide staining rRNA and the position of Nmd3p was monitored by western blotting. As shown in figure 4.9A, in this gel system 60S subunits migrate as a distinct species (lane 1), whereas free Nmd3p migrates into the gel as a diffuse band with lower relative mobility

(lane 2). However, when pre-incubated with 60S subunits, wild-type Nmd3p co-migrated with 60S subunits (Figure 4.9A, lanes 4 and 5). On the other hand, when increasing amounts of Nmd3(I112T, I362T)p were incubated with 60S subunits, no binding was observed (Figure 4.9A, lanes 8 and 9). Nmd3(L291F)p, which was a slightly weaker suppressor of *rpl10* mutants as determined by growth assays (Figure 4.4) also bound free 60S subunits but approximately two to three times more mutant protein was required to achieve levels of binding similar to that of wild-type Nmd3p (Figure 4.9A, lanes 13 and 14). As a negative control, the Nmd3(V340D) loss of function mutant protein showed no detectable binding to 60S subunits (Figure 4.9A, lanes 17 and 18). This mutant, identified in a screen for *nmd3* null mutants, does not support growth and binds only weakly to 60S subunits as measured by co-immunoprecipitation (data not shown and figure 4.10, respectively).

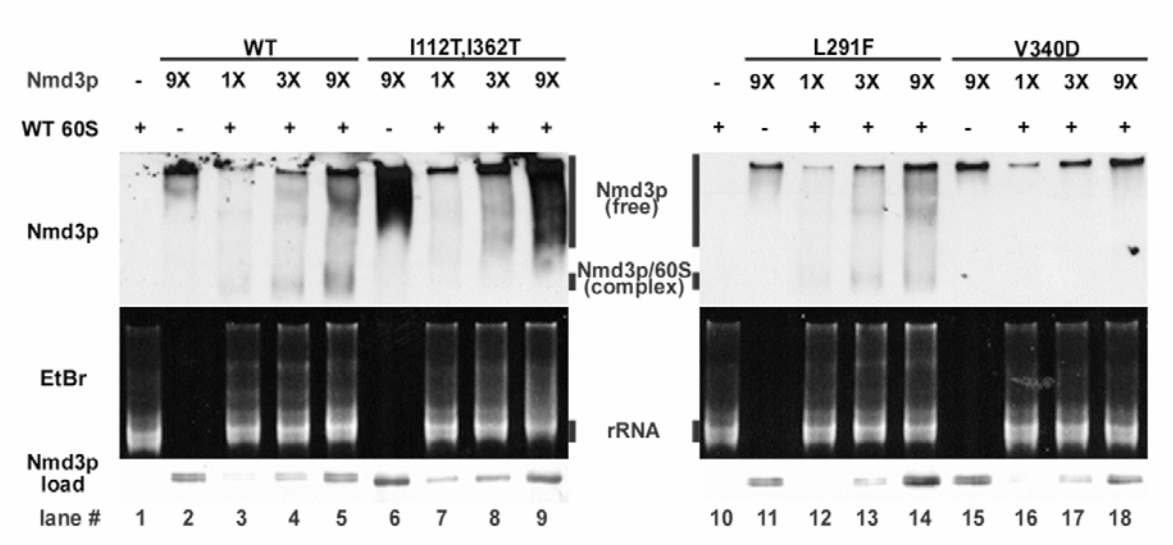

Figure 4.9 Nmd3p suppressors of *rpl10* bind 60S with less affinity than wild-type in vitro.

Three-fold increasing amounts (1X~30ng) of affinity purified GST-Nmd3p wild-type, [I112T,I362T] suppressor, [L291F] suppressor, or [V340D] loss of function mutant proteins were incubated alone or with purified 60S subunits and run on 2.5% acrylamide/0.5% agarose composite gels as described in Chapter 2. The position of Nmd3p and 60S subunits was determined by western blotting using α-GST and ethidium bromide staining, respectively.

Because Nmd3(I112T, I362T)p did not appreciably bind purified subunits in this reconstituted system, the affinity of this mutant for 60S was assayed under more in vivo-like conditions. Oligomeric c-myc-tagged wild-type and mutant Nmd3p proteins were expressed in vivo, immunoprecipitated and assayed for copurification of 60S subunits (Figure 4.10). Indeed, Nmd3(I112T, I362T)p, as well as Nmd3(L291F)p and wild-type Nmd3p, efficiently co-immunoprecipitated 60S subunits, whereas only trace amounts of 60S were associated with Nmd3(V340D)p (Figure 4.10). The difference in binding in these two assays could reflect a difference in affinity for nascent versus mature subunits. Nevertheless, these results show that Nmd3p suppressors have reduced affinity for 60S subunits.

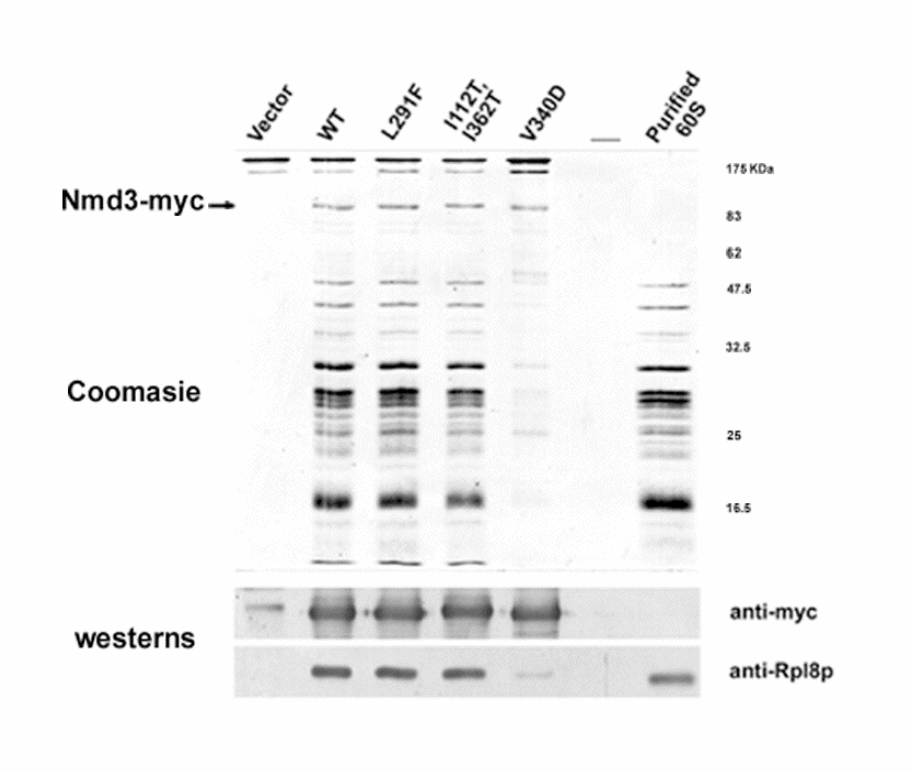

Figure 4.10 Nmd3p suppressors bind 60S with similar affinity to wild-type under in vivo-like conditions.

Extracts were made from strain W303 containing empty vector (pRS425), pAJ538 (*NMD3-myc*), pAJ1315 (*NMD3[I112T,I362T]-myc*), pAJ1070 (*NMD3[L291F]-myc*), or pAJ1299 (*nmd3[V340D]-myc*) and α-myc immunoprecipitations performed as described in Chapter 2. Samples and a purified 60S protein control were run on a 12% SDS-PAGE gel and western blotting performed against Nmd3-myc using α-myc or the 60S protein Rpl8p using α-Rpl8p. After transfer, the gel was stained with Coomasie Blue in order to visualize other 60S ribosome components. Data contributed by Matt West.

Suppression of *rpl10* mutants is correlated with reduced Nmd3p binding to 60S subunits in vitro. However, the null Nmd3(V340D)p showed that only minimal 60S binding under in vivo-like conditions did not provide suppression, indicating that interaction with the 60S subunit must be retained to some extent for Nmd3p activity and suppression of *rpl10*. These findings provide physical evidence to support the notion that enhancing the release of Nmd3p from subunits can bypass the defect of *rpl10* mutants.

4.3.8 Rpl10p dominant negative fragments stably associate with 60S in the presence of Lsg1p dominant negative mutants

As mentioned in the introduction of this dissertation, Lsg1p is a late-acting cytoplasmic GTPase involved in 60S subunit biogenesis/export. Interestingly, *lsg1* mutants lead to a blockage in 60S subunit nuclear export indicated by accumulation of the Rpl25-eGFP reporter protein in the nucle(ol)us (Kallstrom, Hedges et al. 2003). This suggests that Lsg1p acts at one of the last steps in 60S subunit maturation prior to incorporation of 60S into the translation apparatus. More recently, a screen for dominant negative *lsg1* mutants was carried out (West and Johnson, unpublished). This screen identified mutations, including *LSG1[K349T]*, in the Walker A motif that is required for binding and catalysis of GTP to GDP (reviewed in Saraste et al, 1990). Interestingly, the phenotypes observed for Lsg1p dominant negatives are closely shared with those observed in *sqt1* and *rpl10* mutants. Furthermore, these factors act late in the biogenesis pathway, and mutants of all three lead to entrapment of Nmd3p on cytoplasmic 60S subunits. Together these observations suggest that mutations in Rpl10p, Sqt1p or Lsg1p lead to a blockage of a late cytoplasmic step in 60S maturation that prevents release of Nmd3p.

Since Rpl10p and Sqt1p are likely acting in conjunction with Lsg1p, the possibility of Sqt1p and Rpl10p entrapment on Lsg1p dominant negative bound subunits

was addressed. Co-immunoprecipitations of *GAL10* driven oligomeric cmyc-tagged Lsg1p wild-type or two different dominant negative mutants showed enhanced Sqt1p binding (Figure 4.11A).

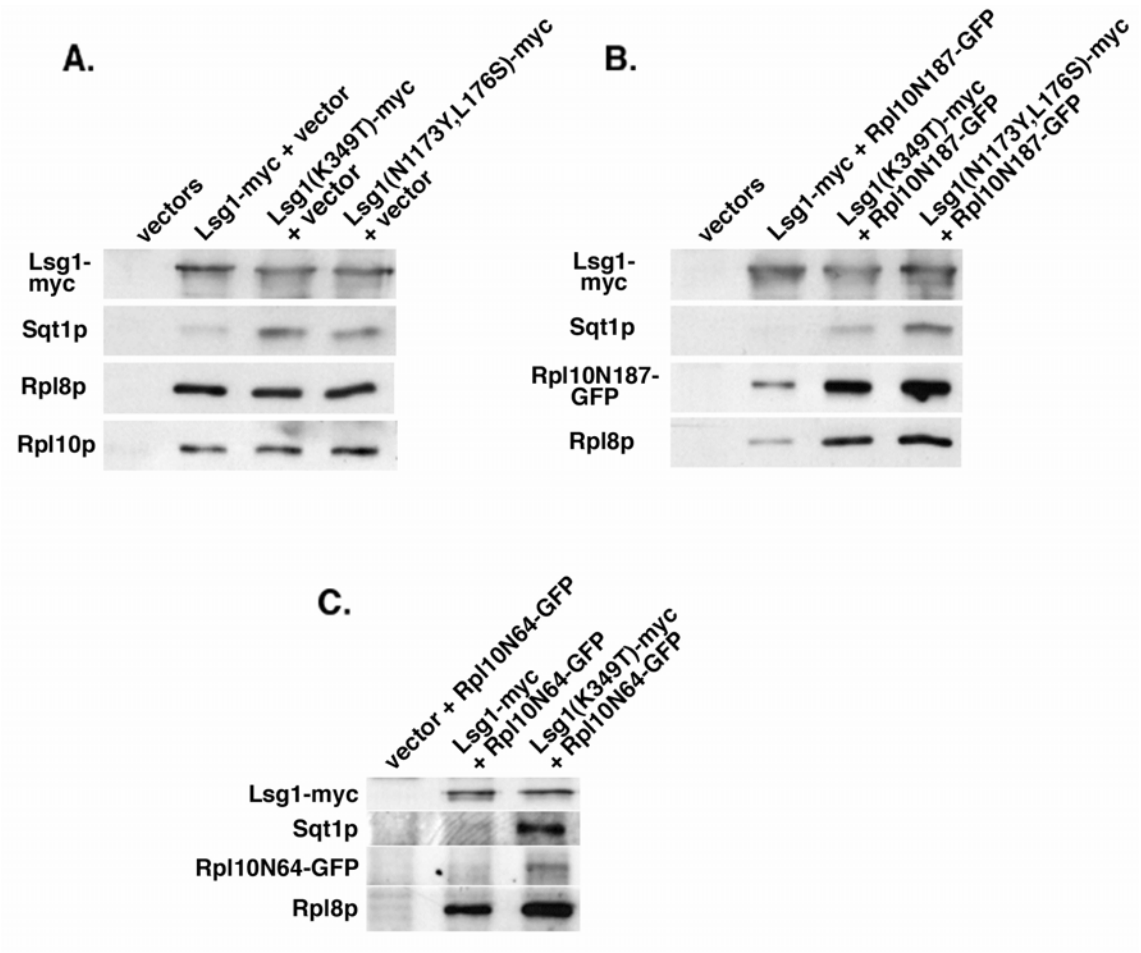

Figure 4.11 Dominant negative mutants of the cytoplasmic GTPase Lsg1p trap wild-type Sqt1p and Rpl10p dominant negative fragments on 60S.

Extracts were made from wild-type strain CH1305 containing (A) empty vector (pRS426) with either pRS425 (empty), pAJ1107 (*GAL10::LSG1-myc*), pAJ1108 (*GAL10::LSG1[K349T]*) or pAJ1105 (*GAL10::LSG1[N173Y,L176S]*) or (B) empty vectors (pRS425 and pRS426) or pAJ1100 (*GAL10::RPL10N187-GFP*) with either pAJ1107, pAJ1108 or pAJ1105 and α-myc immunoprecipitations were performed as described in Chapter 2. (C) Extracts were made from CH1305 containing pRS425 and pAJ1402 (*GAL10::RPL10N64-GFP*), pAJ1107 and pAJ1402, or pAJ1108 and pAJ1402 and immunoprecipitations were carried out as in A and B. Immunoprecipitated samples were run on a 12% SDS-PAGE gel and western blotting performed using α-myc, α-Sqt1p, α-Rpl8p, α-Rpl10p or α-GFP antibodies as described in Chapter 2.

Given that Sqt1p was enriched on Lsg1p dominant negative bound 60S (Figure 4.11A) and that Rpl10p dominant negative fragments sequester Sqt1p (Chapter 3), I assayed the Lsg1p mutant-bound 60S for the presence of Rpl10p dominant negative fragments. This was carried out by co-expressing Lsg1p wild-type or mutant proteins with either *GAL10* driven GFP-tagged *RPL10N187* or *RPL10N64*. Although these dominant negative mutants do not normally show stable binding to 60S subunits, Rpl10N187p (Figure 4.11B) and Rpl10N64p (Figure 4.11C) were co-immunoprecipitated by dominant negative Lsg1p. At the same time, Rpl10p dominant negative fragments seemed to decrease binding of wild-type Lsg1p to subunits. This suggests that Sqt1p loads Rpl10p in the presence of Lsg1p and/or that Sqt1p release is normally concomitant with activation of Lsg1p activity. Without Lsg1p activation, Sqt1p, Rpl10p and Nmd3p are trapped on cytoplasmic subunits.

Since Rpl10p, Lsg1p and Nmd3p are transiently together on the subunit in the cytoplasm as indicated by their co-immunoprecipitation with Lsg1p under normal conditions (Figure 4.11 and (Kallstrom, Hedges et al. 2003)), release of Lsg1p and Nmd3p likely occurs after the point of Sqt1p release and Rpl10p insertion into the subunit. Thus this event is possibly modulated by an as yet unknown factor, such as a protein that resides on the 48S initiation complex prior to 60S binding.

4.4 DISCUSSION

In this body of work, the genetic interactions between *RPL10* and *NMD3* and the requirement for Nmd3p as the export adapter for the large subunit led to the examination of the localization of Nmd3p in *rpl10* and *sqt1* mutants. It was observed that Nmd3p remained cytoplasmic in these mutants. To examine this in more detail, an Nmd3p reporter (Nmd3AAA-GFP) in which three hydrophobic residues within its leucine-rich NES had been changed to alanines was used. This mutant has an export defect causing it

to accumulate in the nucleus. This mutant protein cannot support cell growth if it is the only copy of Nmd3p in the cell and consequently must be expressed ectopically. In *sqt1* and *rpl10* mutants, Nmd3AAA-GFP was retained in the cytoplasm, whereas it accumulated in the nucleus in wild-type cells. These results indicate that Nmd3p shuttling is blocked in *rpl10* and *sqt1* mutants. To support this conclusion the ability of genomically expressed wild-type Nmd3p fused to GFP to recycle to the nucleus under conditions of *RPL10* repression was also examined. In this case, using LMB to trap Nmd3p in the nucleus if it could shuttle, cytoplasmic retention of Nmd3-GFP was again observed. Because Nmd3p is required for 60S subunit export, its retention on cytoplasmic subunits would result in a failure to continue export of 60S subunits. Together, these results suggest that *sqt1* and *rpl10* mutants affect 60S export indirectly by preventing Nmd3p recycling to the nucleus.

RPL10 and *NMD3* show strong genetic interaction. In particular, a dominant allele of *NMD3* (L291F) suppresses the temperature sensitivity of *rpl10[G161D]* (Karl, Onder et al. 1999). Glycine 161 is at the interface of Rpl10p and 25S rRNA and may affect its association with the 60S subunit. To examine the mechanism of suppression by *NMD3[L291F]*, this mutation was incorporated into the Nmd3AAA-GFP reporter. Notably, the L291F or I112T,I362T mutations allowed the reporter to accumulate in the nucleus, thus partially overcoming the retention in the cytoplasm due to the *rpl10[G161D]* mutation. Additionally, neither *NMD3[L291F]* nor *NMD3[I112T,I362T]* alone inhibit 60S subunit or Nmd3p export (data not shown). These results, in conjunction with the same alleles showing weaker affinity for subunits in vitro, suggest that these *NMD3* suppressors act by facilitating release of Nmd3p from *rpl10[G161D]*-containing 60S subunits in the cytoplasm. Identification of Nmd3p partial loss-of-function mutants that also suppress *rpl10[G161D]* corroborates this mechanism of

suppression. This supports the hypothesis that dominant alleles of *NMD3* result from a partial loss of function that facilitates Nmd3p release rather than an allele-specific compensatory function that enhances Nmd3p interaction with the subunit.

Although high copy *NMD3* cannot suppress the lethal effect of repressing *RPL10* expression, it does suppress the nuclear retention of Rpl25-eGFP seen when *RPL10* is repressed. This is inconsistent with Rpl10p being a necessary binding site for Nmd3p on the subunit (Gadal, Strauss et al. 2001) and, instead, suggests that repression of *RPL10* leads to cytoplasmic retention of Nmd3p on 60S subunits, thereby indirectly affecting 60S export. High copy *NMD3* would provide a free pool of Nmd3p available for nuclear re-entry that could support export, even if release of Nmd3p from subunits in the cytoplasm were inhibited. It is significant that *NMD3[L291F]* did not support export of Rpl25-eGFP when *RPL10* was repressed, which favors the idea that *NMD3[L291F]* facilitates release of Nmd3p from the cytoplasmic subunit that contains mutant Rpl10p but cannot readily bypass the loss of Rpl10p from the subunit.

The effects on Nmd3p shuttling described here for *rpl10* and *sqt1* mutants are similar to results obtained with the cytoplasmic G-protein Lsg1p (West and Johnson, unpublished). Lsg1p was originally identified on 60S subunits immunoprecipitated with myc-tagged Nmd3p (Kallstrom, Hedges et al. 2003). Work from our lab showed that overexpression of dominant negative *LSG1* mutants leads to nuclear entrapment of 60S subunits and inhibition of Nmd3p shuttling leading to retention of Nmd3p on cytoplasmic subunits (West and Johnson, unpublished), similar to the effects of *sqt1* and *rpl10* mutants shown here. The growth inhibition as well as the nuclear accumulation of Rpl25-eGFP in *lsg1* mutants can be suppressed by high-copy *NMD3*, indicating that the defect in recycling Nmd3p leads to the defect in 60S biogenesis and export as observed in *rpl10* and *sqt1* mutants. Illustration 4.2 provides a model for the interaction of Sqt1p,

Rpl10p, and Lsg1p with the 60S subunit to coordinate release of the nuclear export adapter Nmd3p in order to maintain the 60S export pathway.

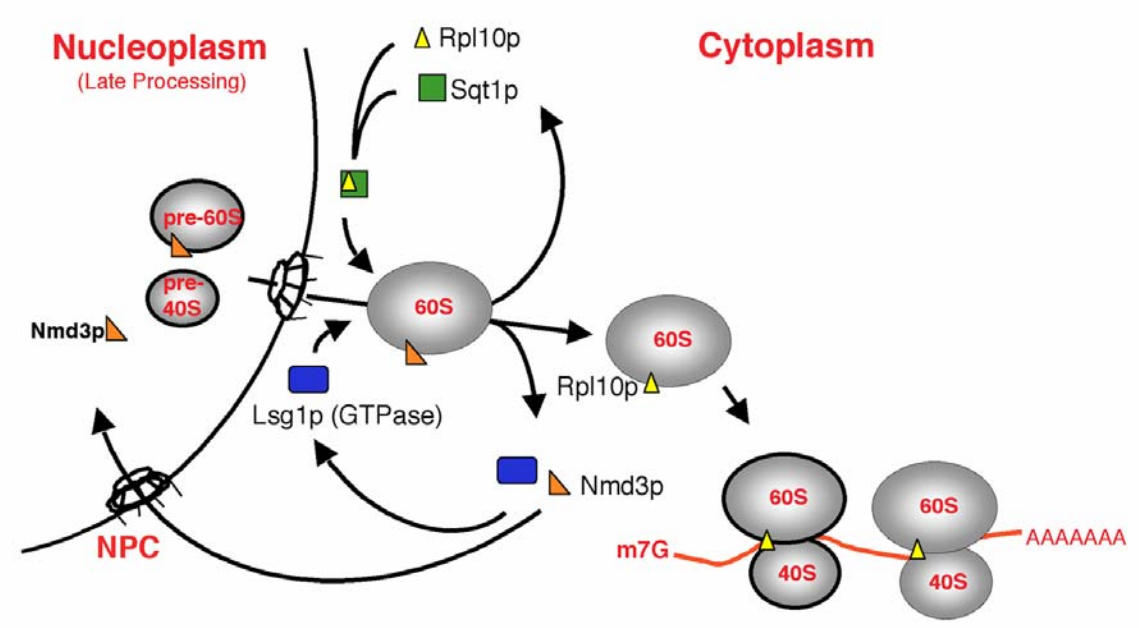

Illustration 4.1 Model for Sqt1p, Rpl10p and Lsg1p modulated release of Nmd3p from cytoplasmic 60S to maintain Nmd3p nuclear recycling and large subunit export.

Nmd3p binds the subunit in the nucleus and facilitates nuclear export though the Crm1p-mediated pathway. Once in the cytoplasm, Sqt1p loads Rpl10p onto the subunit possibly through targeting of these two proteins to the Nmd3p binding site. Subsequently, Rpl10p may provide the signal for Lsg1p loading. Attachment of Lsg1p would then activate its GTPase activity to provide the energy required to modulate Nmd3p release. Alternatively, Lsg1p may modulate insertion of Rpl10p into the 60S subunit leading to the subsequent release of Sqt1p. It would not be until encountering another factor, possibly residing on the 48S initiation complex, that Lsg1p and Nmd3p are released at the point of subunit joining.

The common effects on Nmd3p shuttling, by perturbing either Rpl10p or Lsg1p function, suggests that release of Nmd3p from 60S subunits in the cytoplasm requires the presence of Rpl10p and is mediated by Lsg1p. Rpl10p occupies a functionally important site on the large subunit. It is positioned between the central protuberance and the GTPase stalk, and it is in close proximity to the A-site. The GTPase stalk of bacterial ribosomes provides a binding platform for eEF1A-GTP-aa-tRNA ternary complexes during translation elongation to modulate the loading of charged tRNAs into the A site (Uchiumi, Honma et al. 2002). This site may similarly recruit Lsg1p to modulate the loading and/or unloading of factors such as Rpl10p in this region prior to translation. Lsg1p may sense the correct assembly of Rpl10p in the subunit as a prerequisite for release of Nmd3p, driven by a GTP-dependent conformational change in the subunit or Nmd3p. Such a mechanism could provide a quality control check of subunit structure before its release into the active pool of translating ribosomes.

Chapter 5: Characterization of the interaction between Nmd3p and the 60S subunit

5.1 INTRODUCTION

I began my thesis work with the intention of studying recruitment of Nmd3p to the 60S subunit for nuclear export. To this end, I characterized the interaction of Nmd3p with the 60S subunit by mapping the 60S-binding domain in Nmd3p and by trying to determine the binding site for Nmd3p on the 60S subunit. Furthermore, I also characterized the export sequence of Nmd3p to develop reagents for studying assembly of the export complex. When it was reported that Rpl10p recruits Nmd3p to the subunit, I devoted a considerable effort to understand the interactions of Nmd3p with Rpl10p. As discussed in Chapters 3 and 4, my work provided an alternative explanation for the Nmd3p-Rpl10p interactions: that Rpl10p is needed for release of Nmd3p in the cytoplasm. Consequently, the problem of how Nmd3p is recruited to the subunit in the nucleus remains an open question. Although this analysis of Nmd3p-60S binding is not yet complete, I did develop novel assays for studying these interactions further.

Thus, this chapter provides a more detailed functional analysis of the domains of Nmd3p required for its role in nuclear export of the large ribosomal subunit as well as preliminary analysis of the components of the subunit that facilitate this interaction. Using various truncation mutants, work presented here will first identify the domain within Nmd3p that is required for 60S binding. Point mutants will then be used to study the properties of the Nmd3p NES that give rise to its export function through interaction with the Crm1p export receptor. The chapter will also provide initial identification of the 60S components that are required for Nmd3p binding. Results from this chapter, in combination with results from Chapters 3 and 4, will provide evidence that the current

model for Nmd3p binding to the 60S subunit via Rpl10p is incorrect. The discussion of this chapter will tie together the multiple results that provide a preliminary description of the Nmd3p/60S interaction and will address future work that will be necessary to attain a more accurate depiction of this binding interface.

5.2 BACKGROUND

Our lab became interested in *NMD3* when it was found to be synthetic lethal (SL) with *XRN1*, the major cytoplasmic 5'-3' exoribonuclease in eukaryotic cells (Ho and Johnson 1999). The *nmd3-1* allele found in this SL screen was a frameshift mutant containing six, non-ORF coded amino acids in place of 50 amino acids from the C-terminus of the Nmd3 protein. Interestingly, the *nmd3-1* allele was found to elicit a dominant negative phenotype. Despite its initial isolation in the *XRN1* screen mentioned above, *NMD3* was not found to be involved in mRNA turnover (Ho and Johnson 1999). Instead our lab determined that Nmd3p's primary functional role is in the export of the large subunit export as discussed in the introduction to this thesis (Ho, Kallstrom et al. 2000).

The core of the Nmd3 protein sequence is highly conserved in both eukaryotes and archaebacteria but not eubacteria ((Ho and Johnson 1999) and illustration 5.1). To deal with the added complexity of the nuclear envelope, the eukaryotic version of Nmd3p includes an additional C-terminal extension that contains the nuclear localization signal (NLS) and nuclear export signal (NES) sequences. The reason for a prokaryotic factor to take on the role of an essential nuclear export factor in eukaryotes has yet to be determined. Nonetheless, the basic export function of Nmd3p is conserved in frogs, humans and yeast (reviewed in (Johnson, Lund et al. 2002)).

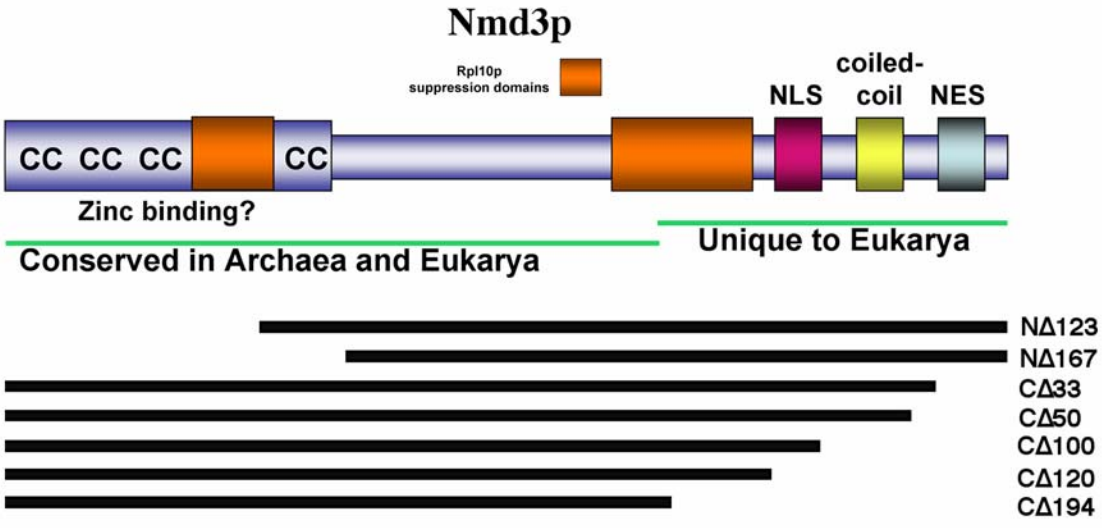

Illustration 5.1 Cartoon of Nmd3p primary structure and truncation mutants used throughout Chapter 5.

In eukaryotic cells ribosomal subunits are assembled in the nucleolus and must be transported through the nuclear pore complexes (NPC) to the cytoplasm. Export of Nmd3p bound 60S subunits occurs via Nmd3p mediated interaction with the export receptor Crm1p (reviewed in (Johnson, Lund et al. 2002)). Additionally, Nmd3p binds both nascent and mature free 60S subunits, but appears to be released prior to 60S loading onto the 48S initiation complex since Nmd3p is not found in translating polysomes (Ho and Johnson 1999).

In yeast, Nmd3p is 518 amino acids in length. It contains a highly acidic region within its C-terminus (amino acids 470-518) that harbors the NES that is essential for protein export via the Crm1p receptor pathway ((Ho, Kallstrom et al. 2000) and illustration 5.1). Based on its biochemical properties, it is predicted to form an amphipathic α-helical structure. Upstream of the NES sequence is a putative coiled-coil region (aa426-465) thought to mediate intra- or inter-molecular protein interactions (reviewed in Burkhard, 2001 and illustration 5.1). It has been suggested that this domain contains a second NES (NES2) (Gadal, Strauss et al. 2001). This coiled-coil domain may interact with other proteins to facilitate the assembly of the "export complex" or to fold against the NES to regulate its accessibility to modulate export function. Additionally, Nmd3p contains a highly basic NLS region (amino acids 399-419) ((Ho, Kallstrom et al. 2000) and illustration 5.1) that mediates the import of Nmd3p into the nucleus in a Kap123p-dependent manner (Sydorskyy, Dilworth et al. 2003). At the N-terminus of the Nmd3 protein are four cysteine-x-x-cysteine repeats reminiscent of zinc binding motifs found in RING fingers and type IV zinc fingers (Mackay and Crossley 1998; Teakle and Gilmartin 1998). This potential zinc-coordinating domain in Nmd3p is likely required for protein-RNA and/or protein-protein interaction with the 60S subunit.

Nmd3p binding to 60S can be reconstituted in vitro (Ho, Kallstrom et al. 2000). Reconstitution of the yeast export complex consisting of Nmd3p, Crm1p and RanGTP has also been accomplished, but not in the presence of 60S binding (Kallstrom and Johnson, unpublished). A similar observation was made with human export complex components (Thomas and Kutay 2003). Furthermore, neither Crm1p nor RanGTP have been purified with any 60S particle isolated by large-scale proteomic analysis to date (reviewed in (Fromont-Racine, Senger et al. 2003)). Together, these data suggest that other transiently associating factors or a specific 60S conformation in the nucleus is required to facilitate export complex formation on the subunit. This may include factors necessary for modulating intramolecular release of the Nmd3p NES from the coiled-coil domain to provide a binding surface for Crm1p.

Nmd3p-Rpl10p interaction suggests that Nmd3p directly interacts with Rpl10p, however other data would indicate otherwise. First, mutations within amino acids 279-336 of Nmd3p, that exchange hydrophobic residues for those having bulky sidechains, were found to be dominant suppressors of an *rpl10* temperature sensitive (ts) allele (Karl, Onder et al. 1999). Second, Rpl10p and Nmd3p were reported to co-purify when expressed in *E. coli* (Gadal, Strauss et al. 2001). However, I have not been able to demonstrate such a specific interaction. In my work, both of these proteins were insoluble in *E. coli*. In addition, GST-Nmd3p does not show specific interaction with in vitro translated Rpl10p. Furthermore, Nmd3p and Rpl10p do not show two-hybrid interaction ((Karl, Onder et al. 1999) and data not shown).

Rpl10p was suggested to load onto the 60S subunit in the nucleus to recruit Nmd3p. This was based on the observation that the GFP tagged Rpl10N64p dominant negative fragment localizes to the nucleus (Gadal, Strauss et al. 2001). However, this also appears to be a misinterpretation of results since immunofluorescent localization of

myc-tagged Rpl10N64p does not show nuclear localization, and this fragment of Rpl10p does not stably associate with subunits (Chapter 3). Even more dramatic was the finding that increasing Nmd3p levels in cells can support nuclear export of subunits when *RPL10* is repressed (Chapter 4). Together, these results support a role for Rpl10p downstream of Nmd3p loading on nuclear pre-60S.

5.3 RESULTS

5.3.1 The amino-terminus of Nmd3p is required for 60S interaction

Domain prediction databases such as Prosite (http://www.expasy.org/prosite/) were initially used to identify potential cellular localization elements in Nmd3p structure based on primary sequence alignments. To map the 60S binding domain of Nmd3p, various N- and C-terminal truncation fragments were subcloned out of wild-type *NMD3* sequence and tagged at their C-terminal ends with an oligomeric c-myc epitope (Illustration 5.1). They were then assayed for 60S binding using either co-immunoprecipitation (Ho and Johnson, unpublished) or sucrose velocity gradient sedimentation (data not shown). Unfortunately, these assays had high background and were not able to clearly distinguish between bound and unbound proteins. Thus, to resolve these issues and to expedite sample processing, I developed a new binding assay using native gel electrophoresis.

This assay utilized composite gels (0.5% agarose, 2.5% polyacrylamide) similar to those in Chapter 4. However, the magnesium concentration of the gels was increased to 16mM, and cycloheximide was added to stabilize 80S couples and polysomes. Extracts were prepared from cells expressing myc-tagged full-length or N-terminally truncated forms of Nmd3p. To increase resolution, samples were mixed with pre-melted 2X agarose composite gel loading buffer instead of the sucrose loading-buffer used

previously as described in Chapter 2. Once each sample had solidified in dry wells, running buffer was added, and the gel was run for 4 hours with continual cooling.

The myc-tagged full-length Nmd3p/60S complex ran as a discrete species by western blotting as compared to the "laddering" of subunits observed by Coomasie Blue staining, which represents 80S and polysome structures (Figure 5.1, lane 2 and (Dahlberg and Grabowski 1990)). Although not detectable by Coomasie staining here, previous assays have shown that 60S runs as a species just below the first "heavy" band representing both 80S and a single polysome (1X) on ethidium bromide stained gels (Figure 5.1 and (Dahlberg and Grabowski 1990)). The bands above 80S represent 2X, 3X, 4X and 5X polysomes, respectively. The discrete full-length Nmd3p band comigrated with the previously determined 60S position, indicated by asterisks in lane 2 (Figure 5.1, Coomasie and western). Similarly, an Nmd3p truncation missing 123 amino acids from its N-terminus, including three cys-x-x-cys motifs, retained binding to 60S (lane 3, denoted by asterisks). Deletion of 167 amino acids, including all four cys-x-x-cys motifs and the N-terminal suppressor domain, completely abolished 60S binding as indicated by lack of comigration between this truncation protein and 60S (lane 4). From these results, it can be concluded that the N-terminus of Nmd3p, which contains a putative zinc-coordinating domain, is required for 60S binding. However, whether removal of the last cys-x-x-cys motif or of the N-terminal suppressor domain leads to the loss of 60S binding remains to be determined (see discussion).

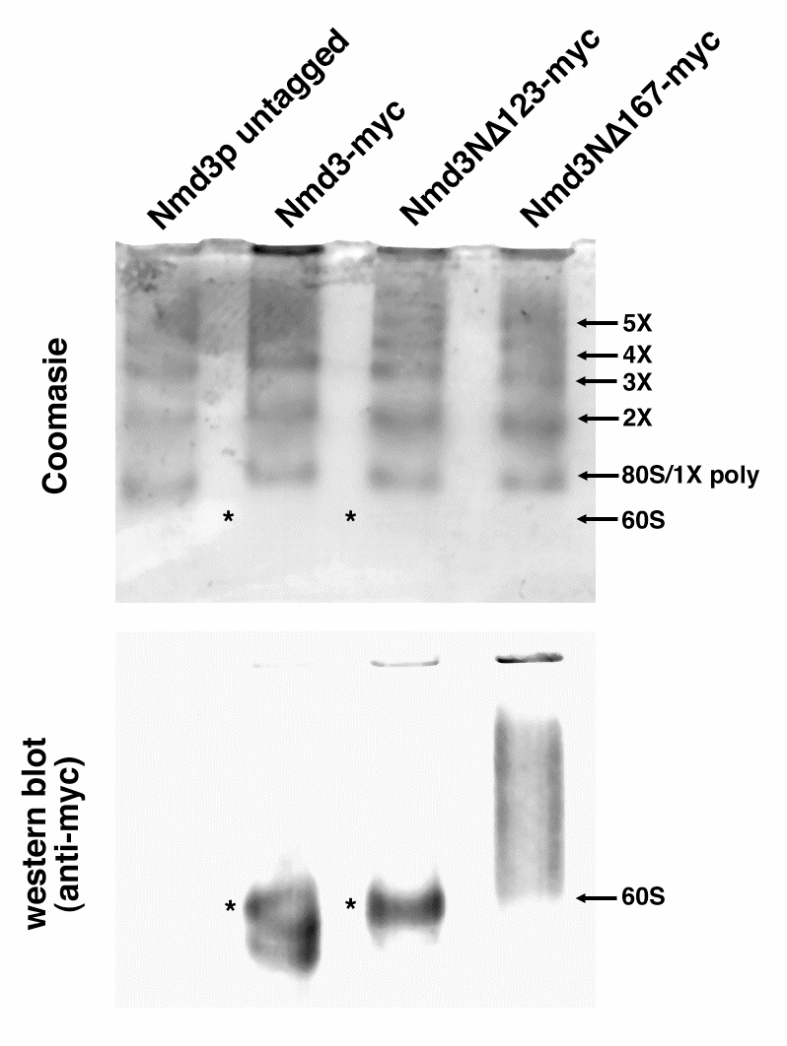

Figure 5.1 Nmd3p N-terminal truncation mutants are deficient for 60S binding.

CH1305 without a vector or containing pAJ414 (*NMD3-myc*), pAJ515 (*nmd3NΔ123-myc*) or pAJ516 (*nmd3NΔ167-myc*) was grown overnight and diluted to OD_{600}~0.15 in 10 ml of appropriate glucose-containing medium. After incubating for 6 hours at 30°C, cultures were treated with 150μg/ml cycloheximide and incubated for 20 minutes on ice before collection. Extracts were made and run on a 2.5% polyacrylamide/0.5% agarose composite gel as described in Chapter 2. Western blotting was performed against Nmd3-myc proteins and the post-transfer gel was stained with Coomasie Blue to visualize ribosomal species. Asterisks denote the relative position of free 60S subunits based on previous observations made with ethidium bromide-stained gels(Dahlberg and Grabowski 1990).

5.3.2 The minimal nuclear export signal sequence of Nmd3p

Previous research in our lab identified Nmd3p as the 60S nuclear export adapter and showed that the nuclear export signal (NES) was within the C-terminal 50 amino acids (Ho, Kallstrom et al. 2000). Within this region is a highly conserved sequence predicted to form an amphipathic helix typical of leucine-rich NESs. In collaboration with Dr. J. Dahlberg, we showed that hydrophobic residues within this peptide are important for export in metazoans. More recently, Nmd3p was suggested to contain a second NES within the coiled-coil domain (Gadal, Strauss et al. 2001). In this same work, the originally characterized NES (Ho, Kallstrom et al. 2000) was found to be dispensable for Nmd3p function.

In order to better define the sequence of yeast Nmd3p necessary for export function, a directed assay using GFP-tagged minimal NES fragments was carried out. This included identification of essential residues in this minimal domain that are required to maintain nuclear export function. To this end, the well-characterized NLS from the large T-antigen of the SV40 virus (Kalderon, Richardson et al. 1984) was fused to the C-terminus of a 175kDa polypeptide fragment of Xrn1p, a 5'→ 3' exonuclease. Green fluorescent protein (GFP) was then added to the C-terminus of the Xrn1-NLS fusion to make Xrn1-NLS(SV40)-GFP (XNG). Cells containing the XNG reporter showed tight nuclear fluorescent signal indicating that the SV40 NLS was functional (Figure 2). Various Nmd3p putative minimal NES peptides were subsequently fused to the C-terminus of this large reporter protein. An Xrn1p fragment was chosen for its size to prevent passive diffusion between the nucleus and cytoplasm that can occur through the NPC for proteins less than 30-40kDa in size.

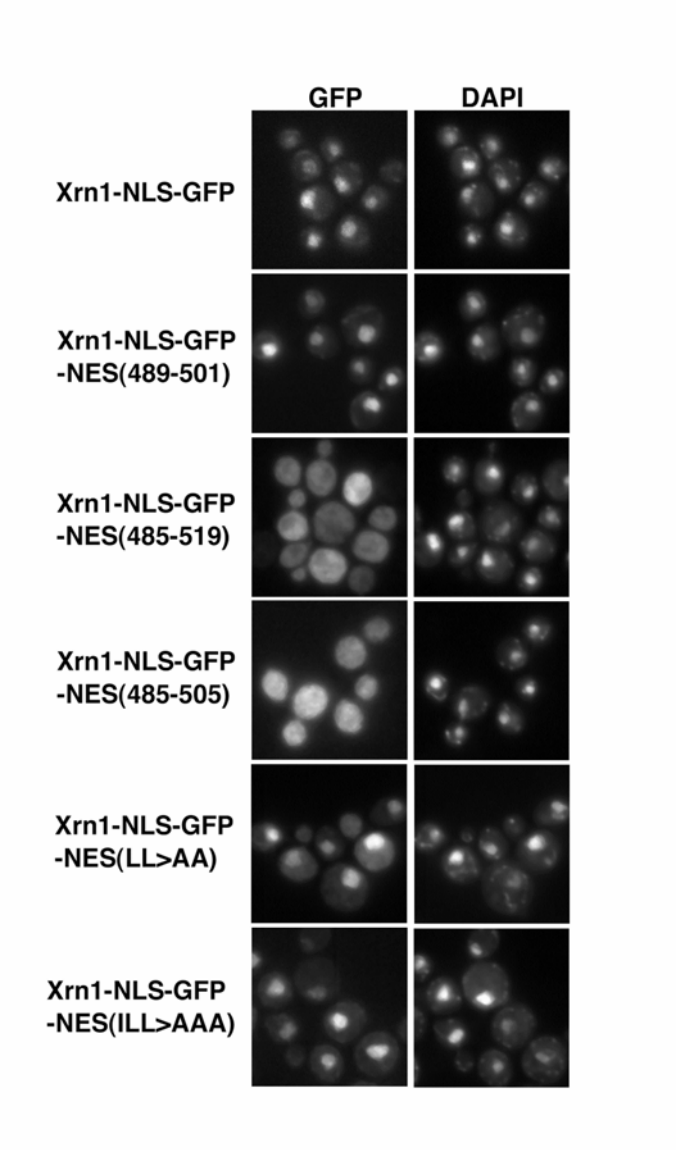

Figure 5.2 Defining the Nmd3p NES.

Wild-type strain W303 containing vectors pAJ670 (*XRN1-NLS-GFP*; *XNG*), pAJ671 (*XNG-NES[489-501]*), pAJ673 (*XNG-NES[485-519]*), pAJ676 (*XNG-NES[485-505]*), pAJ677 (*XNG-NES[LL→AA]*) or pAJ678 (*XNG-NES[ILL→AAA]*) was grown overnight and diluted 20-fold into 2ml of fresh glucose-containing medium. Cultures were grown for 6 hours, fixed, DAPI stained and visualized as according to Chapter 2. Note: the NLS used in these fusions is derived from the SV40 virus large T antigen.

The putative minimal NES sequence of Nmd3p was aligned with well-characterized NES sequences to obtain a map of the most highly conserved residues (Illustration 5.2A). This analysis identified a leucine-rich sequence (amino acids 493-503) that showed high conservation with well-characterized NESs including those from the HIV Rev and protein kinase inhibitor (PKI) proteins and with *NMD3* NES domains from other species. A helical-wheel projection shows that this sequence in yeast forms an amphipathic helix with hydrophobic leucines and isoleucines on one side and acidic residues on the other (Illustration 5.2B, NES1).

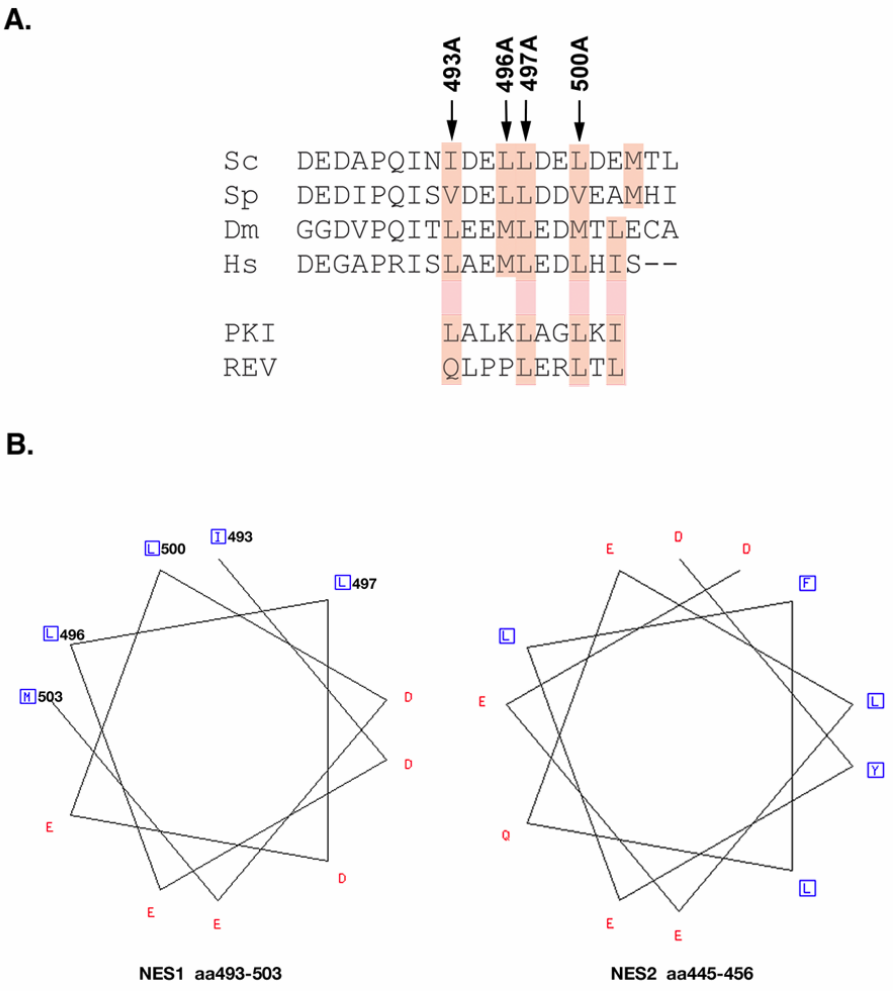

Illustration 5.2 Residues important for Nmd3p NES function.

(A) Alignment of hydrophobic residues in the shortest NES domain that supports Xrn1-NLS-GFP export (aa485-505). Shown are sequences from *Saccharomyces cerevisiae* (Sc), *Schizosaccharomyces pombe* (Sp), *Drosophila melanogaster* (Dm) and human (Hs). For reference, these alignments also include the well-characterized NES domains from the protein kinase inhibitior (PKI) and the HIV-1 Rev proteins. (B) Helical-wheel projections of the primary Nmd3p NES encompassing amino acids 493-503 and of the putative NES2 encompassing amino acids 445-456. Notice the well-defined hydrophobic face of NES1 potentially required for interaction with Crm1p. In contrast, the hydrophobic face of the putative NES2 contains two amino acids containing bulky sidechains, phenylalanine and tryptophan, that are not tolerated in leucine-rich NESs.

Based on the analysis of NES1, a minimal sequence containing only the putative core of the NES (amino acids 489 to 501) was inserted at the C-terminal end of the XNG sequence and found to be insufficient for export function (Figure 5.2). In order to determine if this was due to improper domain folding and/or removal of an essential residue, the remaining C-terminal end of Nmd3p was added to the putative minimal NES. The longer protein fragment, containing amino acids 485-519, supported export of the XNG reporter (Figure 5.2). Based on this observation, a shorter region containing amino acids 485-505 was tested and found to retain nuclear export ability by redistributing the XNG reporter to the cytoplasm (Figure 5.2 and illustration 5.2).

Leucine-rich NESs provide export function through hydrophobic interaction with the Crm1p export receptor. To further test Nmd3p NES function, conserved hydrophobic residues were mutated in the 485-505 amino acid sequence in accordance with studies done with human NMD3 (Trotta, Lund et al. 2003). As a commonly used practice to define residues important in protein function, these hydrophobic residues were mutated to alanines because of their relatively inert properties. Changing conserved leucines 496 and 497 to alanines (LL→AA) led to the accumulation of the XNG reporter in the nucleus (Illustration 5.2A and figure 5.2). A similar result was obtained for the triple mutant I493A, L497A and L500A (ILL→AAA) (Illustration 5.2A and figure 5.2) that correspond with L480, L484 and L487 in hNMD3 (Illustration 5.2A and (Trotta, Lund et al. 2003)). This suggests that the hydrophobic face of the predicted α-helical NES structure is important for nuclear export activity. Correspondingly, this domain is required for mediating CRM1 binding to hNMD3 in vitro (Thomas and Kutay 2003). However, as will be shown in the following section, the effects of these mutations depends heavily on the context of the NES sequence.

5.3.3 Specific mutations in NES1 change the cellular distribution of full-length Nmd3p and define the core domain for export function

As mentioned in the introduction to this chapter, two NESs have been reported in Nmd3p. NES2 in the predicted coiled-coil domain, is just upstream of NES1 (Gadal, Strauss et al. 2001). Removal of this coiled-coil allows growth as assayed by its ability to complement a *Δnmd3* strain (Figure 5.3A). On the other hand, removal of the C-terminal 33 amino acids (NES1) leads to inviability (Figure 5.3A). Contrary to what has been published this suggests that NES1 provides the primary export signal, since NES2 alone was unable to support growth in our hands. Futhermore, helical projections of NES2 do not suggest strong NES activity (Diagram 5.2B, NES2).

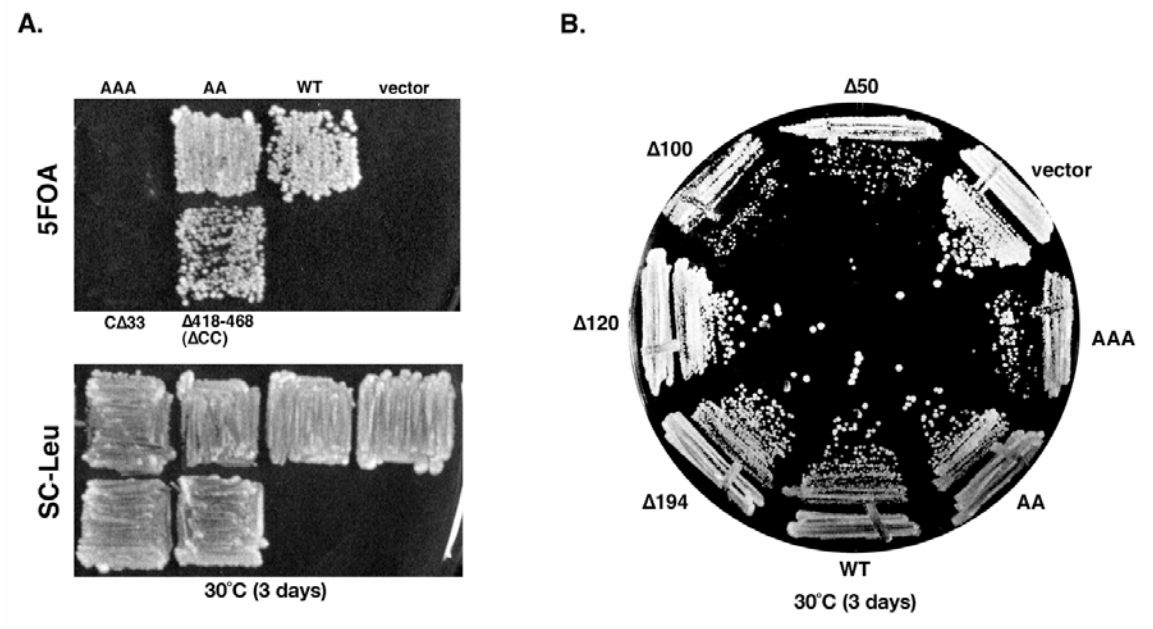

Figure 5.3 Disruption of specific domains in Nmd3p lead to inviability and/or dominant negative growth inhibition.

(A) Strain AJY529 (*nmd3::TRP1*) containing pAJ112 (*NMD3*) was transformed with pAJ24 (vector), pAJ538 (*NMD3*), pAJ751 (*NMD3AA*), pAJ752 (*NMD3AAA*), pAJ377 (*NMD3CΔ33*) or pAJ378 (*NMD3ΔCC[418-468]*) and patched onto either 5FOA to test complementation through loss of pAJ112 or SC-leu as a positive growth control. (B) Wild-type strain W303 containing pAJ24, pAJ751, pAJ752, pAJ538, pAJ534 (*NMD3CΔ50*), pAJ535 (*NMD3CΔ100*), pAJ536 (*NMD3CΔ120*) or pAJ537 (*NMD3CΔ194*) was streaked onto a SC-leu plate and incubated for 3 days at 30°C.

To determine what effects the NES mutations tested in section 5.3.2 have on Nmd3p function, these point mutations were introduced into full-length Nmd3p. The AAA mutation led to entrapment of the Nmd3AAA-GFP reporter in the nucleoplasm as indicated by accumulation of GFP-signal within the boundaries of the nucleus as demarcated by the nucleoporin marker Nic96-mRFP (Figure 5.4). Unexpectedly, the AA mutant was cytoplasmic, indicating that it was efficiently exported (Figure 5.4). In correspondence with their differing effects on export, the AA but not the AAA mutant was also capable of complementing an *Δnmd3* mutant (Figure 5.3A). On the other hand, the AAA mutant elicited a dominant negative phenotype similar to the effect of the CΔ50 truncation mutant (Figure 5.3B). This, combined with the result that the AA mutant did not support export of the XNG reporter, suggests that the surrounding Nmd3p sequence, possibly the coiled-coil, helps in Crm1p recruitment maybe through interaction with accessory factors such as Mtr2p. Thus, less severe disruptions in the primary NES1 domain may be overcome through interaction with this potential second export factor binding-site. In order to identify other factors that may play such a role in 60S export, a synthetic lethal screen using the *NMD3AA* could be carried out. In the event that the function of this secondary factor is disrupted, AA would no longer have the capacity to facilitate export in the context of the full-length protein. Initially, synthetic lethality with *mtr2* could be tested directly.

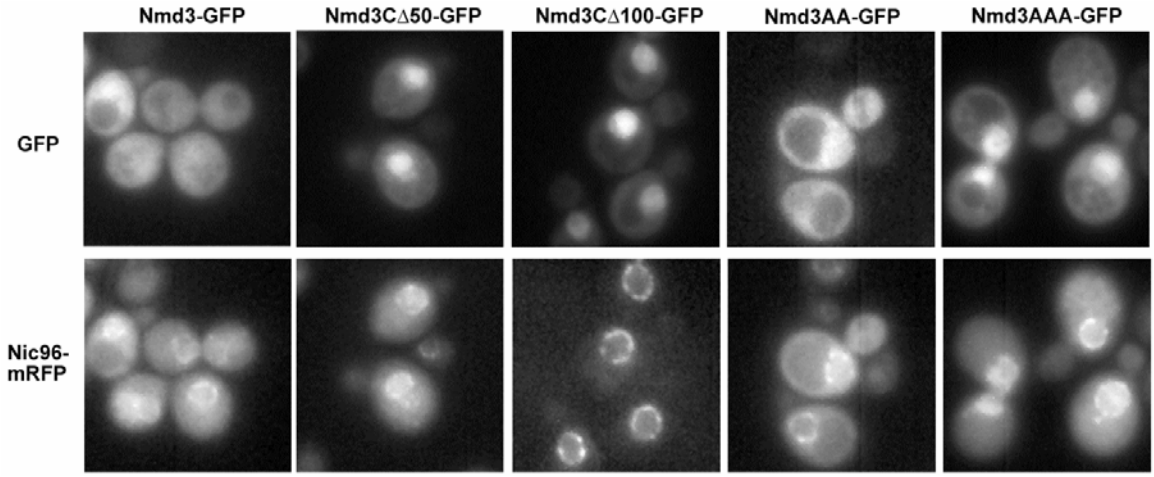

Figure 5.4 Specific mutations in the Nmd3p NES do not affect function in the context of the full-length protein structure.

Strain AJY1849 (*NIC96-mRFP crm1[T539C]*) containing pAJ582 (*NMD3-GFP*), pAJ583 (*NMD3CΔ50-GFP*), pAJ584 (*NMD3CΔ100-GFP*), pAJ753 (*NMD3AA-GFP*), or pAJ754 (*NMD3AAA-GFP*) was grown over a two overnight period and diluted ten-fold into 2ml of fresh glucose-containing medium. Cultures were grown for 6 hours, fixed, DAPI stained and visualized as according to Chapter 2.

In accordance with observations in yeast, work with human NMD3 showed similar, but more striking results. In this system, removal of the last 71 amino acids of hNMD3, comparable to yeast Δ100, led to entrapment of this protein along with 60S ribosomal subunits in nucleoli (Thomas and Kutay 2003). Furthermore, the number of point mutations incorporated into the hNMD3 NES showed a direct correlation with the level of nucle(ol)ar entrapment (Trotta, Lund et al. 2003). Similar mutations trap yeast Nmd3p in the nucleoplasm rather than the nucleolus. This may indicate that yeast Nmd3p loads onto subunits later than hNMD3 or mutations in the yeast Nmd3p NES are not disrupting a nucleolar exit signal similar to the one found in hNMD3 (Trotta, Lund et al. 2003).

In yeast, few pre-rRNA intermediates accumulate in *nmd3* ts or dominant negative mutants indicating that rRNA is almost fully matured prior to the point of Nmd3p function in the 60S biogenesis pathway ((Ho and Johnson 1999) and data not shown, respectively). In contrast however, Rpl25-eGFP accumulates in the nucleolus of cells under the same conditions suggesting that subunits are not released from the nucleolus (Ho, Kallstrom et al. 2000; Gadal, Strauss et al. 2001; Kallstrom, Hedges et al. 2003). Combined, the lack of pre-rRNA processing defects and accumulation of Rpl25-eGFP in the nucleolus of *nmd3* mutants suggest that Nmd3p loads onto pre-60S at the point of nucleolar exit. This would account for the lack of precursor rRNAs being found in pre-60S subunits that are trapped in the nucleolus in the absence of functional Nmd3p.

Along similar lines, NES mutants of hNMD3 that accumulate in nucleoli associate with only late 60S precursor rRNA from frog oocytes (Trotta, Lund et al. 2003). This was determined by injection of maltose binding protein tagged hNMD3 proteins, expressed from bacteria, into oocytes and assaying rRNA components of bound 60S complexes. Nuclear 60S subunits isolated with NES deficient hNMD3 were enriched

with 6S rRNA, a precursor of 5.8S that is cleaved in the cytoplasm in oocytes, but not 28S (25S in yeast) precursors. These results concur with those from yeast indicating that Nmd3p binds to a late 60S particle, likely at the point of release from the nucleolus.

5.3.4 Recruitment of Nmd3p to the 60S subunit

Through pulse-labeling experiments a small set of 60S r-proteins, including Rpl10p, have been identified as exchangeable because of their appearance on ribosomes when no ribosome synthesis is taking place (Warner and Udem 1972; Zinker and Warner 1976). Furthermore, the loading and exchange of Rpl10p on subunits is proposed to occur in the cytoplasm since Rpl10p loads relatively late compared to other subunit proteins (Kruiswijk, Planta et al. 1978). This timing corresponds more with the loading of the acidic P proteins that are well-characterized as cytoplamic loading proteins.

As discussed above, the evidence for Nmd3p binding directly to Rpl10p is questionable. In order to test directly if Rpl10p is needed for Nmd3p binding to the 60S subunit, I began by developing conditions to prepare subunits without Rpl10p. Previously, free 60S subunits lacking Rpl10p were isolated by sucrose velocity gradient fractionation from cells repressed for *RPL10* expression for 16 hours (Eisinger, Dick et al. 1997). These subunits were also shown to be deficient for 40S binding in vitro. Not surprisingly, it was later established that these same conditions also removed several undetermined ribosomal components in addition to Rpl10p indicated by a shift in 60S sedimentation to a lighter position in the gradient and by comparison to the composition of wild-type 60S (B. Trumpower, personal communication). To see such a shift in sedimentation, significant mass depletion must occur. Further, Rpl10p rebinding to subunits prepared under *RPL10* repressed conditions could not be reconstituted in vitro, again suggesting that the 60S structure was drastically altered (Eisinger, Dick et al. 1997).

Based on the effects on 60S subunits when Rpl10p expression is repressed in vivo, I sought to more selectively remove Rpl10p from subunits by various means based on its relatively weak 60S affinity (Dick, Karamanou et al. 1997). To this end I prepared 60S subunits under various buffer conditions, altering ionic strength and magnesium concentration. As a starting point, subunits were prepared on sucrose gradients in the presence of 500mM KCl and heparin and without magnesium as previously described (Dick, Karamanou et al. 1997). Under these conditions, sedimentation of 60S subunits was shown to mildly shift to lighter gradient positions (data not shown). Unfortunately, this shift correlated with results for *RPL10* repression (Eisinger, Dick et al. 1997), suggesting that conditions that remove Rpl10p also remove other factors. The presence of magnesium is required for maintaining proper rRNA structure and ribosome stability. When 60S gradient fractions prepared without magnesium were analyzed for specific r-proteins by western blotting, they were found to be deficient for both Rpl5p and Rpl10p. These proteins accumulated at the top of the gradient (Figure 5.5). On the other hand, Rpl12p, a core ribosomal protein used to indicate the sedimentation position of intact 60S subunits, was found most highly represented in fractions 5 and 6 (Figure 5.5). Since the combined mass of Rpl10p and Rpl5p does not account for the shift in 60S observed during sucrose sedimentation, it appears that these subunits are depleted of several additional ribosomal components.

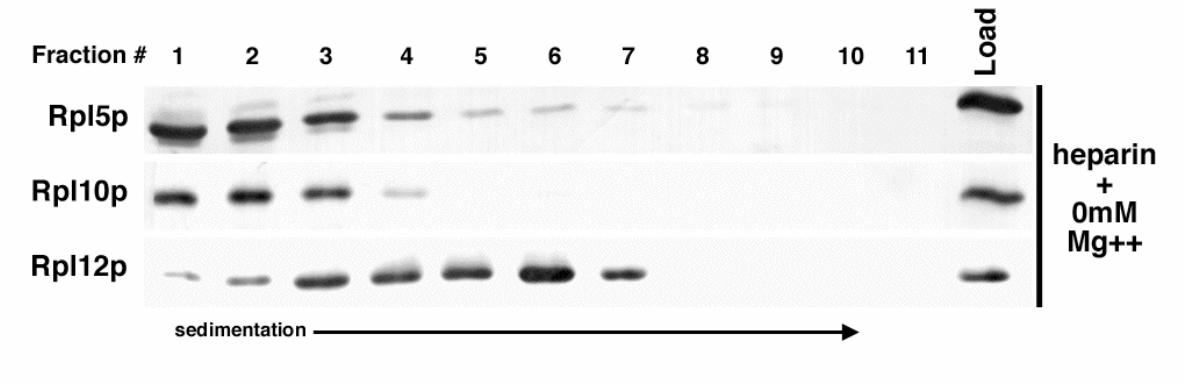

Figure 5.5 Preparation of 60S subunits in the absence of magnesium for in vitro binding assays.

60S subunits were isolated from extracts of wild-type cells on sucrose gradients containing heparin but lacking magnesium as described in Chapter 2. Gradient fractions were collected, TCA precipitated, proteins run on a 12% SDS-PAGE gel and western blotting performed with α-Rpl5p, α-Rpl10p or α-Rpl12p as also described in Chapter 2.

In Xenopus oocytes and mammalian cells, a 5S rRNA/Rpl5p ribonucleoprotein complex is formed prior to assembly into pre-60S subunits ((Picard and Wegnez 1979; Steitz, Berg et al. 1988), respectively). In the case of Xenopus oocytes, 5S is exported to the cytoplasm where it is sequestered to storage sites in association with transcription factor IIIA (TFIIIA) or Rpl5p (Guddat, Bakken et al. 1990; Allison, Romaniuk et al. 1991). TFIIIA associates with RNA Polymerase III to control expression of 5S rRNA in the nucleus. It is believed that the interaction of 5S with TFIIIA acts to sequester TFIIIA to the cytoplasm as a means of controlling 5S transcription levels. 5S is then re-imported into the nucleolus via Rpl5p interaction to associate with pre-60S particles during ribosome biogenesis. Thus, the 5S/Rpl5p complex provides an exception to the rule that ribosomal components are not pre-assembled prior to incorporation into the subunit complexes.

Little is known about the formation of the 5S/Rpl5p complex in yeast. It can be removed from mature subunits as an intact species (Nazar, Yaguchi et al. 1979) and exists as a stable complex when ribosomal subunit assembly is disrupted (Deshmukh, Tsay et al. 1993). From x-ray crystallography studies on subunit structure, Rpl10p makes contacts with 5S (Ban, Nissen et al. 2000); however, whether the 5S/Rpl5p complex loads before or after Rpl10p has not been established. When viewed from the 40S binding face, the 5S/Rpl5p complex constitutes the top and right sides of the central protuberance of the yeast 60S subunit (Illustration 5.3). Because of this position, removing the 5S/Rpl5p complex from subunits would likely destabilize the central protuberance. Subsequently, this could make it easier to remove Rpl10p. This corresponds with the removal of both Rpl10p and Rpl5p from subunits prepared in the absence of magnesium. Thus, these results suggest that the central protuberance and GTPase stalk are significantly altered under such conditions.

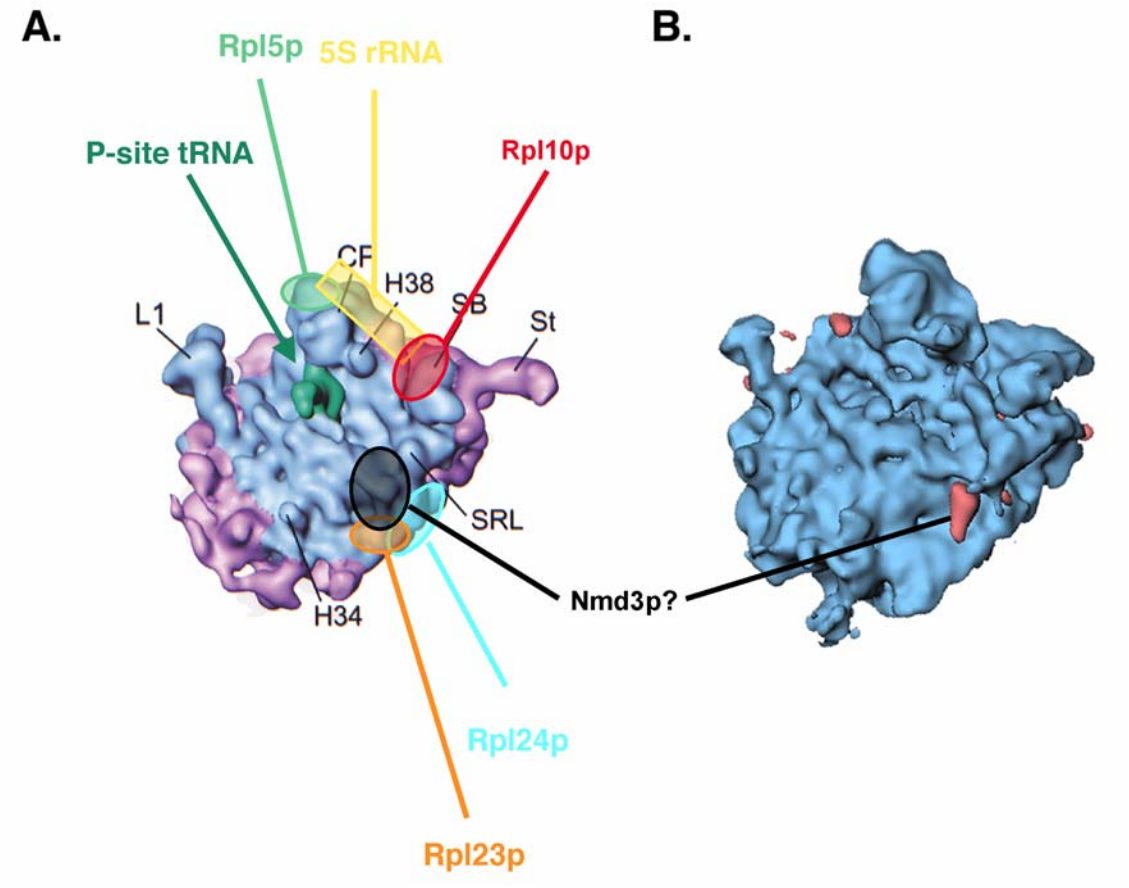

Illustration 5.3 60S components located near Rpl10p and putative Nmd3p binding sites.

(A) Cryo-EM reconstruction of 60S as viewed from the 40S joining face (adapted from (Spahn, Beckmann et al. 2001)). Indicated are proteins and rRNAs near the Rpl10p binding site (including the Rpl5p/5S complex) or near the putative Nmd3p binding site determined by cryo-EM reconstruction of a reconstituted Nmd3p/60S complex shown in (B) (reconstitution was performed by George Kallstrom, cryo-EM performed by Christian Spahn).

In order to find magnesium concentrations that allowed specific removal of Rpl10p, size exclusion chromatography was used. The starting material for these preparations were subunits purified using sucrose velocity gradients under normal magnesium (10mM $MgCl_2$), high salt (500 mM KCl) conditions that dissociated 80S and polysomes, but retained free 40S and 60S subunits as described in Chapter 2. These purified subunits were then further dialyzed for storage in a low magnesium (1mM), low salt (50mM KCl) buffer. EDTA was added to four separate aliquots of 1mM magnesium subunits to further reduce the free Mg^{2+} concentrations to 0.1, 0.2, 0.3 or 0.4mM. Subunits were then passed through a high molecular weight cut-off resin (P300, BioRad) equilibrated in a high salt (500mM KCl) buffer supplemented with 0.1, 0.2, 0.3 or 0.4mM $MgCl_2$. Eluted samples were immediately supplemented with $MgCl_2$ to 10mM in order to stabilize subunits.

P300 fractions from above were collected and run on 12% SDS-PAGE gels in order to characterize the composition of these "stripped" subunits by western blotting (Figure 5.6). Post-transfer gels were then stained with Coomasie Blue to visualize ribosomal protein bands. Because of the 300kDa MWCO of the P300 resin, "intact" large subunits eluted in the void volume (fractions 3 to 5) while free proteins eluted in fractions 8 or higher. Subunits prepared in the presence of 0.1 or 0.2 mM $MgCl_2$ migrated as intact species indicated by the presence of r-proteins in fractions 3, 4 and 5 (Figure 5.6, 0.1 and 0.2mM, Coomasie). However, these subunits no longer contained Rpl5p or Rpl10p as determined by lack of 60S co-elution by western blotting (data not shown and figure 5.6, 0.2mM westerns). At higher magnesium concentrations, 60S species were incrementally more intact, as evidenced by enhanced Rpl5p and Rpl10p retention on these subunits (Figure 5.6, 0.3 and 0.4mM magnesium) as well as by their earlier elution from P300 columns (Figure 5.6, 0.4mM magnesium, Coomasie-stained gel

fractions 2-4). The difference in elution position of 60S at 0.4mM magnesium concentration as compared to that at lower magnesium concentrations suggests that subunits are significantly depleted below the 0.4mM cutoff. However, because of the large mass of these molecules, it is uncertain how differences in elution behavior correlate with differences in subunit size.

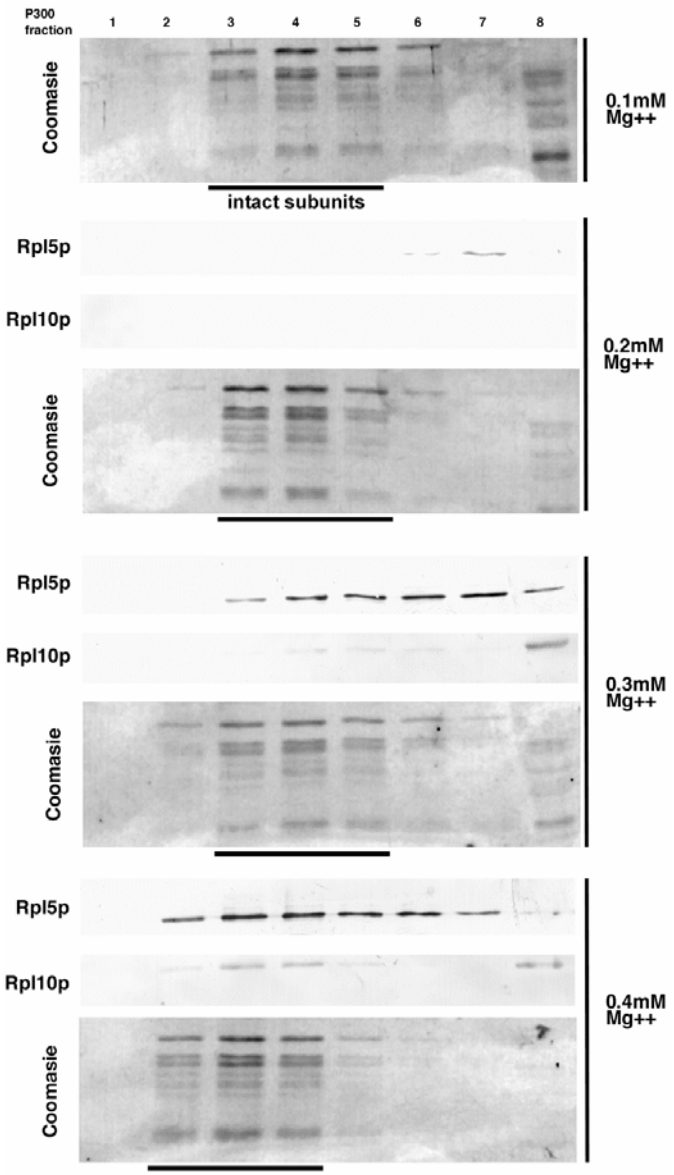

Figure 5.6 Preparation of 60S subunits under low magnesium conditions for in vitro binding assays.

60S subunits purified under normal (10mM) magnesium conditions by sucrose sedimentation were run over BioRad P300 columns under various low magnesium conditions as described in Chapter 2. Elution fractions were collected, run on 12% SDS-PAGE gels and western blotting performed with αRpl5p or αRpl10p as also described in Chapter 2. The post-transfer gels were stained with Coomasie Blue to visualize ribosomal protein bands.

Once isolated, “stripped” subunits were tested for their ability to bind purified GST-Nmd3p using a composite gel assay similar to that used in Chapter 4, but at higher magnesium concentrations. In vitro binding was carried out by incubating a standard amount of GST-Nmd3p (~150ng) with a standard amount of 60S subunits (~$5X10^{-3}$ A_{260}) prepared under each of the conditions described above. After a 30-minute incubation time at 30°C in normal magnesium (10mM $MgOAc_2$) and low salt (60mM KOAc) buffer, samples were run on a 0.5% agarose/2.5% polyacrylamide composite gel made under similar conditions as described in Chapter 2. Analysis by this in vitro method showed that GST-Nmd3p binding to “stripped” subunits (Figure 5.7, lanes 2-6) was significantly less than to intact 60S subunits (Figure 5.7, lane 1). This was based upon lack of comigration with a core ribosomal protein marker (Rpl1a) when examined by western blotting. Nonetheless, Nmd3p did bind to a subcomplex that migrated faster than the intact 60S species (lower band). In the case of the 0.1mM and 0.2mM Mg^{2+} prepared subunits this binding appeared to be bridged by factors other than Rpl5p or Rpl10p because both were deficient from these subunits (Figure 5.6). As a control, GST-Nmd3p alone did not significantly enter the gel indicating that the observed 60S subcomplex was not simply an aggregation of free GST-Nmd3 protein (Figure 5.7, lane 8).

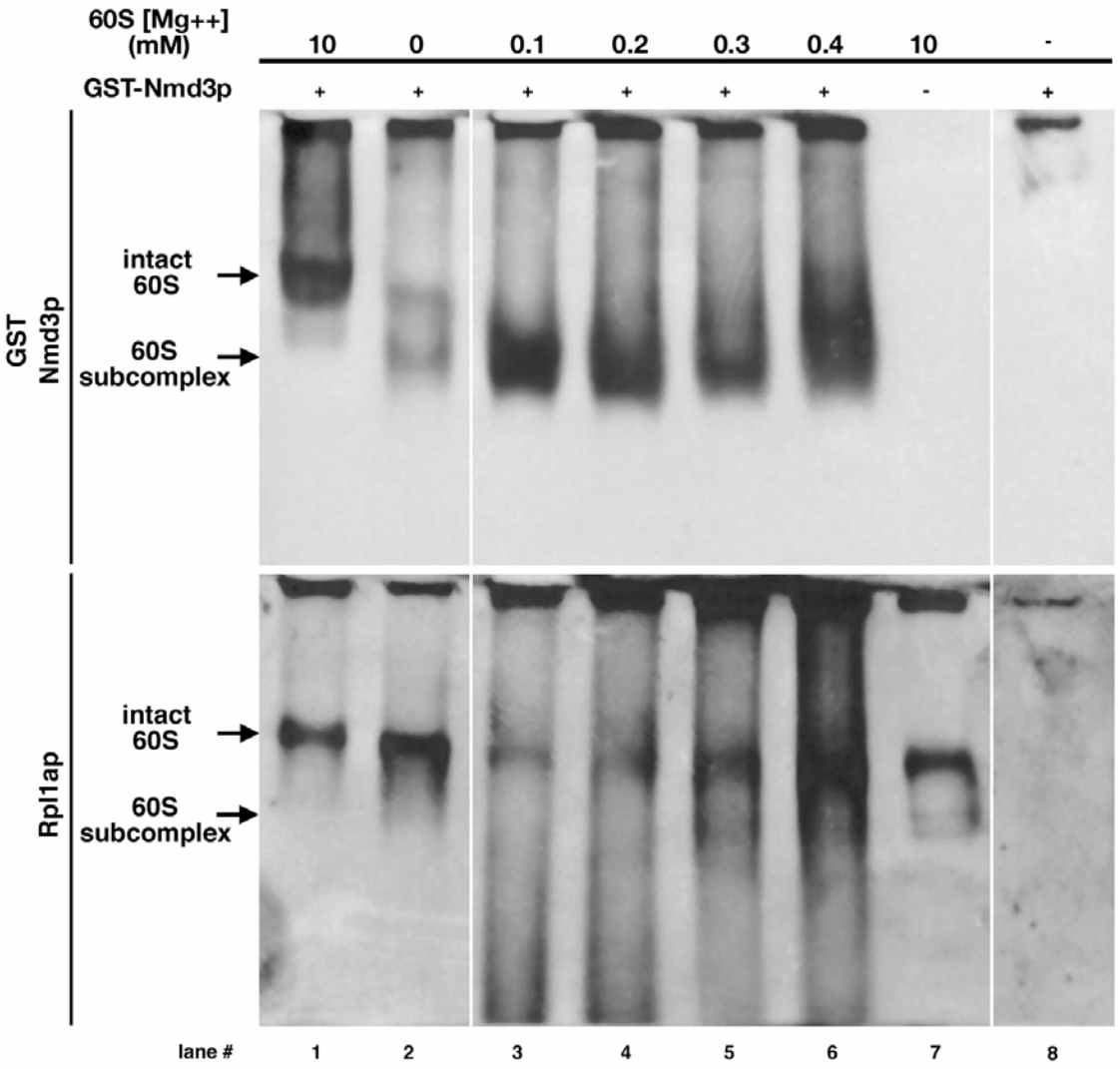

Figure 5.7 Nmd3p binds a 60S subcomplex isolated under low magnesium conditions.

~150ng of affinity purified GST-Nmd3p wild-type protein were incubated alone or with ~$5X10^{-3}$ A_{260} units of 60S subunits isolated under various magnesium concentrations as indicated in the figure. These mixtures were run on a 2.5% polyacrylamide/0.5% agarose composite gel. The position of 60S subunits was determined by western blotting using α-Rpl1ap (Lacroute). The membrane was then stripped and reprobed with α-GST. All methods are described further in Chapter 2.

To determine what rRNA species were present in these preparations, northern blotting was carried out. Since western blot analysis of 60S isolated under low magnesium conditions indicated that the 5S binding protein Rpl5p was missing from some preps, the presence of 5S itself was tested by northern hybridization using a specific DNA oligo probe (AJO249). In accordance with results obtained for Rpl5p, 5S was missing from intact subunits prepared at 0 to 0.2mM magnesium concentrations (Figure 5.8, lanes 1-3). Instead, 5S accumulated at the bottom of these gels indicating that either RNA that was originally co-isolated with subunits under low magnesium conditions is more easily dissociated even in the presence of normal magnesium levels or that the RNA is degraded during pre-incubation with GST-Nmd3p. "Stripped" subunits from 0.1 and 0.2mM magnesium preparations showed a similar result with respect to probing with a 25S specific oligo (AJO192) (Figure 5.8, lane 2 and 3). Surprisingly however, subunits prepared without magnesium but in the presence of heparin retained 25S association (Figure 5.8, lane 1). Thus, subunits prepared under low magnesium conditions in the absence of heparin appear to be inherently unstable which may make them more susceptible to nuclease attack. Regardless of such effects, these results suggest that Nmd3p binding likely involves a protein-protein interaction indicated by the ability of Nmd3p to bind to a "stripped" 60S subcomplex (Figure 5.7) lacking 25 or 5S rRNA species (Figure 5.8).

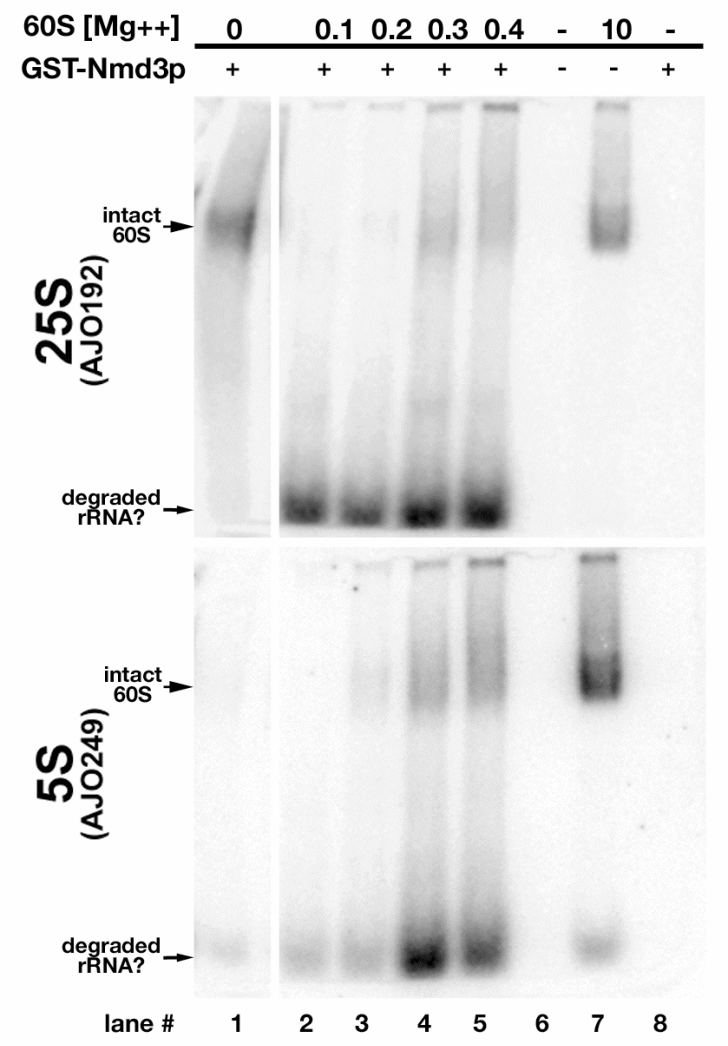

Figure 5.8 A 60S subcomplex bound by Nmd3p is deficient for 25S and 5S rRNAs.

A 2.5%/0.5% composite gel was setup and ran as in figure 5.7. The gel was then transferred to nylon membrane by electrotransfer and assayed by northern blotting for 25S and 5S rRNAs as described in Chapter 2.

The position of 5.8S in this assay was not determined. However, 5.8S makes extensive contact with 25S rRNA and, therefore, is likely present on the same particles, none of which include the putative 60S subcomplex in figure 5.7. Even if 5.8S did provide a binding site for Nmd3p on the subunit, this would place the Nmd3p position on 60S well away from the position of Rpl10p. This is based upon cryo-EM structural analysis showing that 5.8S, which corresponds to the 5' region of 23S in bacteria, is located at the bottom left corner of the joining face, while Rpl10p is located to the upper right of this position, just above the A-site (Illustration 5.3 and (Spahn, Beckmann et al. 2001)).

5.4 DISCUSSION

During the 1960s and 70s, significant advances were made in characterizing the rRNA processing pathway involved in formation of mature 40S and 60S subunits (reviewed in (Kressler, Linder et al. 1999; Venema and Tollervey 1999)). At the same time, isolation of the protein components of each subunit and characterization of the kinetics of subunit formation were made possible through the development of new pulse-chase labeling and 2D gel methodologies. However, after this initial interest, most resources were shifted to the rapidly emerging fields of transcription and replication. In addition, characterization of the multitude of other trans-acting factors that interact with the subunits later in the biogenesis pathway remained elusive due to the lack of adequate isolation and identification procedures. Only recently has our knowledge of late ribosome biogenesis substantially increased through utilization of large-scale proteomic analysis methods involving tandem affinity purification (TAP) in combination with mass spectrometry (Gavin, Bosche et al. 2002).

Prior to the proteomic revolution, identification and characterization of the 60S export adapter function of Nmd3 was carried out (Ho, Kallstrom et al. 2000). A

requirement for such an adapter in 60S export suggested that Nmd3p binding might act as a control point in subunit maturation. Therefore, defining the Nmd3p binding site on the subunit became a necessary requirement for understanding the mechanism of 60S export.

Through collaboration with Christian Spahn, preliminary evidence from cryo-EM imaging of a yeast Nmd3p/60S reconstituted complex showed a mass difference just below the sarcin/ricin loop of the 60S subunit in the crown view that is also the joining face for association with the 40S subunit (Illustration 5.3B). Unfortunately, supporting evidence for this putative binding site has not emerged.

Here, selective disruption trials of this putative binding site were carried out and the resulting subunits were tested for in vitro binding with purified Nmd3p. The results obtained from these lines of experimentation determined that the Nmd3p binding site on 60S is more complex than was initially suggested (Gadal, Strauss et al. 2001). With that said, this analysis has determined that 60S subunits lacking 5S rRNA and r-rproteins Rpl5p and Rpl10p are deficient for Nmd3p binding. However, a complex that migrated at a lower position than 60S on native gels maintained this binding. This "subcomplex" did not contain any 25S or 5S rRNA species as tested for by northern blotting. Isolation of this "subcomplex" for analysis by mass spectrometry and northern blotting with additional probes could be carried out to determine its composition. Nonetheless, in order to identify the full complement of components required for Nmd3p binding on the subunit, more definitive techniques will be needed. At the moment, further cryo-EM imaging of reconstituted Nmd3p/60S complexes seems to be the most viable means to this end.

Identifying the Nmd3p binding site on 60S would provide insight into how cells monitor the assembly of ribosomes. Previously, it was suggested that Rpl10p provides the binding site for Nmd3p on nuclear subunits (Gadal, Strauss et al. 2001), however

results in Chapters 3 and 4 have indicated that Rpl10p likely binds and facilitates release of Nmd3p from 60S in the cytoplasm. Thus, the components that form the Nmd3p binding site on nuclear 60S remain elusive. If Nmd3p is required for "proofreading" of the ribosome structure to determine its "export compentence", then the formation of this binding site is likely critical in this determination. Work presented in Chapter 3 and 4 as well as in this chapter provides further evidence that 60S components other than Rpl10p are required for formation of the Nmd3p binding site on the large subunit.

Although initial characterization of the function of the 60S export adapter Nmd3p had been carried out in the yeast *Saccharomyces cerevisiae*, detailed analysis of domains essential for Nmd3p function had not (Ho, Kallstrom et al. 2000; Gadal, Strauss et al. 2001). Previous work with human NMD3 helped define specific residues essential for export function (Trotta, Lund et al. 2003). Futhermore, interaction of hNMD3 with the CRM1 export adapter has been reconstituted in vitro (Thomas and Kutay 2003). Nonetheless, characterization of the Nmd3p 60S binding site or of the specific domain of Nmd3p required for Crm1p interaction in yeast had not been carried out.

To address these issues I analyzed a collection of Nmd3p mutants by a combination of native gel analysis and cell biology to establish a more detailed map of the regions of Nmd3p required for its export function. The N-terminus of Nmd3p, which contains four cys-x-x-cys motifs, appears to form a domain that interacts with components of the large ribosomal subunit. This binding may be facilitated through r-protein and/or rRNA interaction. Mutations produced within specific regions of the Nmd3p sequence that provide suppression of *rpl10* mutants, through weakened binding to 60S, provide preliminary boundaries for binding domains (Chapter 4). For example, part of the suppressor domain within the N-terminal portion of the protein contains a relatively positively charged region (aa100-115) with a pI of 11.5. This suggests that this

region may facilitate interaction with the RNA of the ribosome. In correlation with this observation, removal of the N-terminal suppressor domain leads to loss of 60S binding (Figure 5.1). On the other hand, the C-terminal suppressor domain contains a hydrophobic region (aa290-350) that may encompass a protein-binding region. This is also consistent with the finding that all C-terminal truncation proteins, except Nmd3CΔ194 that removes part of the C-terminal suppressor region, retain binding to 60S (Illustration 5.1 and data not shown).

Work presented here also identified a small leucine-rich domain that is likely responsible for Crm1p binding. This particular domain is predicted to fold into an amphipathic helix of which its hydrophobic face is predicted to interact with Crm1p in a manner similar to other related NESs from Rev (Fischer, Huber et al. 1995) and PKI (Wen, Meinkoth et al. 1995). In support of this hypothesis, mutations within the hydrophobic face render a minimal Nmd3p NES1 peptide incapable of supporting export of a reporter protein (Figure 5.2. and illustration 5.2A). Not surprisingly, in the context of the full Nmd3p structure, three point mutations within the putative NES rendered the protein nonfunctional indicated by its inability to support growth (Figure 5.3A). This is not consistent with the finding that the far C-terminal domain of Nmd3p (aa474-518), containing NES1, is dispensable for function (Gadal, Strauss et al. 2001). Based on my findings, the only plausible explanation for a c-terminally truncated allele of Nmd3p to retain functionality would be through a gain of function within another cellular component or in Nmd3p itself by the introduction of compensatory mutations.

Although these analyses have provided additional interaction data about the Nmd3p/60S and Nmd3p/Crm1p interfaces, determination of how these interactions are modulated remains elusive. Whether Nmd3p binding affinity for the export complex and the 60S subunit is controlled by accessory factors or changes in the Nmd3p structure

itself is still not known. However, Chapter 4 of this thesis suggests that release of Nmd3p in the cytoplasm is controlled by a complex series of events involving Rpl10p and the cytoplasmic GTPase Lsg1p. If Nmd3p is a necessary control point in the biogenesis pathway, the loading of this protein onto nuclear pre-60S as well as recognition of 60S-bound Nmd3p by Crm1 likely involves careful coordination between trans-acting factors and components of the ribosome itself.

Appendices

APPENDIX A *SQT1* CONDITIONAL AND LOSS OF FUNCTION MUTANTS

Allele	Mutation(s)	Relative Rpl10p binding
wild-type	-	5+
201 ts	L282P	ND
203 ts	Q193S,L194V	ND
204 ts	W256R	ND
2C4 ts	Y182H,G272D	ND
2L1 ts	H73L,M195V	ND
LF2 LOF	T356A	1+
LF5 LOF	E40G,I370T	-
LF6 LOF	N56I	-
LF7 LOF	T165P,R346G	-
LF9 LOF	C115R	1+
LF12 LOF	W92R,L134P,K357R	1+
LF15 LOF	ND	2+

APPENDIX B *NMD3* SUPPRESSOR MUTANTS

Allele	Mutation(s)	Relative *rpl10[G161D]* suppression
57-7h,57-7g	I112T,I362T	5+
57-5h,57-6e	L359P	ND
40-3c	N332D,Y379H	ND
40-1e	V349H,G360D,E476D	2+
40-2d	R113G	1+
40-2e	T105I	ND
nmd3-1(Karl, Onder et al. 1999)	L291F	2+

References

Allison, L. A., P. J. Romaniuk, et al. (1991). "RNA-protein interactions of stored 5S RNA with TFIIIA and ribosomal protein L5 during Xenopus oogenesis." Dev Biol **144**(1): 129-44.

Ban, N., P. Nissen, et al. (2000). "The complete atomic structure of the large ribosomal subunit at 2.4 A resolution." Science **289**(5481): 905-20.

Bassler, J., P. Grandi, et al. (2001). "Identification of a 60S preribosomal particle that is closely linked to nuclear export." Mol Cell **8**(3): 517-29.

Basu, U., K. Si, et al. (2001). "The Saccharomyces cerevisiae TIF6 gene encoding translation initiation factor 6 is required for 60S ribosomal subunit biogenesis." Mol Cell Biol **21**(5): 1453-62.

Becam, A. M., F. Nasr, et al. (2001). "Ria1p (Ynl163c), a protein similar to elongation factors 2, is involved in the biogenesis of the 60S subunit of the ribosome in Saccharomyces cerevisiae." Mol Genet Genomics **266**(3): 454-62.

Carter, A. P., W. M. Clemons, et al. (2000). "Functional insights from the structure of the 30S ribosomal subunit and its interactions with antibiotics." Nature **407**(6802): 340-8.

Ciufo, L. F. and J. D. Brown (2000). "Nuclear export of yeast signal recognition particle lacking Srp54p by the Xpo1p/Crm1p NES-dependent pathway." Curr Biol **10**(20): 1256-64.

Dahlberg, A. E. and P. J. Grabowski (1990). Gel electrophoresis of ribonucleoproteins. Gel Electrophoresis of Nucleic Acids: A Practical Approach. D. Rickwood and B. D. Hames. Oxford, Oxford University Press**:** 275-289.

Deshmukh, M., Y. F. Tsay, et al. (1993). "Yeast ribosomal protein L1 is required for the stability of newly synthesized 5S rRNA and the assembly of 60S ribosomal subunits." Mol Cell Biol **13**(5): 2835-45.

Dick, F. A., D. P. Eisinger, et al. (1997). "Exchangeability of Qsr1p, a large ribosomal subunit protein required for subunit joining, suggests a novel translational regulatory mechanism." FEBS Lett **419**(1): 1-3.

Dick, F. A., S. Karamanou, et al. (1997). "QSR1, an essential yeast gene with a genetic relationship to a subunit of the mitochondrial cytochrome bc1 complex, codes for a 60 S ribosomal subunit protein." J Biol Chem **272**(20): 13372-9.

Dragon, F., J. E. Gallagher, et al. (2002). "A large nucleolar U3 ribonucleoprotein required for 18S ribosomal RNA biogenesis." Nature **417**(6892): 967-70.

Eisinger, D. P., F. A. Dick, et al. (1997). "SQT1, which encodes an essential WD domain protein of Saccharomyces cerevisiae, suppresses dominant-negative mutations of the ribosomal protein gene QSR1." Mol Cell Biol **17**(9): 5146-55.

Eisinger, D. P., F. A. Dick, et al. (1997). "Qsr1p, a 60S ribosomal subunit protein, is required for joining of 40S and 60S subunits." Mol Cell Biol **17**(9): 5136-45.

Fatica, A. and D. Tollervey (2002). "Making ribosomes." Curr Opin Cell Biol **14**(3): 313-8.

Fischer, U., J. Huber, et al. (1995). "The HIV-1 Rev activation domain is a nuclear export signal that accesses an export pathway used by specific cellular RNAs." Cell **82**(3): 475-83.
Fornerod, M., M. Ohno, et al. (1997). "CRM1 is an export receptor for leucine-rich nuclear export signals." Cell **90**(6): 1051-60.
Fried, H. and U. Kutay (2003). "Nucleocytoplasmic transport: taking an inventory." Cell Mol Life Sci **60**(8): 1659-88.
Fromont-Racine, M., B. Senger, et al. (2003). "Ribosome assembly in eukaryotes." Gene **313**(2003): 17-42.
Gadal, O., D. Strauss, et al. (2001). "A nuclear AAA-type ATPase (Rix7p) is required for biogenesis and nuclear export of 60S ribosomal subunits." Embo J **20**(14): 3695-704.
Gadal, O., D. Strauss, et al. (2001). "Nuclear export of 60s ribosomal subunits depends on Xpo1p and requires a nuclear export sequence-containing factor, Nmd3p, that associates with the large subunit protein Rpl10p." Mol Cell Biol **21**(10): 3405-15.
Garrett, R. A. (2000). The Ribosome: structure, function, antibiotics, and cellular interaction. Washington, D. C., ASM Press.
Gavin, A. C., M. Bosche, et al. (2002). "Functional organization of the yeast proteome by systematic analysis of protein complexes." Nature **415**(6868): 141-7.
Gorlich, D. and U. Kutay (1999). "Transport between the cell nucleus and the cytoplasm." Annu Rev Cell Dev Biol **15**: 607-60.
Grandi, P., V. Rybin, et al. (2002). "90S pre-ribosomes include the 35S pre-rRNA, the U3 snoRNP, and 40S subunit processing factors but predominantly lack 60S synthesis factors." Mol Cell **10**(1): 105-15.
Grosshans, H., K. Deinert, et al. (2001). "Biogenesis of the signal recognition particle (SRP) involves import of SRP proteins into the nucleolus, assembly with the SRP-RNA, and Xpo1p-mediated export." J Cell Biol **153**(4): 745-62.
Guddat, U., A. H. Bakken, et al. (1990). "Protein-mediated nuclear export of RNA: 5S rRNA containing small RNPs in xenopus oocytes." Cell **60**(4): 619-28.
Ho, J. H. and A. W. Johnson (1999). "NMD3 encodes an essential cytoplasmic protein required for stable 60S ribosomal subunits in Saccharomyces cerevisiae." Mol Cell Biol **19**(3): 2389-99.
Ho, J. H., G. Kallstrom, et al. (2000). "Nascent 60S ribosomal subunits enter the free pool bound by Nmd3p." Rna **6**(11): 1625-34.
Ho, J. H., G. Kallstrom, et al. (2000). "Nmd3p is a Crm1p-dependent adapter protein for nuclear export of the large ribosomal subunit." J Cell Biol **151**(5): 1057-66.
Hovland, P., J. Flick, et al. (1989). "Galactose as a gratuitous inducer of GAL gene expression in yeasts growing on glucose." Gene **83**(1): 57-64.
Huh, W. K., J. V. Falvo, et al. (2003). "Global analysis of protein localization in budding yeast." Nature **425**(6959): 686-91.
Hurt, E., S. Hannus, et al. (1999). "A novel in vivo assay reveals inhibition of ribosomal nuclear export in ran-cycle and nucleoporin mutants." J Cell Biol **144**(3): 389-401.

Iouk, T. L., J. D. Aitchison, et al. (2001). "Rrb1p, a yeast nuclear WD-repeat protein involved in the regulation of ribosome biosynthesis." Mol Cell Biol **21**(4): 1260-71.
Johnson, A. W. (2004). Nuclear Export of Ribosomal Subunits. The Nucleolus. M. O. J. Olson. New York, Klumer Academic/Plenum Publishers**:** 286-296.
Johnson, A. W., E. Lund, et al. (2002). "Nuclear export of ribosomal subunits." Trends Biochem Sci **27**(11): 580-5.
Kaiser, C., S. Michaelis, et al. (1994). Methods in yeast genetics. Cold Spring Harbor, N.Y., Cold Spring Harbor Laboratory Press.
Kalderon, D., W. D. Richardson, et al. (1984). "Sequence requirements for nuclear location of simian virus 40 large-T antigen." Nature **311**(5981): 33-8.
Kallstrom, G., J. Hedges, et al. (2003). "The putative GTPases Nog1p and Lsg1p are required for 60S ribosomal subunit biogenesis and are localized to the nucleus and cytoplasm, respectively." Mol Cell Biol **23**(12): 4344-55.
Kapp, L. D. and J. R. Lorsch (2004). "The molecular mechanics of eukaryotic translation." Annu Rev Biochem **73**: 657-704.
Karl, T., K. Onder, et al. (1999). "GRC5 and NMD3 function in translational control of gene expression and interact genetically." Curr Genet **34**(6): 419-29.
Katahira, J., K. Strasser, et al. (1999). "The Mex67p-mediated nuclear mRNA export pathway is conserved from yeast to human." Embo J **18**(9): 2593-609.
Kelley, L. A., R. M. MacCallum, et al. (2000). "Enhanced genome annotation using structural profiles in the program 3D-PSSM." J Mol Biol **299**(2): 499-520.
Kranz, J. E. and C. Holm (1990). "Cloning by function: an alternative approach for identifying yeast homologs of genes from other organisms." Proc Natl Acad Sci U S A **87**(17): 6629-33.
Kressler, D., P. Linder, et al. (1999). "Protein trans-acting factors involved in ribosome biogenesis in Saccharomyces cerevisiae." Mol Cell Biol **19**(12): 7897-912.
Kruiswijk, T., R. J. Planta, et al. (1978). "The course of the assembly of ribosomal subunits in yeast." Biochim Biophys Acta **517**(2): 378-89.
Lafontaine, D., J. Vandenhaute, et al. (1995). "The 18S rRNA dimethylase Dim1p is required for pre-ribosomal RNA processing in yeast." Genes Dev **9**(20): 2470-81.
Lake, J. A. (1976). "Ribosome structure determined by electron microscopy of Escherichia coli small subunits, large subunits and monomeric ribosomes." J Mol Biol **105**(1): 131-9.
Lake, J. A. (1982). "Ribosomal subunit orientations determined in the monomeric ribosome by single and by double-labeling immune electron microscopy." J Mol Biol **161**(1): 89-106.
Longtine, M. S., A. McKenzie, 3rd, et al. (1998). "Additional modules for versatile and economical PCR-based gene deletion and modification in Saccharomyces cerevisiae." Yeast **14**(10): 953-61.
Lowe, T. M. and S. R. Eddy (1999). "A computational screen for methylation guide snoRNAs in yeast." Science **283**(5405): 1168-71.
Mackay, J. P. and M. Crossley (1998). "Zinc fingers are sticking together." Trends Biochem Sci **23**(1): 1-4.

Maden, B. E., R. R. Traut, et al. (1968). "Ribosome-catalysed peptidyl transfer: the polyphenylalanine system." J Mol Biol **35**(2): 333-45.
Mangiarotti, G. and S. Chiaberge (1997). "Reconstitution of functional eukaryotic ribosomes from Dictyostelium discoideum ribosomal proteins and RNA." J Biol Chem **272**(32): 19682-7.
Mattaj, I. W. and L. Englmeier (1998). "Nucleocytoplasmic transport: the soluble phase." Annu Rev Biochem **67**: 265-306.
Milkereit, P., O. Gadal, et al. (2001). "Maturation and intranuclear transport of pre-ribosomes requires Noc proteins." Cell **105**(4): 499-509.
Mitchell, D. A., T. K. Marshall, et al. (1993). "Vectors for the inducible overexpression of glutathione S-transferase fusion proteins in yeast." Yeast **9**(7): 715-22.
Moazed, D. and H. F. Noller (1989). "Intermediate states in the movement of transfer RNA in the ribosome." Nature **342**(6246): 142-8.
Moazed, D. and H. F. Noller (1991). "Sites of interaction of the CCA end of peptidyl-tRNA with 23S rRNA." Proc Natl Acad Sci U S A **88**(9): 3725-8.
Moy, T. I. and P. A. Silver (1999). "Nuclear export of the small ribosomal subunit requires the ran-GTPase cycle and certain nucleoporins." Genes Dev **13**(16): 2118-33.
Moy, T. I. and P. A. Silver (2002). "Requirements for the nuclear export of the small ribosomal subunit." J Cell Sci **115**(Pt 14): 2985-95.
Nakagawa, A., T. Nakashima, et al. (1999). "The three-dimensional structure of the RNA-binding domain of ribosomal protein L2; a protein at the peptidyl transferase center of the ribosome." Embo J **18**(6): 1459-67.
Nazar, R. N., M. Yaguchi, et al. (1979). "The 5-S RNA binding protein from yeast (Saccharomyces cerevisiae) ribosomes. Evolution of the eukaryotic 5-S RNA binding protein." Eur J Biochem **102**(2): 573-82.
Neville, M. and M. Rosbash (1999). "The NES-Crm1p export pathway is not a major mRNA export route in Saccharomyces cerevisiae." Embo J **18**(13): 3746-56.
Nguyen, Y. H., A. A. Mills, et al. (1998). "Assembly of the QM protein onto the 60S ribosomal subunit occurs in the cytoplasm." J Cell Biochem **68**(2): 281-5.
Nissan, T. A., J. Bassler, et al. (2002). "60S pre-ribosome formation viewed from assembly in the nucleolus until export to the cytoplasm." Embo J **21**(20): 5539-47.
Nissen, P., J. Hansen, et al. (2000). "The structural basis of ribosome activity in peptide bond synthesis." Science **289**(5481): 920-30.
Noller, H. F., V. Hoffarth, et al. (1992). "Unusual resistance of peptidyl transferase to protein extraction procedures." Science **256**(5062): 1416-9.
Oender, K., M. Loeffler, et al. (2003). "Translational regulator RpL10p/Grc5p interacts physically and functionally with Sed1p, a dynamic component of the yeast cell surface." Yeast **20**(4): 281-94.
Pestova, T. V., V. G. Kolupaeva, et al. (2001). "Molecular mechanisms of translation initiation in eukaryotes." Proc Natl Acad Sci U S A **98**(13): 7029-36.
Picard, B. and M. Wegnez (1979). "Isolation of a 7S particle from Xenopus laevis oocytes: a 5S RNA-protein complex." Proc Natl Acad Sci U S A **76**(1): 241-5.

Planta, R. J. and W. H. Mager (1998). "The list of cytoplasmic ribosomal proteins of Saccharomyces cerevisiae." Yeast **14**(5): 471-7.
Popa, I., M. E. Harris, et al. (2002). "CRM1-dependent function of a cis-acting RNA export element." Mol Cell Biol **22**(7): 2057-67.
Ramakrishnan, V. (2002). "Ribosome structure and the mechanism of translation." Cell **108**(4): 557-72.
Raychaudhuri, P., E. A. Stringer, et al. (1984). "Ribosomal subunit antiassociation activity in rabbit reticulocyte lysates. Evidence for a low molecular weight ribosomal subunit antiassociation protein factor (Mr = 25,000)." J Biol Chem **259**(19): 11930-5.
Ribbeck, K. and D. Gorlich (2002). "The permeability barrier of nuclear pore complexes appears to operate via hydrophobic exclusion." Embo J **21**(11): 2664-71.
Rohl, R. and K. H. Nierhaus (1982). "Assembly map of the large subunit (50S) of Escherichia coli ribosomes." Proc Natl Acad Sci U S A **79**(3): 729-33.
Sanchez, M. E., D. Urena, et al. (1990). "In vitro reassembly of active large ribosomal subunits of the halophilic archaebacterium Haloferax mediterranei." Biochemistry **29**(39): 9256-61.
Santos-Rosa, H., H. Moreno, et al. (1998). "Nuclear mRNA export requires complex formation between Mex67p and Mtr2p at the nuclear pores." Mol Cell Biol **18**(11): 6826-38.
Saveanu, C., D. Bienvenu, et al. (2001). "Nog2p, a putative GTPase associated with pre-60S subunits and required for late 60S maturation steps." Embo J **20**(22): 6475-84.
Saveanu, C., A. Namane, et al. (2003). "Sequential protein association with nascent 60S ribosomal particles." Mol Cell Biol **23**(13): 4449-60.
Schlenstedt, G., D. H. Wong, et al. (1995). "Mutants in a yeast Ran binding protein are defective in nuclear transport." Embo J **14**(21): 5367-78.
Senger, B., D. L. Lafontaine, et al. (2001). "The nucle(ol)ar Tif6p and Efl1p are required for a late cytoplasmic step of ribosome synthesis." Mol Cell **8**(6): 1363-73.
Sengupta, J., J. Nilsson, et al. (2004). "Identification of the versatile scaffold protein RACK1 on the eukaryotic ribosome by cryo-EM." Nat Struct Mol Biol **11**(10): 957-62.
Sonenberg, N. and T. E. Dever (2003). "Eukaryotic translation initiation factors and regulators." Curr Opin Struct Biol **13**(1): 56-63.
Spahn, C. M., R. Beckmann, et al. (2001). "Structure of the 80S ribosome from Saccharomyces cerevisiae--tRNA-ribosome and subunit-subunit interactions." Cell **107**(3): 373-86.
Stade, K., C. S. Ford, et al. (1997). "Exportin 1 (Crm1p) is an essential nuclear export factor." Cell **90**(6): 1041-50.
Stage-Zimmermann, T., U. Schmidt, et al. (2000). "Factors affecting nuclear export of the 60S ribosomal subunit in vivo." Mol Biol Cell **11**(11): 3777-89.
Steitz, J. A., C. Berg, et al. (1988). "A 5S rRNA/L5 complex is a precursor to ribosome assembly in mammalian cells." J Cell Biol **106**(3): 545-56.

Stultz, C. M., R. H. Nambudripad, et al. (1997). Predicting Protein Structure with Probabilistic Models. Protein Structural Biology in Bio-Medical Research. N. Allewell and C. Woodward. Greenwich, JAI Press. **22B:** 447-506.
Suyama, M., T. Doerks, et al. (2000). "Prediction of structural domains of TAP reveals details of its interaction with p15 and nucleoporins." EMBO Rep **1**(1): 53-8.
Sydorskyy, Y., D. J. Dilworth, et al. (2003). "Intersection of the Kap123p-mediated nuclear import and ribosome export pathways." Mol Cell Biol **23**(6): 2042-54.
Teakle, G. R. and P. M. Gilmartin (1998). "Two forms of type IV zinc-finger motif and their kingdom-specific distribution between the flora, fauna and fungi." Trends Biochem Sci **23**(3): 100-2.
Thomas, F. and U. Kutay (2003). "Biogenesis and nuclear export of ribosomal subunits in higher eukaryotes depend on the CRM1 export pathway." J Cell Sci **116**(Pt 12): 2409-19.
Trapman, J. and R. J. Planta (1976). "Maturation of ribosomes in yeast. I Kinetic analysis by labelling of high molecular weight rRNA species." Biochim Biophys Acta **442**(3): 265-74.
Trapman, J., J. Retel, et al. (1975). "Ribosomal precursor particles from yeast." Exp Cell Res **90**(1): 95-104.
Trotta, C. R., E. Lund, et al. (2003). "Coordinated nuclear export of 60S ribosomal subunits and NMD3 in vertebrates." Embo J **22**(11): 2841-51.
Tschochner, H. and E. Hurt (2003). "Pre-ribosomes on the road from the nucleolus to the cytoplasm." Trends Cell Biol **13**(5): 255-63.
Uchiumi, T., S. Honma, et al. (2002). "Translation elongation by a hybrid ribosome in which proteins at the GTPase center of the Escherichia coli ribosome are replaced with rat counterparts." J Biol Chem **277**(6): 3857-62.
Udem, S. A. and J. R. Warner (1972). "Ribosomal RNA synthesis in Saccharomyces cerevisiae." J Mol Biol **65**(2): 227-42.
Udem, S. A. and J. R. Warner (1973). "The cytoplasmic maturation of a ribosomal precursor ribonucleic acid in yeast." J Biol Chem **248**(4): 1412-6.
Venema, J. and D. Tollervey (1999). "Ribosome synthesis in Saccharomyces cerevisiae." Annu Rev Genet **33**: 261-311.
Warner, J. R. (1966). "The assembly of ribosomes in HeLa cells." J Mol Biol **19**(2): 383-98.
Warner, J. R. (1971). "The Assembly of Ribosomes in Yeast." J Biol Chem **246**(2): 447-454.
Warner, J. R. (2001). "Nascent ribosomes." Cell **107**(2): 133-6.
Warner, J. R. and S. A. Udem (1972). "Temperature sensitive mutations affecting ribosome synthesis in Saccharomyces cerevisiae." J Mol Biol **65**(2): 243-57.
Wen, W., J. L. Meinkoth, et al. (1995). "Identification of a signal for rapid export of proteins from the nucleus." Cell **82**(3): 463-73.
Winey, M., D. Yarar, et al. (1997). "Nuclear pore complex number and distribution throughout the Saccharomyces cerevisiae cell cycle by three-dimensional reconstruction from electron micrographs of nuclear envelopes." Mol Biol Cell **8**(11): 2119-32.

Youngman, E. M., J. L. Brunelle, et al. (2004). "The active site of the ribosome is composed of two layers of conserved nucleotides with distinct roles in peptide bond formation and peptide release." Cell **117**(5): 589-99.
Yusupov, M. M., G. Z. Yusupova, et al. (2001). "Crystal structure of the ribosome at 5.5 A resolution." Science **292**(5518): 883-96.
Zinker, S. and J. R. Warner (1976). "The ribosomal proteins of Saccharomyces cerevisiae. Phosphorylated and exchangeable proteins." J Biol Chem **251**(6): 1799-807.
Zuk, D., J. P. Belk, et al. (1999). "Temperature-sensitive mutations in the Saccharomyces cerevisiae MRT4, GRC5, SLA2 and THS1 genes result in defects in mRNA turnover." Genetics **153**(1): 35-47.

Vita

John Benjamin Hedges was born in Scott City, Kansas on September 18, 1975 to Sharon Marie Hedges and Eric Samuel Hedges. After graduating from Scott Community High School in 1994, he attended the University of Kansas, Lawrence, where he received a Bachelor of Arts in December 1998. After completing his undergraduate degree, he was employed by the Midwest Research Institute, Kansas City, Missouri. In August of 1999 he entered the Graduate School at the University of Texas.

Permanent address: 1209 Elizabeth, Scott City, Kansas, 67871

This dissertation was typed by the author.